2017

Generation of recombinant human respiratory syncytial viruses to study antigenic subtype differences, attachment glycoprotein evolution, and polymerase localization

BOSTON UNIVERSITY

SCHOOL OF MEDICINE

Thesis

GENERATION OF RECOMBINANT HUMAN RESPIRATORY SYNCYTIAL VIRUSES TO STUDY ANTIGENIC SUBTYPE DIFFERENCES, ATTACHMENT GLYCOPROTEIN EVOLUTION, AND POLYMERASE LOCALIZATION

by

GRACE YOONHEEKEE OLINGER

B.S., University of Missouri, 2013

Submitted in partial fulfillment of the

requirements for the degree of

Master of Science

2017

Approved by

First Reader _____

W. Paul Duprex, Ph.D.
Professor of Microbiology

Second Reader _____

John H. Connor, Ph.D.
Associate Professor of Microbiology

DEDICATION

I would like to dedicate this work to my late mother, who passed away from her battle with cancer. She is the inspiration for my passion in biomedical research.

ACKNOWLEDGMENTS

I would like to thank my mentor, Dr. W. Paul Duprex for his guidance and support. I would also like to thank the current and former laboratory members of Duprex laboratory, Dr. Linda Rennick, Dr. Sham Nambulli, Dr. Natasha Tilston-Lunel, Gregory Ho, Andrew Acciardo, and Dr. Martin Ludlow, who have been helpful and supportive. I would also like to thank the department of Microbiology at Boston University School of Medicine, the chair of the department, Dr. Ronald Corley, and Director of Graduate Studies, Dr. Gregory Viglianti. I am also grateful for members of my former committee, Dr. Rachel Fearns, Dr. Rahm Gummuluru, Dr. Jay Mizgerd, and especially for Dr. John Connor, who is also my second thesis reader, for their guidance.

I am eternally grateful for my friends and loved ones who have been encouraging and supportive in all my endeavors and have been like a family to me; special thanks to Leandro Creatini, Raquel Rodriguez, Daniel Taub, Alicia Wooten, Tia Mei Potts, and Supapan Thammanok. Finally, I would like to thank my late parents, who have instilled in me a passion for knowledge, inspired me to be a better person, and taught me that no dream is too big.

GENERATION OF RECOMBINANT HUMAN RESPIRATORY SYNCYTIAL VIRUSES TO STUDY ANTIGENIC SUBTYPE DIFFERENCES, ATTACHMENT GLYCOPROTEIN EVOLUTION, AND POLYMERASE LOCALIZATION

GRACE YOONHEEKEE OLINGER

ABSTRACT

Human respiratory syncytial virus (HRSV) is a negative sense, single strand RNA virus that causes respiratory tract infection with common cold-like symptoms, which can be severe in children, immunocompromised, and the elderly. Even with 60 years of research, the need for vaccine and effective treatment has not been met. In this work, recombinant viruses have been generated which will be valuable in gaining a better understanding of HRSV subtypes, glycoprotein evolution, and the polymerase localization, which would contribute to HRSV vaccine and therapeutics development.

The differences in the fitness of A and B antigenic subtypes of HRSV and how it affects the regional circulation pattern is not well understood. To study and compare the two subtypes, it is important to use clinically relevant recombinant viruses and to use animal models that best represent human infection. Using a wild-type virus strain (A11 and B05) from each HRSV subtype, a wild-type like recombinant (r) virus, rHRSV^{A11}, and recombinant viruses expressing fluorescent proteins, rHRSV^{A11}EGFP(5) and rHRSV^{B05}dTom(5), were generated. Characterization of rB05 viruses demonstrated that the differences in the

fluorescent protein expressed did not affect virus growth kinetics. To prepare for an experiment in cotton rats, recombinant HRSVs generated were used to infect cotton rat lung cells *in vitro*. With confirmation of infection of cotton rat lung cells by rHRSV, cotton rat co-infection experiment was planned for the recombinant A11 and B05 viruses and a microneutralization assay was developed for post-infection processing of the *in vivo* samples.

The BA genotype of HRSV B subtype is a strain of HRSV B subtype containing a 60 nucleotide duplication in the glycoprotein (G) gene. HRSV BA genotype was first isolated in 1998 and has quickly become the predominant genotype circulating globally. Although a role of immune evasion by the strains of BA genotype has been suggested to explain this phenomenon, few studies have supported this hypothesis. To compare the HRSV B subtype virus with and without the duplication, rB05 virus lacking the duplication, rHRSV^{B05}EGFP(5)GΔ60b, and containing an epitope tag within the duplication, rHRSV^{B05}EGFP(5)Gmycb, were generated. A serial passage experiment was set up using rHRSV^{B05}EGFP(5) and rHRSV^{B05}EGFP(5)GΔ60b to understand the mutations that accumulate in the G protein gene of each virus. This will be valuable in setting up a similar experiment in the presence of immune pressure to understand the advantage that is conferred to the virus containing the duplication. Expression of Gmyc was confirmed in rHRSV^{B05}EGFP(5)Gmyc infection, which validated that this virus can be used to study the HRSV^{B05} G protein and modifications in the duplicated region.

The HRSV large (L) protein is essential in HRSV transcription and replication, but is difficult to study due to lack of immunologic reagents and challenges with purification. Recombinant viruses expressing reporter and polymerase fusion proteins have been generated and used for studying various other viral polymerases. Expression plasmids for HRSV L protein containing a reporter protein in its variable region 2 have been published. However, the modification resulted in downregulation in the function of the protein and rHRSV expressing modified L protein have not yet been published. In this study, rHRSV^{B05}LVenus was generated to study the effects of modification of HRSV L protein variable region and the localization of HRSV L protein. LVenus protein in rHRSV^{B05}LVenus infected cells was visualized by confocal laser scanning microscopy and the expression levels were examined by immunoblotting. rHRSV^{B05}LVenus was compared to rHRSV^{B05}EGFP(5) with unmodified L protein to show that modification of HRSV L protein had no effect on virus replication. Viruses had equivalent growth kinetics and were equally sensitive to ribavirin, a known HRSV inhibitor.

The recombinant viruses generated in this study are valuable tools in answering questions that are difficult to pursue without clinically relevant recombinant viruses. Characterization of the rHRSVs demonstrated that these viruses will have many applications. In this study, viruses were characterized for

the basic growth kinetics, expression of proteins of interest, and assay development. With these validated tools, questions such as the cause of the epidemiological pattern observed for HRSV A and B subtypes, the role of host immune response in advantage conferred to HRSV BA genotype, and the effects of inhibitors to formation of HRSV polymerase complex can be addressed.

TABLE OF CONTENTS

LIST OF TABLES

LIST OF FIGURES

LIST OF ABBREVIATIONS

(-)RNA .....negative sense RNA

(+)RNA ..... positive sense RNA

A .....adenine

aa ..... amino acid

BA.....Buenos Aires genotype containing duplication in G protein

bp .....base pairs

BU ..... Boston University

c..... cellular

CD ..... conserved domain

COOH..... carboxy terminus

CPE ..... cytopathic effect

CR .....conserved region

CLSM .....confocal laser scanning microscopy

CT..... cytoplasmic tail

CX3CR1 ..... CX3C chemokine receptor 1

d.p.i..... days post-infection

DAPI .....4',6-diamidinmo-2-phenylindole

DC ..... dendritic cell

DC-SIGN ..... DC-specific intercellular adhesion molecule-3-grabbing non-integrin

ddH_2O ..... double distilled water

DPBS ..... Dulbecco's phosphate buffered saline

EBSS ..... Earle's balanced salt solution

EGFP ..... enhanced green fluorescent protein

ER ..... endoplasmic reticulum

F ..... HRSV fusion glycoprotein

FBS ..... fetal bovine serum

FDA ..... Food and Drug Administration

G (nucleotide) ..... guanine

G (protein) ..... HRSV attachment glycoprotein

GE ..... gene end

GS ..... gene start

GTP ..... guanosine triphosphate

HRSV ..... human respiratory syncytial virus

HSPG ..... heparin sulfate proteoglycans

I_1 ..... insert 1

I_2 ..... insert 2

I_A ..... insert A

I_B ..... insert B

ICAM ..... intercellular adhesion molecule

Ig ..... intergenic

IVIG ..... intravenous immunoglobulin

L ..... HRSV large protein

LB ..... lysogeny broth

Le ..... leader

L-SIGN ..... lymph node-specific ICAM-3 grabbing non-integrin

M ..... HRSV matrix protein

MEM ..... minimal essential medium

MLD ..... mucin-like domain

MOI ..... multiplicity of infection

MT ..... methyltransferase

MVA-T7 ..... modified vaccinia virus expressing T7 RNA polymerase

N ..... HRSV nucleoprotein

NEB ..... New England Biolabs

NH_2 ..... amino terminus

NNS ..... nonsegmented, negative sense

NS ..... HRSV nonstructural protein

nt ..... nucleotide

ORF ..... open reading frame

P ..... HRSV phosphoprotein

p ..... plasmid

p.f.u. ..... plaque forming units

PBS ..... phosphate buffered saline

P*n* ..... passage (*number)*

QUB ..... The Queen's University, Belfast

r ..... recombinant

RACE ..... rapid amplification of cDNA ends

RdRp ..... RNA dependent RNA polymerase

RNP ..... ribonucleoprotein

rpm ..... revolutions per minute

sc ..... subclone

SH ..... HRSV small hydrophobic protein

T ..... thymine

T75 flask ..... 75 cm^2 tissue culture flask

$TCID_{50}$ ..... tissue culture infectious dose 50

TM ..... transmembrane domain

Tr ..... trailer

U ..... uracil

VR ..... variable region

CHAPTER 1: INTRODUCTION

1.1 HRSV disease

Human respiratory syncytial virus (HRSV) is a nonsegmented, negative (-) sense (NNS) single stranded RNA virus in the *Pneumoviridae* family (Afonso et al., 2016; Collins et al., 2013). It infects airway epithelial cells and causes an acute respiratory tract infection with symptoms similar to common cold. Infection lasts about a week, although prolonged fatal lower respiratory tract infections can occur in children, immunocompromised individuals, and the elderly (Byington et al., 2015; Hall et al., 2013; Ramirez, 2008; Walsh and Falsey, 2012). HRSV is the leading cause of bronchiolitis and pneumonia in children under age of five in the United States and about 33.8 million children under age of five worldwide were infected in 2005 (Hall et al., 2009; Nair et al., 2010). Severe disease is caused by high viral load (DeVincenzo et al., 2005; Kim et al., 2015) and by a robust immune response to the infection which includes leukocyte infiltration and cytokine production (Farrag and Almajhdi, 2015; Johnson and Graham, 1999; Kim et al., 1969). Reinfections occur throughout life, because HRSV specific antibodies are only partially protective, may be subtype or strain specific, and do not last for a long time (Habibi et al., 2015; Hall et al., 1991; Openshaw et al., 2017).

1.2 HRSV therapeutics

HRSV was first isolated from a throat swab from an infant in 1957 (Chanock et al., 1957). After sixty years of research, there is no vaccine for HRSV (Neuzil, 2016) and there is still a need for safe and effective treatments (Graham, 2011; Simões et al., 2015). There is only one Food and Drug Administration (FDA) approved prophylaxis, palivizumab, and one therapeutic treatment, ribavirin, for HRSV infection and both are only used for individuals at high risk (Committee on Infectious Diseases, 1993; The IMpact RSV Study Group, 1998). Palivizumab is a FDA approved humanized monoclonal antibody against the HRSV fusion (F) glycoprotein used as an injectable prophylactic in high risk patients, such as preterm infants and children with chronic lung disease (American Academy of Pediatrics Committee on Infectious Diseases and American Academy of Pediatrics Bronchiolitis Guidelines Committee, 2014; Mochizuki et al., 2017; Subramanian et al., 1998). Ribavirin is a nucleoside analog used for various viral infections for its ability to inhibit virus RNA synthesis, mRNA capping, and depletion of intracellular pools of guanosine triphosphate (GTP) (De Clercq and Li, 2016). However, its exact mechanism of action in HRSV infected patients is unclear and because of the side effects associated with the high therapeutic dosage, it is only used in individuals at the highest risk, such as those who are immunocompromised (Conrad et al., 1987; Gross and Bryson, 2015; Smith et al., 1991). Development of vaccines and treatments has been difficult due to the high mutation rate of HRSV which can generate escape mutants (Power, 2008). In addition, the underlying

causes leading to HRSV reinfections in the presence of preexisting immunity is unclear (Habibi et al., 2015; Power, 2008; Schmidt et al., 2012, 2014; Zhao and Sullender, 2005; Zhu et al., 2011).

1.2 HRSV genes and replication

The HRSV genome is 15.2 kb in length and contains 10 genes which encode 11 proteins (Figure 1.1A) (Collins et al., 2013). The leader (Le) noncoding sequence at 3' terminus of the genome contains signals for HRSV genome replication, transcription and encapsidation by nucleo-(N) protein (Fearns et al., 2002; Mink et al., 1991). Trailer (Tr) noncoding sequence at 5' terminus of HRSV genome contains an antigenome promoter for initiation of replication of anti-sense viral genome (Fearns et al., 2002; Mink et al., 1991; Peeples and Collins, 2000). Each gene is preceded by a gene start (GS) sequence, which is essential for transcription initiation, and followed by a gene end (GE) sequence, which is essential for transcription termination and mRNA polyadenylation (Collins et al., 1986; Hardy et al., 1999; Kuo et al., 1997). Noncoding intergenic (Ig) sequences between one to 52 nucleotides (nt) long are present at each gene junction between the GE and GS sequences (Moudy et al., 2004). Nonstructural (NS) proteins are encoded by NS1 and NS2 genes and these interfere with host innate immune response (Spann et al., 2005; Swedan et al., 2011; Teng et al., 2000). The N protein encapsidates the (-) RNA genome and positive (+) RNA antigenome in a helical ribonucleoprotein (RNP). This prevents degradation of the RNA, prevents

its detection by host innate immune response, and assists in processive RNA replication by the large (L) protein (Fearns and Deval, 2016; Fearns et al., 1997; Noton and Fearns, 2011). Together with L protein and a cofactor phospho-(P) protein, RNP is the basic unit of infectivity (Fearns and Deval, 2016). P protein is a cofactor for HRSV RNA dependent RNA polymerase (RdRp) and mediates polymerase complex formation (Castagné et al., 2004; Dupuy et al., 1999). Matrix (M) protein is essential in assembly of virions and for maturation of the viral filaments (Ghildyal et al., 2006; Henderson et al., 2002; Marty et al., 2004; Mitra et al., 2012). Small hydrophobic (SH) protein is a transmembrane protein believed to act as a viroporin, forming an ion channel in host cell membranes (Carter et al., 2010; Gan et al., 2012). Attachment glyco-(G) protein contains an amino terminal cytoplasmic tail domain, transmembrane domain, and carboxy terminal ectodomain (Levine et al., 1987; McLellan et al., 2013) (section 1.5). The F glycoprotein binds host proteins at the surface of the cell and initiates fusion of virion with the plasma membrane (Krzyzaniak et al., 2013; McLellan et al., 2013). M2-1 and M2-2 proteins are encoded by the M2 gene and play regulatory roles in transcription and replication of the viral genome (Bermingham and Collins, 1999; Fearns and Collins, 1999). The L gene with a 68 nt overlap with M2 gene (Hardy et al., 1999) encodes the L protein which is the major component of the RdRp and is involved in mRNA capping and polyadenylation (Cox and Plemper, 2015; Fearns and Deval, 2016) (section 1.3).

Binding of virion to the cell plasma membrane and fusion is mediated by the G and F glycoproteins (McLellan et al., 2013). After fusion, the (-)RNP is released into the cytoplasm (Collins et al., 2013). HRSV genome is transcribed and replicated by the RdRp. A start-stop transcription process leads to the generation of a transcription gradient of HRSV mRNAs, in which genes at the 3' end of the genome are expressed at a higher level than those at the 5' end (Barik, 1992). The L protein initiates replication of (-)RNA at the 3' end of the genomoe to generate encapsidated (+)RNA, the antigenome. Genome replication at the trailer complement sequence of the antigenome and generates (-)RNA genome (Fearns et al., 2000). These newly replicated viral antigenome and genome are both encapsidated by N protein to form (+) and (-)RNPs. Viral proteins and (-)RNP are assembled into virions at the plasma membrane (Figure 1.1B). This process is mediated by the M protein (Bajorek et al., 2014; Meshram et al., 2016). Virions bud from the host cell at the plasma membrane at the apical surface in ciliated airway epithelial cells (Roberts et al., 1995) and *in vitro* cell-to-cell fusion in nonpolarized cells can be mediated by F glycoprotein to cause syncytia (Huong et al., 2016; Zhang et al., 2002).

1.3 HRSV L protein

HRSV L protein is a 250 kDa subunit of RdRp complex. The L and P proteins form a basic polymerase complex which is sufficient to initiate RNA

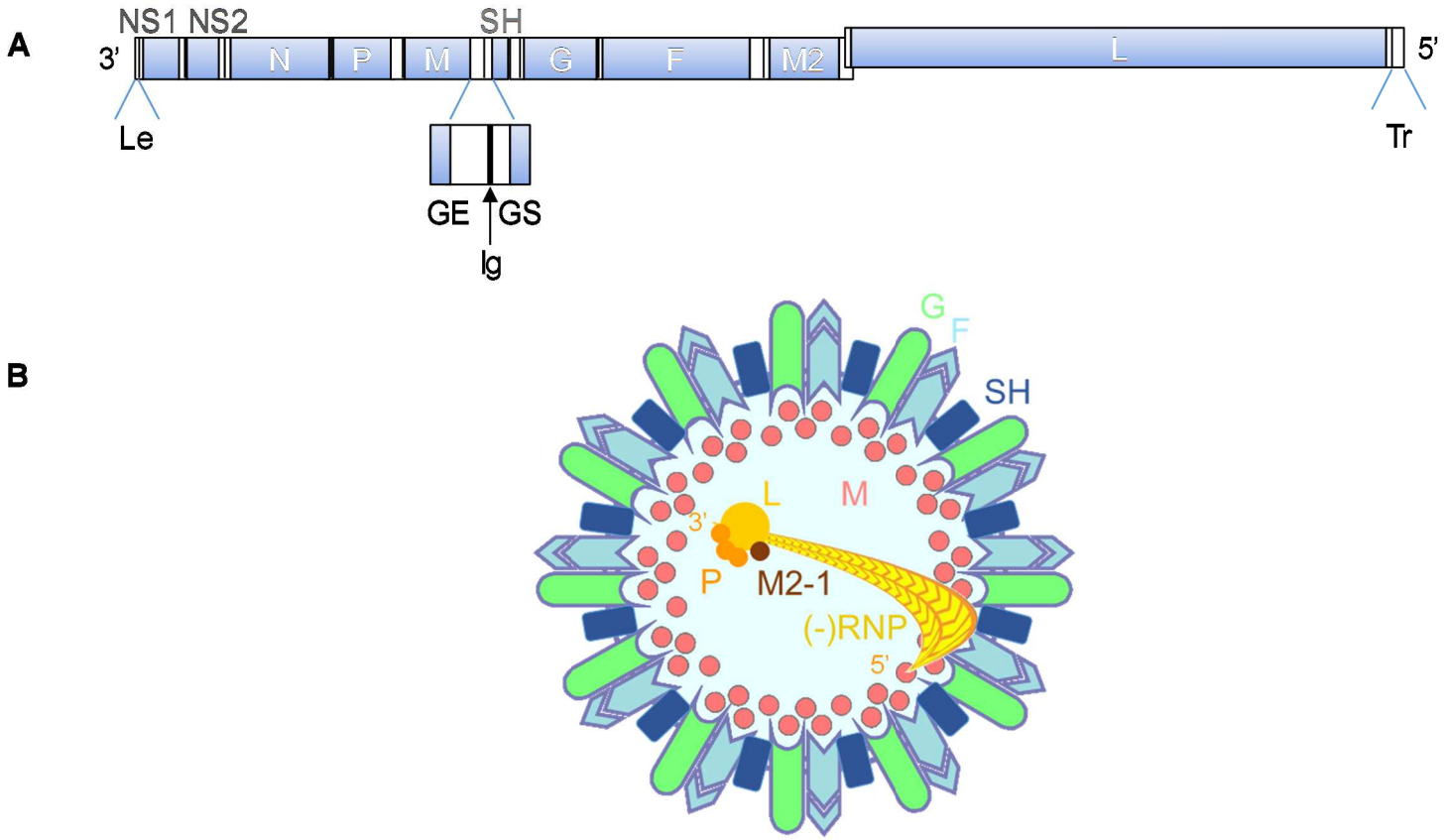

Figure 1.1: Schematic diagram of HRSV genome (Each component drawn in scale to length) and virion. (A) HRSV genome demonstrating the gene (blue) order. At each gene junction, left box represents gene end (GE) of the upstream gene, vertical line represents the intergenic (Ig) sequence, and the right box represents the gene start (GS) of the downstream gene (enlarged example shown for M-SH gene junction). The white boxes at 3' and 5' end of the genome represents leader (Le) and trailer (Tr). There is a 68 nucleotide overlap in the M2 and L protein gene. (B) HRSV virion is enveloped and contains three surface glycoproteins (SH, G, and F proteins). M protein, (-)RNP, RdRp complex (P, M2, and L proteins) are within the virion.

synthesis and transcription, but M2-1 is needed for efficient transcription elongation (Collins et al., 1996). Due to its large size and difficulties with purification of the protein, L protein atomic structure has not been determined. Functional domains (Poch et al., 1990; Svenda et al., 1997), such as the polymerase domain and the capping domain, of HRSV L protein were identified by mutagenesis studies (Fix et al., 2011; Liuzzi et al., 2005). Six highly conserved regions (CR) were identified (Figure 1.2) by comparing primary amino acid sequences of L proteins of NNS RNA viruses and these are separated by variable linker region (VR) (Poch et al., 1990; Svenda et al., 1997). CR I to III are essential for RdRp function and CR IV to VI are essential for the mRNA capping. The VR between CR V and CR VI, also known as the hinge region, in other NNS RNA viruses, tolerates insertion of epitopes, such as cellular (c)-myc, and fluorescent proteins, such as enhanced green fluorescent protein (EGFP) and mCherry. Insertion of open reading frames (ORF) of fluorescent proteins into the L gene attenuates the wild-type virus and reduce polymerase activity in morbilliviruses and rhabdoviruses (Brown et al., 2005; Duprex et al., 2002; Ruedas and Perrault, 2014). The resulting recombinant (r) viruses have been used for rational attenuation of the virus (Silin et al., 2007) and for visualizing the RdRp complex in infected cells (Brown et al., 2005; Hoenen et al., 2012; Ruedas and Perrault, 2009).

HRSV L protein has been difficult to study due to its large size, problems with purifying the protein, and lack of useful antibodies which bind the protein

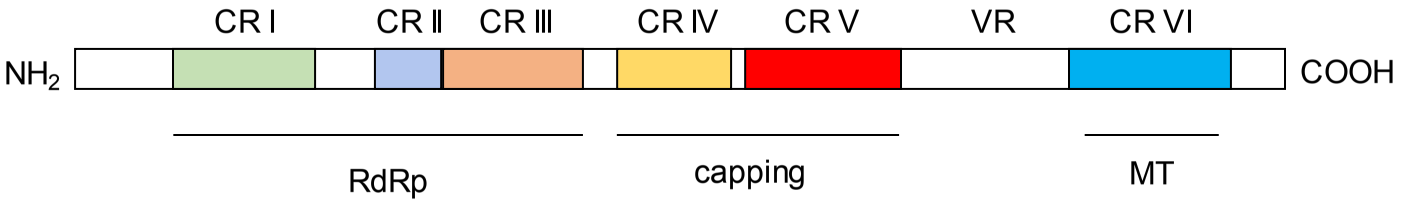

Figure 1.2: Schematic diagram of structural and functional domains of NNS virus L proteins. Conserved regions (CR) I through VI are represented in colored boxes and variable region (VR) is labeled. Functional domains are denoted with black lines; RdRp domain is responsible for transcription and replication of RNA. Capping domain is responsible for polyribonucleotidyltransferase activity in RNA capping. Methyltransferase (MT) domain is responsible for methylation of the cap. NH_2 denotes amino terminus and COOH denotes carboxy terminus of the protein.

unambiguously. One way to overcome these problems has been to generate reporter protein tagged L proteins. EGFP and mCherry sequences have been into the HRSV L expression plasmids at the sequence encoding VR. The resulting protein showed that there was downregulation of RdRp activity of modified L protein in minigenome replication transcription assay (Fix et al., 2011). As yet, an rHRSV modified L protein containing fluorescent protein has not been reported.

1.4 Antigenic subtypes of HRSV

In the 1980s, two antigenic groups of HRSV were described based on the binding of a panel of monoclonal antibodies generated from HRSV immunized mice to viruses (Anderson et al., 1985; Mufson et al., 1985). These two groups are known as antigenic subtypes A and B. Recently, it has become more common to determine HRSV subtype using subtype specific primers at the G protein ectodomain, since the majority of sequence differences between the subtypes are located there (Coggins et al., 1998; Peret et al., 1998; Sullender et al., 1993; Tan et al., 2013). The G proteins of HRSV A and B subtypes have approximately 50% amino acid sequence homology (Johnson et al., 1987). Multiple strains of each subtype co-circulate in a population, but during any given season, one subtype tends to predominate (Peret et al., 1998, 2000). Results from A and B subtype sequence and epidemiological differences suggest that lack of cross protection to a subtype circulating in previous season contributes to the predominance of

strains from the other subtype the following year (Schobel et al., 2016; White et al., 2005). Much of HRSV research is based on prototypic laboratory adapted strains of subtype A (Collins et al., 1995; Moore et al., 2009). HRSV strains of subtype A cause higher viral load in patients compared to subtype B (Kim et al., 2015). This may have an impact on disease severity which is greater in patients infected with HRSV subtype A strains (Devincenzo, 2004; DeVincenzo et al., 2005; Hall et al., 1990; Jafri et al., 2013; McConnochie et al., 1990; Zhou et al., 2015).

1.5 Intragenic duplication in HRSV G protein gene

The HRSV G protein is a type II transmembrane glycoprotein comprised of 289 to 327 amino acids depending on the strain. It has an amino terminal cytoplasmic tail (CT) domain followed by a transmembrane (TM) domain (McLellan et al., 2013) (Figure 1.3A). The carboxy terminal ectodomain of HRSV G protein contains a highly conserved domain (CD) flanked by two highly variable mucin-like domains (MLD) (Wertz et al., 1985, 1989). The CD contains a heparin binding domain and a disulfide bridge formed by four cysteine residues (Gorman et al., 1997). Like mucin, the two MLDs are rich in serine, threonine, and proline residues, heavily glycosylated, and contain unfolded secondary structures (Wertz et al., 1985). HRSV G protein is translated in the endoplasmic reticulum (ER) as 32 kDa unmodified protein. Glycosylation increases the molecular weight of mature G protein to 55 to 100 kDa in transformed cell lines and 180 kDa in primary airway epithelial cells (García-Beato et al., 1996; Kwilas et al., 2009). HRSV G protein

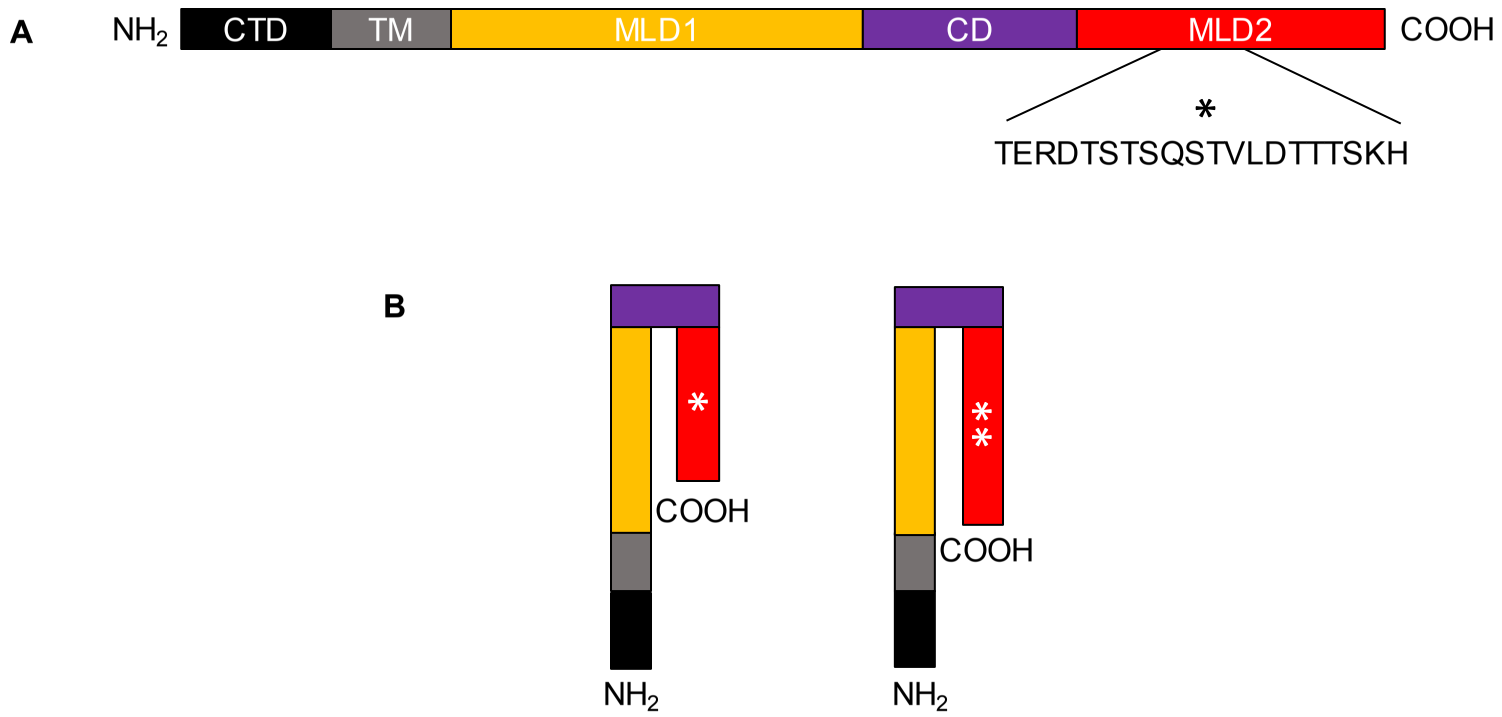

Figure 1.3: Schematic diagram of HRSV G protein structure of pre-BA and BA genotypes. (A) From amino terminus to carboxy terminus: cytoplasmic tail domain (CTD), transmembrane domain (TM), mucin like domain 1 (MLD1), conserved domain (CD), mucin like domain 2 (MLD2). The duplicated sequence in MLD2 is marked with an asterisk and the amino acid sequence is shown. (B) Structural representation of the G protein domains. The left shows a diagram of a G protein without the duplication in MLD2 (pre-BA genotype) and right shows a diagram of G protein of BA genotype containing the duplication.

exists in both membrane bound and secreted forms, where the secreted protein is translated from the second AUG of the mRNA which is located within the TM encoding sequence (Hendricks et al., 1987, 1988). HRSV G protein binds heparin sulfate proteoglycans (HSPG) (Feldman et al., 1999), CX3C chemokine receptor 1 (CX3CR1) (Johnson et al., 2015; Stobart et al., 2015), surfactant A (Hickling et al., 2000), annexin II (Malhotra et al., 2003), dendritic cell-specific intercellular adhesion molecule-3-grabbing non-integrin (DC-SIGN) (Johnson et al., 2012), and lymph node-specific ICAM-3 grabbing non-integrin (L-SIGN) (Johnson et al., 2012). Infection of cells that express HSPGs at a high level suggests that G protein is not essential for virus entry (Techaarpornkul et al., 2002). However, G protein seemed to play an important role *in vitro* in differentiated human airway epithelial cells and *in vivo* in mice (Teng et al., 2001).

HRSV G protein tolerates major changes in primary sequence. Typically, these are caused by changes in G protein gene such as frame-shift mutations (García-Barreno et al., 1990), generation of premature stop codons (Martínez et al., 1997), and adenosine to guanine hypermutations (Martínez et al., 1997). In late 1990's, isolates of HRSV B subtype containing a 60 nt duplication within the G protein gene were isolated (Trento et al., 2003). HRSV genotypes containing this duplication were named BA, because they were first isolated in Buenos Aires, Argentina. The original BA isolates contained a 60 nt duplication that resulted in 20 amino acid tandem repeat in MLD2 (Figure 1.3B). The BA genotype has spread

globally, replacing preexisting strains of HRSV B subtypes in less than a decade (Trento et al., 2010). Although, B subtype strains lacking the duplication have been isolated recently, the BA genotype is still the predominant HRSV B strain genotype circulating globally (Agoti et al., 2013). A 72 nt duplication, resulting in 36 amino acid repeat in MLD2, was found in HRSV A subtypes isolated in Ontario, Canada (Eshaghi et al., 2012). The genotype of HRSV A containing this duplication was named ON1, and like BA, it is becoming the predominant globally circulating HRSV A genotype. Phylogenetic analysis suggest that the duplications in MLD2 have been positively selected based on the high frequency of nonsynonymous mutations seen in various strains of HRSV (Botosso et al., 2009; Melero et al., 1997). The nonsynonymous mutations in several amino acid residues in MLD2 can revert supporting the hypothesis of role of immune pressure, which changes over time in populations, in providing selective pressure to the G protein (Botosso et al., 2009). However, there has only been one study which sought to elucidate the role of 60 nt duplication in HRSV BA genotype. An rHRSV was generated containing HRSV A subtype genome with consensus sequence from BA genotype G protein genes. There was a slight increase in HRSV BA G protein attachment to host cells compared to duplication deletion mutant and no effect on virus neutralization by F glycoprotein specific antibody (Hotard et al., 2015).

1.6 In vivo models of HRSV infection

HRSV only infects humans and there is no known animal reservoir (Sacco et al., 2015). Mice are the most commonly used animal model for HRSV infection, for approximately 77% of published HRSV animal studies (Sa et al., 2010). The BALB/c strain is more susceptible than most strains of mice, but infection still results in minimal clinical signs of disease and low virus yield compared to the input virus (Stark et al., 2002). In mice HRSV infection is restricted to in alveolar pneumocytes, in contrast to humans, where ciliated airway epithelial cells are the main cell type involved in HRSV infection (Moore et al., 2008). Cotton rats (*Sigmodon hispidus*) are increasingly used as a model in HRSV research, because virus replicates in the respiratory tract of cotton rat and the pathology more closely resembles human infection (Boukhvalova et al., 2009; Sacco et al., 2015). Similar to human infants, cotton rats receive maternal passive immunity to HRSV which last up to 18 months (Prince et al., 1983).

1.7 Reverse genetics of HRSV

Reverse genetics allows modification of viral genome and examination of the changes in phenotype (Bridgen, 2012; Conzelmann, 2004). Approaches to generate rHRSV were developed in 1995 and the prototype rHRSV^{A2}, a laboratory-adapted strain of rHRSV used in HRSV research, was recovered (Collins et al., 1995). Full-length antigenomic (+)RNA was transcribed from a plasmid containing HRSV cDNA downstream of a T7 RNA polymerase promoter and containing T7

RNA polymerase terminator at its 3' end. Sequences of hammerhead ribozyme were inserted downstream of HRSV Tr cDNA sequence to cleave the 5' of the antigenome when transcribed. This antigenomic plasmid and plasmids for N, P, M2-1, and L protein expression were transfected into cells expressing T7 RNA polymerase due to infection by modified vaccinia virus, MVA-T7. After 3 days, cytopathic effect (CPE) in transfected cells became visible and the recombinant virus were isolated (Bukreyev et al., 1996; Collins et al., 1995).

Recently modifications to the original protocol includes addition of hammerhead ribozyme sequence between the T7 promoter and HRSV Le cDNA sequence in the antigenomic plasmid and Hepatitis delta ribozyme sequence between the HRSV Tr cDNA sequence and the T7 terminator to generate authentic 3' and 5' of the (-)RNA genome (Been and Wickham, 1997; Bridgen, 2012; Hotard et al., 2012). A range of rHRSV have been generated to study clinically isolated strains of HRSV (Lemon et al., 2015), modifications in HRSV proteins (Corry et al., 2015; Hotard et al., 2015; Schmidt et al., 2014), and attenuated HRSV for possible vaccine candidates (Le Nouën et al., 2017; Rostad et al., 2016; Stobart et al., 2015). To visualize infected cells, fluorescent protein expressing reporter viruses have been generated by inserting an additional transcription unit (ATU) containing fluorescent protein gene into the viral genome (Figure 1.4) (Duprex et al., 1999; Lemon et al., 2015; Ludlow et al., 2012; Schmidt et al., 2011; Whitlow et al., 2006). These ATUs contain the coding region of the fluorescent protein gene with GS

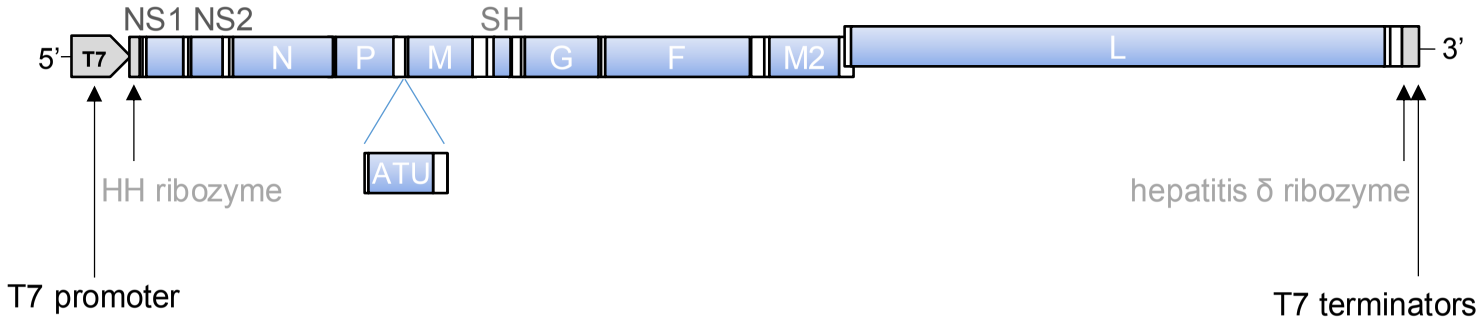

Figure 1.4: Schematic diagram of HRSV antigenomic plasmid used for recovery of rHRSV^{B05}. HRSV cDNA sequence is inserted into a plasmid under the control of T7 RNA polymerase promoter and contains a T7 RNA polymerase terminators at its 3' end. This plasmid also contains sequences that will be transcribed into hammerhead ribozyme (upstream of Le) and hepatitis δ ribozyme (downstream of Tr). Together these two ribozymes will generate the HRSV genome termini by post-transcriptional cleavages. EGFP gene sequence was inserted into an additional transcription unit (ATU) at position 5 to recover rHRSV^{B05} expressing EGFP.

and GE signals of viral genes (Hotard et al., 2012; Lemon et al., 2015; Schnell et al., 1996). A recombinant subgroup B HRSV, HRSV^{B05}EGFP(5), which closely resembles wild-type, was described which contains EGFP ATU at the position 5 of HRSV genome (Figure 1.4) (Lemon et al., 2015). With unmodified sequence as compared to the clinical isolate and low passage number, this virus would better represent clinical isolates than laboratory-adapted rHRSV (Kumaria et al., 2011; Villenave et al., 2011).

1.8 Aims and objectives

The goal of chapter 3 was to examine the differences between HRSV of each subtype and to prepare for a coinfection model. Therefore, rHRSV of A and B subtypes expressing two different fluorescent proteins were generated and characterized. In preparation for *in vivo* coinfection study in cotton rats, rHRSV were tested for infectivity in cotton rat cells and protocols were developed for testing the presence of neutralizing antibodies.

The goal of chapter 4 was to determine the role of the 60 nt duplication in G protein gene of HRSV BA genotype. Therefore, rHRSV^{B05} containing modifications in the MLD2 region were generated. These viruses were characterized for expression of the modified G protein and G protein gene stability over passages. We hypothesize that immune pressure confers replicative

advantage to the rHRSV BA genotype. The rHRSV characterization will lead to experiments that are more complex to test our hypothesis.

The goal of chapter 5 was to visualize HRSV L protein in infected cells for studying trafficking of L protein and its response to inhibitors. Therefore, rHRSV^{B05} containing Venus fluorescent protein gene in the VR of HRSV L protein was generated. The expression of modified L protein was characterized. When compared, L protein modified virus resembled rHRSV^{B05}EGFP(5), which does not contain modified L protein, for growth kinetics and its sensitivity to ribavirin.

CHAPTER 2: MATERIALS AND METHODS

2.1 Cells

2.1.1 Cell lines

HEp-2 cells (CCL-23), Vero cells (CCL-81), and cotton rat lung cells (PTA-3930) were purchased from ATCC.

2.1.2 Cell growth medium

All tissue culture media, solutions, and fetal bovine serum (FBS) were purchased from Thermo Fisher Scientific unless noted otherwise. HEp-2 cells were cultured in OptiMEM I Reduced Serum Medium supplemented with 3% (v/v) FBS. Vero cells were cultured in AdvancedMEM supplemented with 1% (v/v) GlutaMAX and 10% (v/v) FBS. Cotton rat lung cells were cultured in minimal essential medium (MEM) with Earle's Balanced Salt Solution (EBSS) with 2 mM L-glutamine (Hyclone) supplemented with 10% (v/v) FBS. Live cell imaging growth medium was prepare using Leibovitz medium without phenol red (Gibco) supplemented with 20% (v/v) FBS and 100 U/ml of penicillin/streptomycin. Prior to usage, all medium was preheated to 37ºC.

2.1.3 Cell biology equipment

DMIL LED microscope (Leica) was used for routine observing of cells for maintenance. For observing cells by phase and UV microscopy, Leica DMI3000B

inverted microscope was used. Images were obtained using LAS imaging software (Leica). For confocal laser scanning microscopy (CLSM), Leica SP5 II confocal microscope was used and images were obtained using LAS AF software (Leica).

For centrifugation of samples containing cells and cell debris, Allegra X-15R centrifuge (Beckman Coulter) was used unless noted otherwise. Vari Mix Platform Rocker (Thermo Fisher Scientific) was used for all protocols requiring rocking of samples for over 1 minute. Cells were maintained in Series 8000 WJ incubator (Thermo Fisher Scientific).

2.1.4 Cell maintenance

Cells were cultured 75cm^2 (T75) flasks (Fisher Scientific) for routine maintenance. Cells were split when they were 70% to 90% confluent to maintain optimal viability. Cells were checked for confluency using an inverted microscope (Leica), growth medium was removed, and cells were rinsed with Dulbecco's phosphate buffered saline (DPBS). The cells were treated with 0.25% (w/v) trypsin-EDTA with phenol red (1ml) and incubated at 37ºC with 5% (v/v) CO_2 for up to 10 minutes to allow cells to detach from the flask. Growth medium (section 2.1.2) was added to the flask, cells were suspended by pipetting, and 8% to 50% of the cells were added to a new T75 flask. Growth medium was added to the new flask up to volume of 15 ml. The cells were incubated at 37ºC in a 5% (v/v) CO_2 environment. When an exact cell count was needed, cells were counted manually using a

hemocytometer (Sigma-Aldrich) and the concentration of cells was determined by the following formula:

$$Concentration\ of\ cells\ = \frac{Number\ of\ cells \times 10{,}000}{Number\ of\ squares\ counted} \times dilution\ factor$$

All tissue culture plates were purchased from Fisher Scientific, unless noted otherwise. Following volumes of growth medium were used for various tissue culture plates: 6-well plates (2 ml), 12-well plates (1.5 ml), 24-well plates (1 ml), 96 well plates (0.2 ml).

2.2 Viruses

2.2.1 Virus strains

HRSV^{B05} has been previously described (Lemon et al., 2015). HRSV^{A11} was isolated from a clinical sample collected in Belfast, UK during the 2011 HRSV season.

2.2.2 Recovery of rHRSV

One day before transfection, 2 x 10^6 HEp-2 cells were added to wells in 6-well plates and incubated at 37ºC, 5% (v/v) CO_2 for up to 24 hours. Modified vaccinia virus expressing T7 RNA polymerase (MVA-T7) stock (15 µl) in OptiMEM (3 ml) was added to each well of cells at an multiplicity of infection (MOI) of approximately 0.5 in 6-well plates and incubated at 37ºC, 5% (v/v) CO_2 for 25

minutes. Infected cells were centrifuged at 1,200 revolutions per minute (rpm), 30ºC for 20 minutes. Inoculum was removed and each well of cells was transfected with pCG-HRSV-N (1.6 µg), pCG-HRSV-P (1.2 µg), pCG-HRSV-M2-1 (0.8 µg), pCG-HRSV-L (0.4 µg), and full-length HRSV antigenomic plasmid (1.6 µg) using Lipofectamine 2000 (Thermo Fisher Scientific) according to the manufacturer's specification. OptiMEM was added to the transfected cells which were incubated at 37ºC, 5% (v/v) CO_2 for at least 18 hours at which point OptiMEM was replaced with HEp-2 growth medium. Each day, growth medium was replaced. Cells were maintained at 37ºC, 5% (v/v) CO_2. When over 80% of the cells were infected as determined by CPE or expression of EGFP or Tomato fluorescent tags, cells were trypsinized and added to a T75 flask containing 2.5 x 10^5 HEp-2 cells and 15 ml HEp-2 growth medium. Cells were maintained at 37ºC, 5% (v/v) CO_2. Each day, growth medium was replaced. At the peak of infection, when there was over 80% infection and the monolayer disruption was observed, cells and supernatant were frozen at -80ºC. Samples were thawed at room temperature and centrifuged at 3,000 rpm for 5 minutes at 4ºC to pellet the cell debris. Cleared supernatant was collected and mixed with equal volume of 50% (w/v) sucrose to produce rHRSV P0 stock, which were stored at -80ºC.

2.2.3 Plaque pick method of recovering passage 1 virus

Virus was recovered by the method described in section 2.2.2, but when over 30 infected cells were found in a single plaque, these infected cells were

scraped and collected using a p200 micropipette and OptiMEM (30 µl). The plaque suspension was used to infect 10^5 HEp-2 cells in a 24-well plate for rHRSV passage 1 infection.

2.2.4 rHRSV passage

2 x 10^5 HEp-2 cells were put into 6 wells of 6-well plate with of growth medium (2 ml) and each well received varying volume of virus (0.4 µl, 3.2 µl, 4 µl, 12 µl, 40 µl) or left uninfected. Growth medium was replaced daily. When multiple wells have reached over 80% infectivity, the supernatant from the well with the least amount of input virus with over 80% infectivity was collected. This virus was used to repeat the 6 well dilution passage as described above until P2 or P3. These stocks were titered by tissue culture infectious dose 50 ($TCID_{50}$) assay (section 2.2.6) and used for the generation of stock virus.

2.2.5 rHRSV stock generation

In a T75 flask, 5 x 10^6 HEp-2 cells were infected with titered virus at an MOI of 0.02. Growth medium was replaced daily. When extensive cell monolayer disruption was observed, cells were scraped and collected with the supernatant. Supernatant was centrifuged at 3,000 rpm for 5 minutes at 4ºC and the cleared supernatant was mixed with equal volume of 50% (w/v) sucrose to produce the stock virus. Stock virus was stored at -80ºC.

2.2.6 rHRSV titer determination: $TCID_{50}$ assay

Virus was diluted 1:10 (10^{-1}) in OptiMEM (1 ml) in triplicate. Each of the triplicate 1:10 dilution was serially diluted (1:10) seven times. Each dilution (200 µl) was added to quadruplicate wells of 96-well plates, which contained 2 x 10^4 Vero cells in each well. Cells were observed by phase and UV microscopy 7 days post-infection (d.p.i.) and HRSV infected Vero cells were counted for each well. The titer in $TCID_{50}$/ml was calculated using Reed and Muench 50% endpoint method (Reed and Muench, 1938).

2.2.7 rHRSV titer determination: immunoplaque assay

For each virus to be titered, 12 wells were plated with 1.5 x 10^5 cells HEp-2 cells the day before the assay was set up. Virus was diluted 1:10 (10^{-1}) in OptiMEM (250 µl) and serial dilution (1:10) was carried out five times in duplicate. Growth medium from the HEp-2 cells were removed and 200 µl of each dilution (10^{-1} to 10^{-6}) was added. Infections were carried out in 37ºC 5% (v/v) CO_2 for an hour. Inoculum was removed and replaced with 0.8% (w/v) methylcellulose solution overlay (1 ml). 0.8% (w/v) methylcellulose solution was made using sterilized methylcellulose (Sigma-Aldrich) dissolved in HEp-2 growth medium (section 2.1.2). Cells were kept at 37ºC with 5% (v/v) CO_2 for at least 2 days and the plaques were observed by UV microscope. When the plaques became easily identifiable (3 to 4 d.p.i.), the overlay was removed and the cells were fixed with

80% (v/v) methanol (Sigma-Aldrich) at 4ºC for 30 minutes and removed. Methanol fixation step was repeated once more. Dried milk powder was mixed into DPBS to generate 5% (w/v) milk solution to be used as blocking buffer. Cells were rinsed with ddH_2O four times and blocking buffer (1 ml) was added. The plate of cells was rocked for 1 hour and cells were rinsed with ddH_2O three times. Each well of cells received 1:200 goat polyclonal anti-RSV antibody (200 µl) (Abcam) in blocking buffer and plate was incubated at room temperature with rocking for 1 hour. Antibody was removed and cells were rinsed 3 times with ddH_2O. Cells received 1:1000 rabbit anti-goat HRP (200 µl) (Abcam) in blocking buffer and incubated at room temperature for 1 hour with rocking. Antibody was removed and cells were rinsed three times with ddH_2O. Peroxidase substrate stock was made by dissolving 4-chloronaphthol (Pierce) in ethanol at 3 mg/ml concentration. Immediately before use, the stock solution was diluted 1:10 in with PBS (10 ml) and 3% (v/v) hydrogen peroxide (0.1 ml) (Sigma-Aldrich). Diluted peroxidase solution (200 µl) was added to the cells and incubated for 15 minutes on a rocker at room temperature. Reaction was stopped by rinsing the cells with ddH_2O. Plaque forming units (p.f.u.) per ml was calculated for each set of duplicate and averaged to determine the titer.

2.2.8 Multistep growth analysis of rHRSV

For each time point assayed, 3×10^5 HEp-2 cells were infected with rHRSV at an MOI of 0.2. The total volume of cell/virus mix was equal to 3 ml for each time point. Infected cells (1 ml) were added to 24-well plate in triplicate. At each time

point, 50% (w/v) sucrose was added to three wells of infected HEp-2 cells at an equal volume to the growth medium. The cells were stored at -80ºC. This process was repeated for triplicate wells at each time point. After the collection of last time point, all samples were defrosted and supernatants were used to set up $TCID_{50}$ assay in Vero cells (section 2.2.6).

2.2.9 Microneutralization assay of rHRSV^{B05}EGFP(5)

Six hours prior to infection, 2 x 10^4 Vero cells were plated in 3 wells of 96-well plate per dilutions of human intravenous immunoglobulin (IVIG) (CSL Behring) or human serum (Atlanta Biologicals) being tested. Cells were incubated at 37ºC, 5% (v/v) CO_2. Dilutions of IVIG or human serum were made in OptiMEM. A rHRSV^{B05}EGFP(5) stock was made to contain 300 p.f.u. of virus per 50 µl. IVIG/human serum dilution (50 µl) was added to 300 p.f.u. virus in triplicate. This mixture was incubated at 37ºC for 1 hour. The growth medium on Vero cells were removed and IVIG/human serum treated virus (100 µl) was added. Cells were incubated at 37ºC, 5% (v/v) CO_2 for 30 minutes before the plate was manually agitated. Cells were incubated for an additional 30 minutes and supernatant was removed. To each well of cells, 0.8% (w/v) carboxymethylcellulose growth medium solution (100 µl) was added. Cells were observed using UV microscopy at 1 d.p.i. Foci of infection were counted and p.f.u. per ml was calculated.

2.2.10 Immunoblot analysis

Transfected or infected cells were treated with 4x Laemmli buffer (Boston BioProducts), Halt protease inhibitor cocktail (Thermo Fisher Scientific), and EDTA (Thermo Fisher Scientific). DPBS was added to each well of cells and stored in -20ºC. After two freeze-thaw cycles to lyse the cells, samples were collected into microcentrifuge tubes and the DNA was sheared hydrodynamically. Laemmli buffer (5 µl) and NuPAGE reducing agent (1.5 µl) (Thermo Fisher Scientific) were added to an aliquot (10 µl) of the cell lysate and was heated at 70ºC for 10 minutes. Cell lysates were loaded onto NuPAGE 10% Bis-Tris protein gel (Thermo Fisher Scientific) and the proteins were separated by gel electrophoresis using NuPAGE MOPS SDS running buffer (Thermo Fisher Scientific). Proteins were transferred to a nitrocellulose blot using the iBlot dry blotting system (Thermo Fisher Scientific) at 20V for 7 minutes and 10 seconds. PBS-T solution was produced by supplementing 1x PBS with 0.1% (v/v) Tween-20. Blot was rinsed with PBS-T and blocked using 5% (w/v) milk solution for 18 hours at 4ºC. After the detection of protein of interest with specific primary and secondary antibodies (Appendix 2), blot was exposed and image was obtained by Odyssey CLx Imaging System (LI-COR) using LI-COR Image Studio software (LI-COR).

2.2.11 Indirect immunofluorescence

Growth medium was removed from the cells and cells were rinsed with DPBS. DPBS was removed and 10% (v/v) buffered formalin (Fisher Scientific) was

added to each well of cells at room temperature for 10 minutes to fix the cells. Fixative was removed and cells were rinsed with DPBS. Cells were permeabilized using 0.5% (v/v) Triton X-100 in DPBS (500 µl) and incubated at room temperature for 15 minutes. Cells were rinsed and blocked using Image-iT FX signal enhancer ready probes reagent (Molecular Probes) at room temperature for 30 minutes and the reagent was removed. Cells were rinsed and treated with BlockAid blocking solution (Molecular Probes) at room temperature for 30 minutes and the blocking solution was removed. Cells were rinsed with DPBS. Primary antibody dilution (Appendix 2) in BlockAid blocking solution was added to cells and was incubated at 37ºC for 1 hour. Cells were rinsed with DPBS and secondary antibody dilution (Appendix 2) in BlockAid blocking solution was added. Cells were rinsed with DPBS and coverslips on which cells were adhered were mounted onto glass slides (VWR) using VECTASHIELD HardSet Antifade Mounting Medium with 4',6-diamidinmo-2-phenylindole (DAPI) (Vector Laboratories).

2.2.12 Live cell imaging preparation for confocal laser scanning microscopy (CLSM)

Growth medium was removed from cells in 35 mm µ-Dish glass bottom plate (Ibidi) and primary antibody dilution (Appendix 2) in growth medium was added. Cells were incubated at room temperature for 10 minutes and the antibody mix was removed. Cells were rinsed with DPBS and live cell imaging growth medium

(1 ml) (section 2.1.2), 3 drops of NucBlue live probe (Molecular Probes), and 0.1mM of Trolox (Vector Laboratories) were added.

2.3. Molecular biology

2.3.1 Sequence analysis

Clone/primer design, computer clone generation, and polymerase chain reaction/restriction digestion plans were completed using SeqBuilder software (DNASTAR). Sequence alignment and analysis were completed using SeqMan Pro software (DNASTAR).

2.3.2 Molecular biology equipment

DNA concentration was measured using NanoDrop 1000 spectrophotometer (Thermo Fisher Scientific). Bacterial liquid culture incubation for DNA preparation was completed in MaxQ 5000 incubator shaker (Thermo Fisher Scientific). Mixing samples by vortex agitation was completed using Vortex-2 Genie (Scientific Industries). Samples in microcentrifuge tubes were centrifuged using benchtop centrifuge 5424 (Eppendorf) or benchtop centrifuge 5417C (Eppendorf). To heat and cool samples in microcentrifuge tubes, Thermomixer R heat block (Eppendorf) was used.

2.3.3 Restriction digestion

Restriction enzymes were purchased from New England Biolabs (NEB). Digestion contained at least 1 µg of the DNA to be cut, enzyme dependent buffers at 1x, at least 10 units of each enzyme for the reaction, and nuclease free water (Invitrogen). The reaction mix was incubated at the temperature provided by the manufacturer for 1 to 24 hours.

2.3.4 DNA gel electrophoresis

DNA fragments were separated by gel electrophoresis in 1% (w/v) agarose gel containing ethidium bromide (Sigma-Aldrich) for DNA fragments larger than 500 bp and 2% (w/v) agarose gel containing ethidium bromide for smaller DNA fragments. DNA fragments in gel were visualized and analyzed using MultiImage II gel imager (Alpha Innotech). DNA fragment in the gel was excised using gel extractor (USA Scientific) and the DNA was purified using QIAQuick gel extraction kit (QIAGEN) according to the manufacturer's specifications.

2.3.5 Polymerase chain reaction (PCR)

Primers (Appendix 1) were synthesized by Sigma-Aldrich. PCR reactions were carried out using Phusion high-fidelity DNA polymerase (NEB) and Phusion HF buffer. The reaction mix was set up according to the manufacturer's specifications and 10 to 100 ng of template DNA was used. C1000 thermocycler

(BioRad) was used to set up cycle conditions according to the Phusion enzyme manufacturer's specifications.

2.3.6 Gibson assembly

Gibson assembly reaction was set up according to the manufacturer's (NEB) specifications to allow assembly of multiple DNA fragments with 15 to 40 nt overlaps. The 20 µl reaction contained Gibson assembly master mix (10 µl), 0.01 to 0.25 pM of vector, 3 times the vector amount of each of the insert. The reaction was incubated at 50ºC for 1 hour.

2.3.7 Ligation

Gel purified vector was treated with Antarctic phosphatase according to the manufacturer's specification using 5 units of the enzyme. T4 DNA ligase (400 U) (NEB) was used to ligate vector and insert according to the manufacturer's specification. For all ligations, vector to insert ratio was maintained at 1:3. The reaction was incubated at room temperature for at least 2 hours or at 16ºC for 18 hours.

2.3.8 Bacterial transformation

DH5α chemically competent cells (NEB) stored in -20ºC were thawed out on ice and aliquoted into 8 – 15 µl aliquots. Ligation/Gibson assembly reaction (1 – 5 µl) or plasmid (10 – 50 ng) was added to the cells. Cells were left on ice for

30 minutes and incubated at 42ºC water bath for 90 seconds. Cells were incubated in ice for 5 minutes, SOC medium (100 µl) (NEB) was added, and incubated at 37ºC for at least 20 minutes. Cells were plated onto an LB agar (BD Biosciences) plate containing ampicillin (Sigma-Aldrich) or kanamycin (Sigma-Aldrich) as determined by the antibiotic resistance of the clone. The plates were incubated at 30ºC for at least 24 hours (plasmids containing HRSV G protein gene) or at 37ºC for at least 12 hours.

2.3.9 Small scale plasmid DNA preparation

A single colony from a transformation (section 2.3.8) was picked and added into LB broth (3 ml) (BD biosciences) containing 100 µg/ml ampicillin (Sigma-Aldrich) or 50 µg/ml kanamycin (Sigma Aldrich) depending on the antibiotic resistance of the clone. The liquid culture was incubated in a shaker at 37ºC for at least 18 hours for plasmids smaller than 12,000 bp in length and 30ºC for at least 24 hours for longer plasmids. Bacterial culture was removed from the shaker, culture (1.5 ml) was added to a microcentrifuge tube, centrifuged at 13,000 rpm for 1 minute in a benchtop centrifuge. Most of the supernatant was removed and the pellet was suspended in remaining supernatant. TENS solution was produced just prior to the plasmid preparation using 20 mM TRIS with 2 mM EDTA and 0.2 M NaOH with 1% (w/v) SDS. To the bacterial suspension, TENS solution (300 µl) and 3M sodium acetate (150 µl) (Sigma-Aldrich) were added and mixed using a vortex. Samples were centrifuged at 13,000 rpm for 5 minute in a benchtop

centrifuge and the supernatant was transferred to microcentrifuge tubes containing 4°C 100% ethanol and mixed by inversion of the tubes. The samples were centrifuged at 13,000 rpm for 5 minutes and 70% (v/v) ethanol (400 µl) was added. Samples were centrifuged at 13,000 rpm for 3 minutes and the DNA pellet was dried. Pellet was suspended in 10 mM TRIS buffer (Sigma-Aldrich) supplemented with 25 µg/ml RNAse A (Sigma-Aldrich).

2.3.10 Large scale plasmid preparation

A single colony from a transformation (section 2.3.8) or 0.5 ml of a small scale bacterial liquid culture (section 2.3.9) was added to LB broth (3 ml) containing 100 µg/ml ampicillin (Sigma-Aldrich) or 50 µg/ml kanamycin (Sigma-Aldrich) depending on the antibiotic resistance of the plasmid. This culture was incubated at 30ºC for plasmids longer than 12,000 bp in length or 37 ºC for at least 6 hours for plasmids shorter than 12,000 bp in length. Liquid culture was added to LB broth (200 to 400 ml) containing ampicillin (Sigma-Aldrich) or kanamycin (Sigma-Aldrich). This culture was incubated at 30ºC for 26 hours for plasmids longer than 12,000 bp in length or 37ºC for 16 hours for plasmids shorter than 12,000 bp in length in a shaker. Liquid culture was put into a bottle and centrifuged at 4,650 rpm in 4ºC for 30 minutes in Allegra X-15R centrifuge (Beckman Coulter) to pellet the bacterial cells. Plasmids were purified using HiSpeed Plasmid Maxi Kit (Qiagen) and the manufacturer's specification.

2.3.11 Sanger dideoxy sequencing

Primers (Sigma-Aldrich) used for sequencing are listed in Appendix 1. The Sanger dideoxy sequencing was completed by GENEWIZ (New Jersey, USA). Results were provided as electrochromatograms which were used to align with the expected sequence using SeqMan Pro software (section 2.3.1).

2.3.12 RNA isolation

To prepare the lysate for RNA isolation, virus stock (250 µl) was mixed with TRIzol LS (750 µl) (Thermo Fisher Scientific) by inversion of the tube and samples were incubated at room temperature for 5 minutes. Chloroform (200 µl) (Sigma-Aldrich) was added and samples were incubated at room temperature for 3 minutes. Sample were centrifuged at 13,000 rpm in 4ºC. The aqueous phase was removed and was used for RNA isolation according to the TRIzol LS manufacturer's specification.

2.3.13 DNase treatment of RNA samples

To remove DNA from purified RNA samples, TURBO DNase buffer (2 µl) (Life Technologies) and TURBO DNase (2 U) (Life Technologies) were added to RNA samples (20 µl). Samples were incubated at 37°C for 30 minutes and DNase inactivation reagent (2 µl) (Life Technologies) was added and incubated at room temperature for 5 minutes. Samples were centrifuged at 11,000 rpm for 1.5 minutes and supernatant was collected.

2.3.14 Sequencing HRSV full-length genome

RNA samples were used for cDNA synthesis using SuperScript III reverse transcriptase (Invitrogen) and HRSV forward primers (Table 2.1), which generated overlapping cDNA fragments. Reactions were set up according to the SuperScript III manufacturer's specification. Using the cDNAs generated from RNA or a full-length antigenomic plasmid, multiple overlapping amplicons of HRSV genome was generated by PCR (section 2.3.5). Phusion High-Fidelity PCR kit (New England Biolabs) and gene specific primers (Table 2.2) were used for amplification using the Phusion High-Fidelity PCR kit manufacturer's specifications. The presence of amplicons of expected sizes were verified by gel electrophoresis in 1% agarose gel and the DNA fragment was purified (section 2.3.4). The purified DNA fragments were used for Sanger dideoxy sequencing (section 2.3.11) usinG protein gene specific primers (Table 2.3)

2.3.15 Rapid amplification of cDNA ends (RACE) for rHRSV leader

Total RNA isolated from virus stock (section 2.3.12) was polyadenylated on the Le side using *E. coli* polyA polymerase (NEB). Reaction consisted of RNA (7.375 µl), 10x SuperScript III RT buffer (1.25 µl) (Invitrogen), 25 mM $MgCl_2$ (2.5 µl) (NEB), 10 mM ATP (0.625 µl) (Invitrogen), RNAseOUT (40 U) (NEB), and PolyA polymerase (1.25 U) (NEB). Reactions were incubated at 37ºC for 30 minutes and 65ºC for 20 minutes. Polyadenylated RNA was used as a template for cDNA

A

cDNA name	Primer
1	priHRSV-A10-42+
2	priHRSV-A10-5046+
3	priHRSV-A10-12600+

B

cDNA name	Primer
1	priHRSV-B05-33+
1b	priHRSV-B05-2554+
2	priHRSV-B05-5087+
3	priHRSV-B05-10127+

Table 2.1: Primers used to amplify HRSV^{A11} and HRSV^{B05} cDNA fragments from RNA samples. (A) Three cDNA fragments (1, 2, 3) were generated from HRSV^{A11} RNA samples and (B) four cDNA fragments (1, 1b, 2, 3) were generated from HRSV^{B05} RNA samples using the primers listed. The sequences corresponding to each primer are listed in Appendix 1.

Amplicon	cDNA template	Forward primer	Reverse primer
A	1	priHRSV-A11-42+	priHRSV-A10-2617-
B1*	1	priHRSV-A10-2558+	priHRSV-A10-3285-
B2*	1	priEGFP-685+	priHRSV-A10-5095-
B	1	priHRSV-A10-2558+	priHRSV-A10-5095-
C	2	priHRSV-A10-5046+	priHRSV-A10-7607-
D	2	priHRSV-A10-7577+	priHRSV-A10-10150-
E	3	priHRSV-A10-10076+	priHRSV-A10-10150-
F	3	priHRSV-A10-12600+	priHRSV-A10-15171-

Table 2.2A: Primers used to amplify overlapping amplicons from HRSV^{A11} cDNA. Multiple amplicons were generated using the cDNA template listed in Table 2.1a. * amplicons generated instead of amplicon B only if the genome contained EGFP ATU. The sequences corresponding to each primer are listed in Appendix 1.

Amplicon	cDNA template	Forward primer	Reverse primer
A	1	priHRSV-B05-33+	priHRSV-B05-2579-
B1a*	1b	priHRSV-B05-2554+	priXFP-698-
B1b*	1b	priXFP-22+	priHRSV-B05-3767-
B1	1	priHRSV-B05-2554+	priHRSV-B05-3767-
B2	1	priHRSV-B05-3698+	priHRSV-B05-5650-
C	2	priHRSV-B05-5087+	priHRSV-B05-7609-
D	2	priHRSV-B05-7574+	priHRSV-B05-10145-
E	3	priHRSV-B05-10127+	priHRSV-B05-12687-
F	3	priHRSV-B05-12609+	priHRSV-B05-15214-

Table 2.2B: Primers used to amplify overlapping amplicons from HRSV^{B05} cDNA. Multiple amplicons were generated using the cDNA template listed in Table 2.1b. * amplicons generated instead of amplicon B only if the genome contained EGFP or dTom ATU. The sequences corresponding to each primer are listed in Appendix 1.

Template amplicon	Primer
A	priHRSV-A10-278-
A	priHRSV-A10-103+
A	priHRSV-A10-913+
A	priHRSV-A10-1569+
A	priHRSV-A10-1946+
A	priHRSV-A10-2576+
B/B1	priHRSV-A10-2924-
B/B1	priHRSV-A10-2803+
B/B1	priHRSV-A10-3203+
B1	priEGFP-339+
B1	priEGFP-591+
B/B2	priHRSV-A10-3285-
B/B2	priHRSV-A10-3845+
B/B2	priHRSV-A10-4390+
C	priHRSV-A10-5786-
C	priHRSV-A10-5305+
C	priHRSV-A10-6231+

Template amplicon	Primer
C	priHRSV-A10-6707+
C	priHRSV-A10-7158+
D	priHRSV-A10-8281-
D	priHRSV-A10-8168+
D	priHRSV-A10-8617+
D	priHRSV-A10-9102+
D	priHRSV-A10-9781+
E	priHRSV-A10-10771-
E	priHRSV-A10-10401+
E	priHRSV-A10-11023+
E	priHRSV-A10-11648+
E	priHRSV-A10-12273+
F	priHRSV-A10-13291-
F	priHRSV-A10-12910+
F	priHRSV-A10-13537+
F	priHRSV-A10-14144+
F	priHRSV-A10-14854+

Table 2.3A: Primers used to sequence each amplicon of HRSV^{A11} cDNA. Amplicons generated using primers from Table 2.2A were used for Sanger sequencing reactions with primers listed. The sequences corresponding to each primer are listed in Appendix 1.

Template amplicon	Primer
A	priRSV-B-285R
A	priHRSV-B05-169+
A	priHRSV-B05-739+
A	priHRSV-B05-1262+
A	priHRSV-B05-1745+
A	priHRSV-B05-2225+
B1/B1a	priHRSV-B05-3084-
B1/B1a	priHRSV-B05-2916+
B1a	priXFP22+
B1b	priXFP698-
B1/B1b	priRSV-B-3267+
B2	priHRSV-B05-4109-
B2	priHRSV-B05-3936+
B2	priHRSV-B05-4524+
B2	priHRSV-B05-5014+
C	priHRSV-B05-5599-
C	priHRSV-B05-5555+

Template amplicon	Primer
C	priHRSV-B05-6251+
C	priHRSV-B05-6743+
C	priHRSV-B05-7435+
D	priHRSV-B05-7870-
D	priHRSV-B05-7788+
D	priHRSV-B05-8230+
D	priHRSV-B05-8734+
D	priHRSV-B05-9476+
E	priHRSV-B05-10581-
E	priHRSV-B05-10309+
E	priHRSV-B05-10747+
E	priHRSV-B05-11757+
E	priHRSV-B05-12230+
F	priHRSV-B05-13104-
F	priHRSV-B05-12815+
F	priHRSV-B05-13598+
F	priHRSV-B05-14176+
F	priHRSV-B05-14604+

Table 2.3B: Primers used to sequence each amplicon of HRSV^{B05} cDNA. Amplicons generated using primers from Table 2.2B were used for Sanger sequencing reactions with primers listed. The sequences corresponding to each primer are listed in Appendix 1.

synthesis using SuperScript III reverse transcriptase (Invitrogen) and priAdaptor-dT17 (Appendix 1) using manufacturer's specifications. cDNA was purified using QIAquick PCR purification kit (QIAGEN) according to the manufacturer's specifications. Purified cDNA was used as a template for amplification of the leader end of the genome using Phusion High Fidelity polymerase (NEB), priAdaptor, priAdaptor-dT17, and gene specific reverse primer. Amplicon was verified by gel electrophoresis and the DNA fragment was gel extracted (section 2.3.4). The purified amplicon was used for Sanger dideoxy sequencing using a gene specific reverse primer.

2.3.16 Rapid amplification of cDNA ends (RACE) for rHRSV trailer

RNA isolated from virus stock (section 2.3.12) was used as a template for cDNA synthesis using SuperScript III reverse transcriptase (Invitrogen) and gene specific forward primers using SuperScript III manufacturer's specifications. cDNA was purified using QIAquick PCR purification kit (QIAGEN) according to the manufacturer's specifications. Purified cDNA was tailed using terminal transferase (NEB) and dATP. The reaction contained cDNA (30 µl), 10X terminal transferase buffer (5 µl) (NEB), 2.5 mM $CoCl_2$ (5 µl) (NEB), 10 mM dATP (1 µl) (Invitrogen), terminal transferase (10 U) (NEB), and nuclease free water (8.5 µl). Reaction was carried out at 37ºC for 30 minutes and heat inactivated at 70ºC for 10 minutes. Tailed cDNA was purified using QIAquick purification kit (QIAGEN) according to the manufacturer's specifications. End of the HRSV cDNA was amplified by PCR

using purified tailed cDNA, Phusion High Fidelity polymerase (NEB), priAdaptor, priAdaptor-dT17, and a gene specific forward primer. The size of the amplicon was verified by gel electrophoresis and the DNA fragment was gel extracted (section 2.3.4). purified amplicon was used for Sanger dideoxy sequencing using a gene specific forward primer.

2.3.17 RNA ligation

RNA isolated from virus stock (section 2.3.12) was denatured at 90ºC for 3 minutes and was ligated using T4 RNA ligase I kit (NEB). Reaction containing denatured RNA (8 µl), 10x T4 RNA ligation reaction buffer (2 µl) (NEB), RNase inhibitor (0.5 µl) (NEB), 50% PEG 8000 (4 µl) (NEB), 10mM ATP (0.1 µl) (NEB), T4 RNA ligase (10 U) (NEB), and nuclease free water (5.4 µl) was incubated at 16ºC for 18 hours and was heat inactivated at 95ºC for 5 minutes. Ligated RNA was purified using RNeasy RNA purification kit (QIAGEN) according to the manufacturer's specifications.

CHAPTER 3: HRSV SUBTYPE DIFFERENCES

3.1 Generation of plasmids to express HRSV^{A11} proteins

To recover rHRSV, HEp-2 cells are transfected with a full-length antigenomic plasmid and plasmids which express the HRSV N, P, M2-1, and L proteins (section 1.8). Plasmids expressing HRSV^{A11} N, P, and M2-1 proteins were available. A plasmid expressing HRSV^{A11} L was constructed.

Plasmid encoding HRSV^{A11} L protein, pCG-HRSV^{A11}L, was generated using pscCG-HRSV^{A11}LΔBam (Figure 3.1A) provided by Dr. Sham Nambulli at Boston University (BU). The subclone (sc) was digested with *Bam* HI (section 2.3.3), the 5,434 bp DNA fragment was gel extracted (section 2.3.4), and dephosphorylated with Antarctic phosphatase to generate a linear vector (section 2.3.7). A plasmid, pHRSV^{A11}, containing the complete antigenome of HRSV^{A11} was generated by Dr. Ken Lemon at the Queen's University in Belfast (QUB). Large scale plasmid preparation of pHRSV^{A11} was optimized to yield higher concentration of plasmid by adjusting the *E. coli* culture growth conditions (section 2.3.10). pHRSV^{A11} (Figure 3.1B) was digested with *Bam* HI and the 5,529 bp DNA fragment was gel extracted to generate an insert. One to three ratio of vector and insert were ligated with T4 DNA ligase (section 2.3.7) and the ligation was used to transform *E. coli* DH5α competent cells (section 2.3.8). This ratio was kept constant for all following transformations from ligated product. The transformed cells were plated onto LB

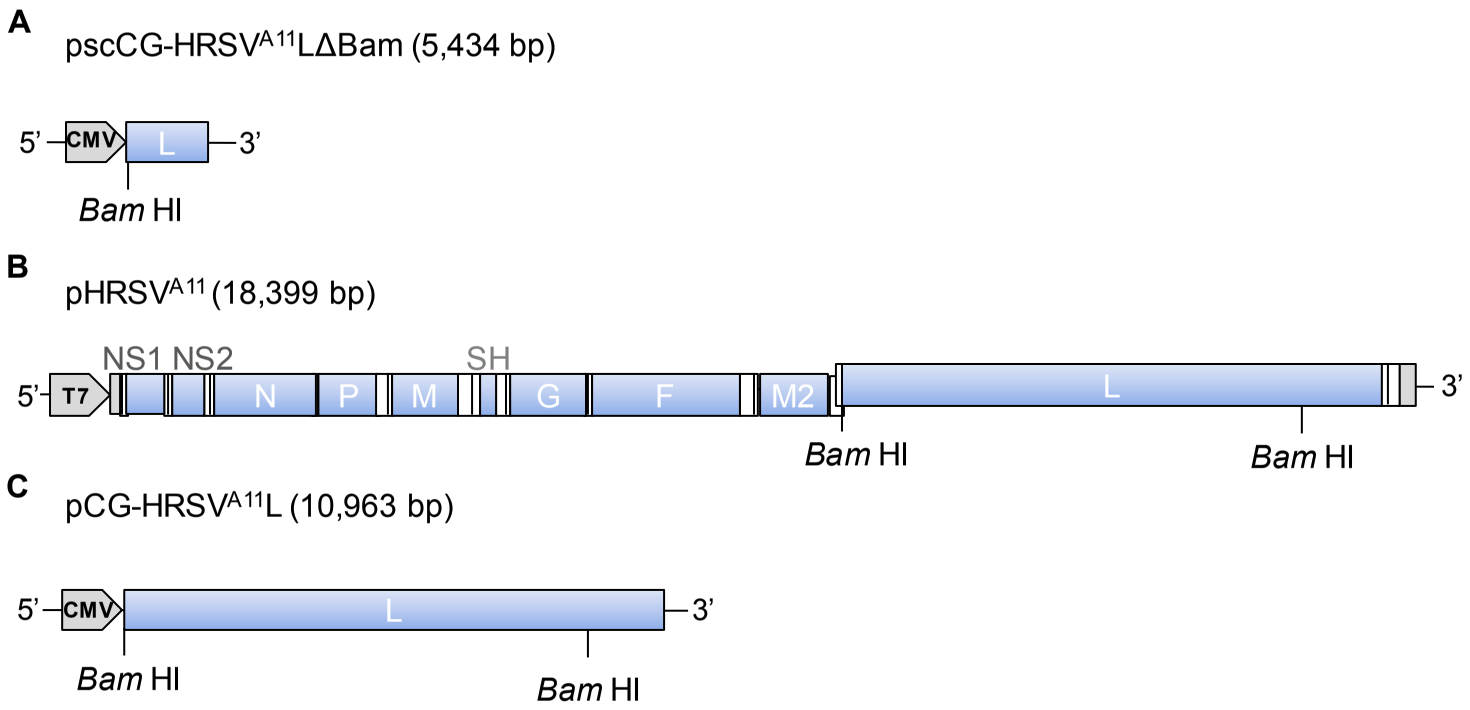

Figure 3.1: Schematic diagram of construction of pCG-HRSV^{A11}L. (A) pscCG-HRSV^{A11}LΔBam (Dr. Sham Nambulli, BU) was digested with *Bam* HI, the 5434 bp DNA fragment was gel extracted, and dephosphorylated with Antarctic phosphatase to generate a linear vector. (B) pHRSV^{A11} (Dr. Ken Lemon, QUB) was digested with *Bam* HI and a 5529 bp DNA fragment was gel extracted to generate insert. (C) A schematic diagram of pCG-HRSV^{A11}L and the *Bam* HI sites which were used for constructing the plasmid. The grey pentagons at the 5' end indicate either the CMV or T7 promoters used to control the expression of the plasmids.

agar plates containing ampicillin. Six colonies were amplified in liquid culture containing ampicillin and plasmids were isolated by small scale plasmid preparation (section 2.3.9). Plasmids were screened by diagnostic restriction digestion (section 2.3.3) to examine if ligation was successful and three plasmids were identified which contained the insert. Liquid culture containing ampicillin was inoculated with a single bacterial clone. This culture was used to isolate pCG-HRSV^{A11}-L by large scale plasmid preparation (section 2.3.10). Plasmid was digested using *Ava* I and *Nco* I restriction enzymes (section 2.3.3). Presence of 3217, 2822, 2465, 685, 632, 583, 444, and 115 bp DNA fragments was confirmed by gel electrophoresis (Figure 3.2A). Restriction digestion is presented as an example and will not be shown for other cloning results in this thesis. This plasmid was sequence verified by Sanger dideoxy sequencing using pripCG+, priRSV-A10-8489+, priRSV-A10-9102+, priRSV-A10-10401+, priRSV-A10-11023+, priRSV-A10-11648+, priRSV-A10-12273+, priRSV-A10-12910+, priRSV-A10-13537+, priRSV-A10-14144+, and, pripCG-b (Appendix 1) to check the sequence across the *Ava* I sites used for cloning (Figure 3.2B) and across the L gene (data not shown). Sequences were aligned with the pCG-HRSV^{A11}L (Figure 3.1C) computer clone using DNASTAR SeqMan Pro software and no spurious mutations were found.

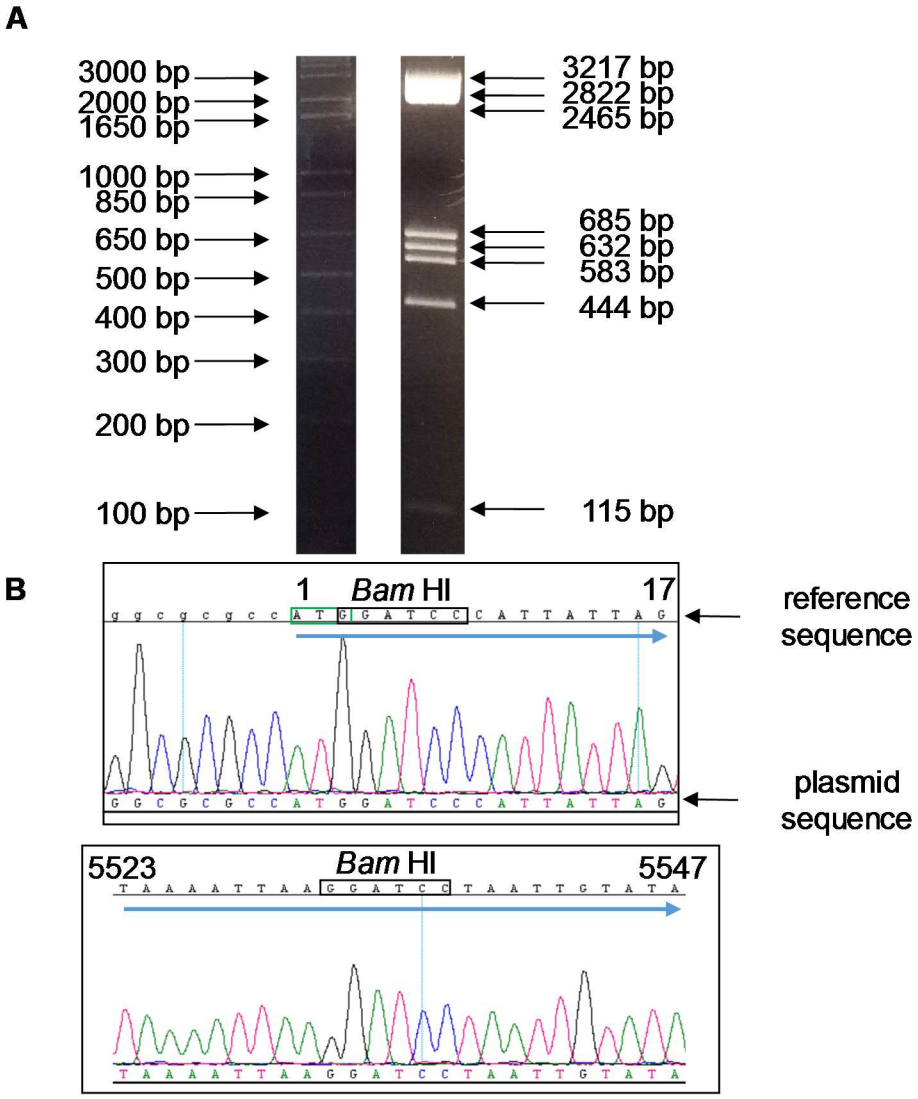

Figure 3.2: Molecular analysis of pCG-HRSV^{A11}L by diagnostic restriction digestion and sequence analysis. (A) Gel image of restriction digestion analysis of pCG-HRSV^{A11}L using *Ava* I and *Nco* I enzymes. (B) pCG-HRSV^{A11}L electrochromatogram data across the two *Bam* HI restriction sites (black boxes) used for the construction of the plasmid. The upper electrochromatogram shows pCG vector sequence (lower case letters) followed by HRSV^{A11} L protein gene (capital letters, blue arrow). The first *Bam*HI restriction site overlaps with the start codon (green box) in the HRSV^{A11} L protein gene. Lower electrochromatogram shows the second *Bam* HI restriction site begins at nucleotide 5532 of HRSV^{A11} L protein gene.

3.2 Generation of pHRSV^{A11}EGFP(5)

The sequence of HRSV^{A11} strain was obtained directly from a clinical sample (Dr. Ken Lemon, QUB). Amplicons were used to construct an antigenomic plasmid, pHRSV^{A11} (Dr. Ken Lemon, QUB). This plasmid was used to generate, pHRSV^{A11}EGFP(5), which would be used to recover an rHRSV^{A11} which expresses EGFP. This recombinant HRSV would allow comparisons to be made between the two subtypes of HRSV, using rHRSV^{B05}EGFP(5) (Lemon et al., 2015). Previous studies demonstrated there were significant difficulties cloning plasmids containing G protein genes of HRSV, therefore a subclone lacking these sequences, pscHRSV^{A11}EGFP(5)ACD, was constructed. pscHRSV^{A11}ACD lacks 3,157 bp fragment B encoding from the end of SH gene to beginning of L gene (Dr. Ken Lemon, QUB). This subclone was used to insert an ATU containing EGFP gene sequence to reduce the difficulties associated with growing full-length plasmids containing sequences of G protein gene. pscHRSV^{A11}ACD (Figure 3.3A) was digested with *Ava* I and the 12,666 bp DNA fragment was gel extracted (section 2.3.4) to produce the linear vector. pMK-HRSV^{A11}EGFP(5) (Figure 3.3B) was synthesized by GeneArt to contain the ATU containing EGFP gene sequence after P gene of HRSV^{A11} antigenome flanked by HRSV^{A11} sequences up to two *Ava* I sites. pMK-HRSV^{A11}EGFP(5) was digested with *Ava* I, the 2,556 bp DNA fragment was gel extracted (section 2.3.4), and dephosphorylated with Antarctic phosphatase to produce the insert. Vector and insert were ligated using T4 DNA

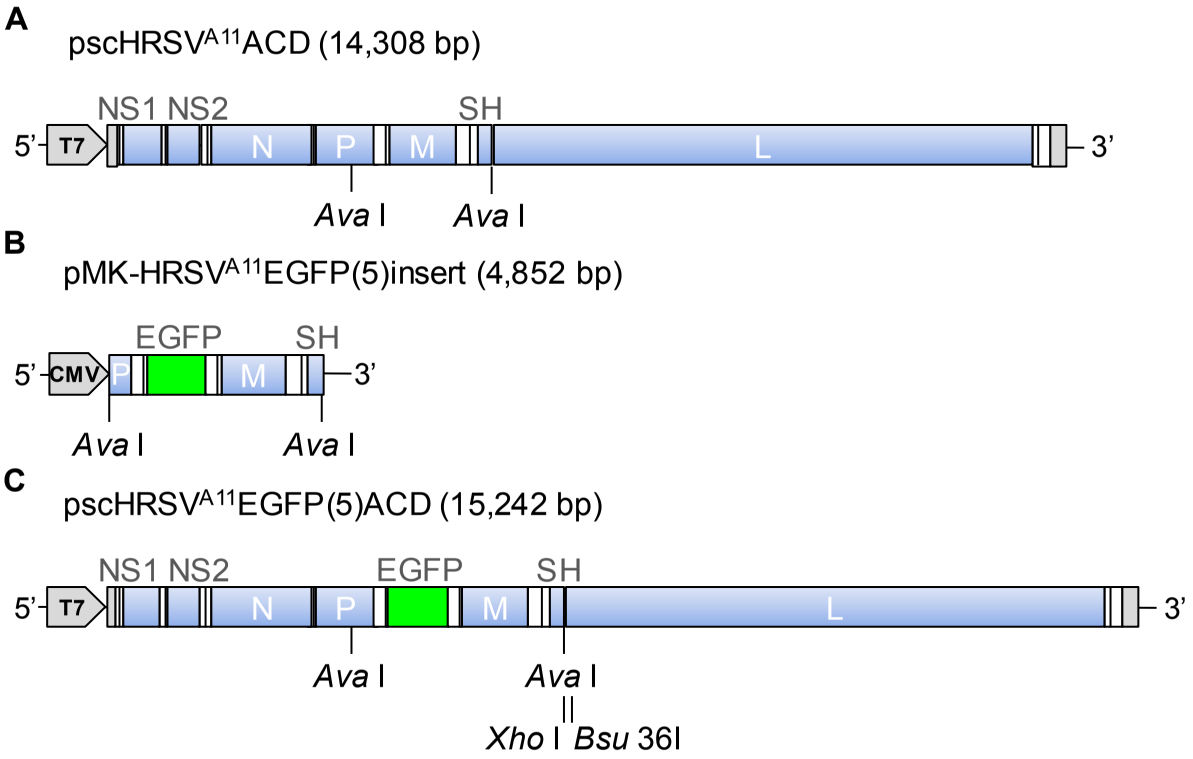

Figure 3.3: Schematic diagram of construction of pscHRSV^{A11}EGFP(5)ACD. (A) pscHRSV^{A11}ACD (Dr. Ken Lemon, QUB) was digested with *Ava* I to generate the linear vector. (B) pMK-HRSV^{A11}EGFP(5)insert was digested with *Ava* I to generate a 2556 bp insert containing the EGFP ATU. (C) A schematic diagram of pscHRSV^{A11}EGFP(5)ACD. *Ava* I sites were used to construct this plasmid. This plasmid was digested with *Xho* I and *Bsu* 36I to generate a linear vector for construction pHRSV^{A11}EGFP(5). The grey pentagons at the 5' end indicate either the CMV or T7 promoters used to control the expression of the plasmids.

ligase (section 2.3.7) and *E. coli* DH5α competent cells were transformed with one fourth of the ligation (section 2.3.8). The transformed cells were plated onto an LB agar plate containing ampicillin. Six colonies were amplified in liquid culture containing ampicillin and plasmids were isolated by small scale plasmid preparation (section 2.3.9). Plasmids were screened by diagnostic restriction digestion to examine if ligation was successful (section 2.3.3). Two plasmids shown to contain the insert were sequenced by Sanger dideoxy sequencing using priRSV-A10-2576+, priRSV-A-2637+, priRSV-A-3528+, priHRSV-A10-8639-, priRSV-A-9051-, priRSV-A-14854+, priHRSV-A10-15838+, and priEGFP591+ (Appendix 1) across the insert (section 2.3.11). Sequences were aligned with the computer clone of pscHRSV^{A11}EGFP(5)ACD (Figure 3.3C) using DNASTAR SeqMan Pro software and no spurious mutations were identified (Figure 3.4).

A full-length HRSV^{A11} antigenomic plasmid with an ATU encoding EGFP, pHRSV^{A11}EGFP(5), was constructed by inserting in HRSV^{A11} fragment B into pscHRSV^{A11}EGFP(5)ACD. pscHRSV^{A11}EGFP(5)ACD (Figure 3.3C) was digested with *Xho* I and *Bsu* 36I restriction enzymes (section 2.3.3) to generate 15,255 bp linear vector. pHRSV^{A11} (Figure 3.5A) was digested with *Xho* I and *Bsu* 36I to generate a 4,104 bp insert. Vector and insert were gel extracted (section 2.3.4), ligated using T4 DNA ligase (section 2.3.7), and ligation was used to transform *E. coli* DH5α competent cells (section 2.3.8). Transformed cells were plated onto LB agar plates containing ampicillin. Eleven colonies were amplified in liquid

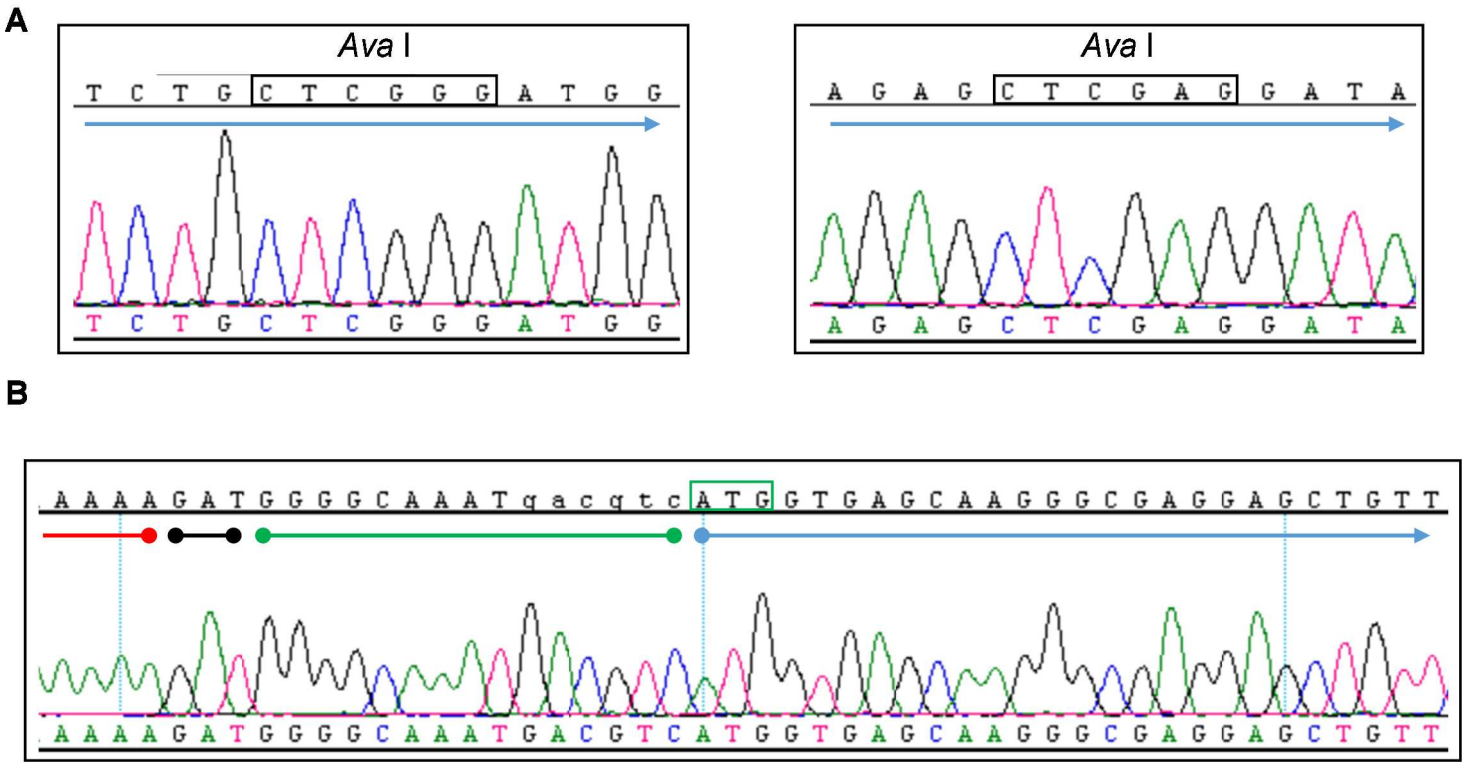

Figure 3.4: Sequence analysis of pscHRSV^{A11}EGFP(5)ACD across the restriction sites used for construction of each plasmid and EGFP ATU. (A) Sequence across the two *Ava* I sites in pscHRSV^{A11}EGFP(5)ACD as aligned with sequence of its computer clone. The *Ava* I sites, first one (left) located in the P gene (blue arrow) and the second (right) in the SH gene (blue arrow), are enclosed in black boxes. (B) Sequence across the junction between P GE to EGFP ATU that has been inserted. P GE (green line), intergenic sequence (black line), EGFP ATU GS (green line), and EGFP gene (blue arrow) are shown here. The start codon sequence for EGFP gene is marked with a green box.

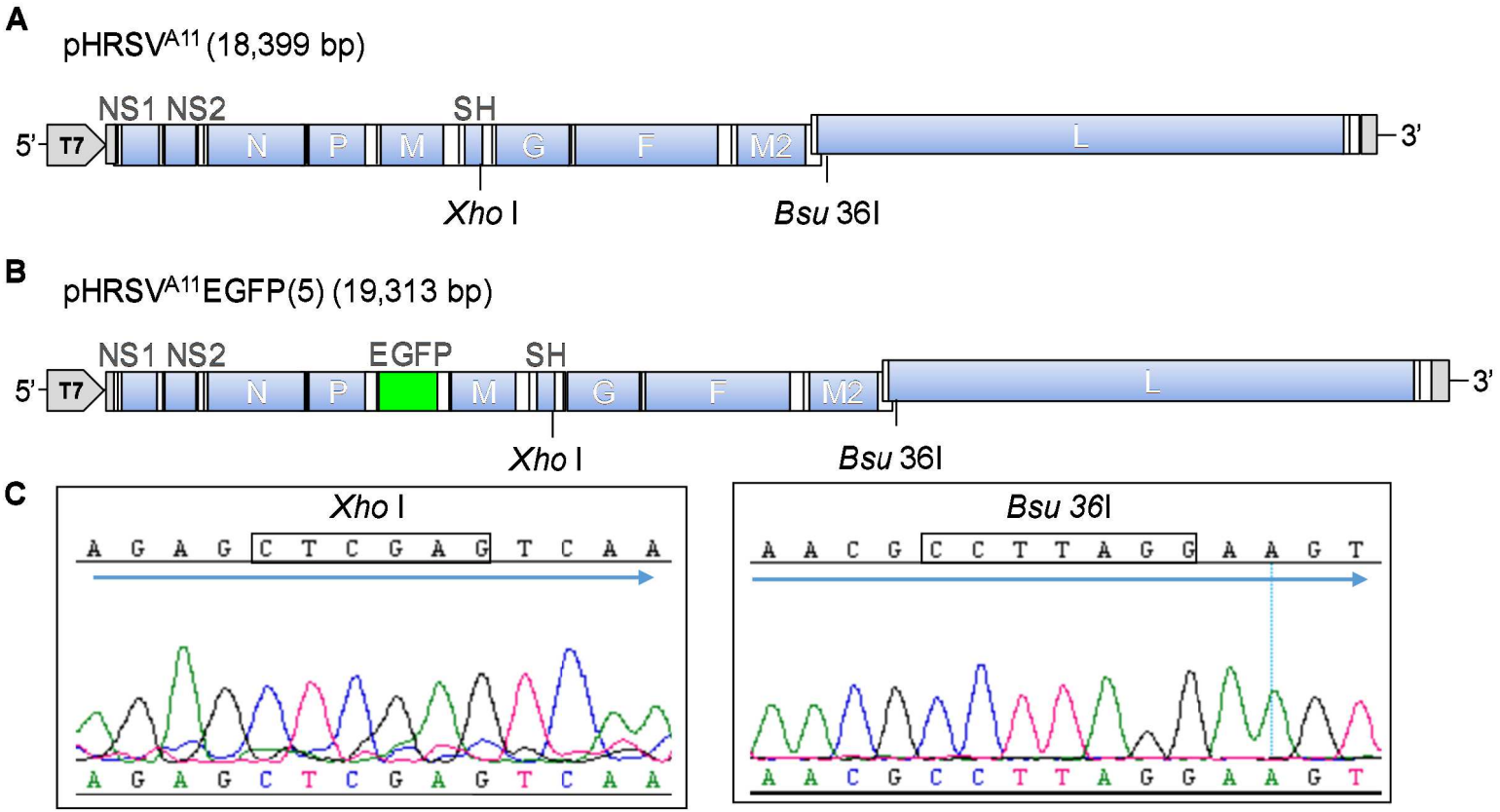

Figure 3.5: Schematic diagram of construction of pHRSV^{A11}EGFP(5) and sequence analysis across the two restriction sites used for cloning. (A) pHRSV^{A11} was digested with *Xho* I and *Bsu* 36I to generate a 4104 bp insert containing HRSV^{A11} genome from SH gene to L protein gene. (B) A schematic diagram of pHRSV^{A11}EGFP(5). Restriction sites used for construction of this plasmid are shown. (C) pHRSV^{A11}EGFP(5) electrochromatogram data across *Xho* I site (left) located in SH gene (blue arrow) and *Bsu* 36I site (right) located in L protein gene (blue arrow). Each restriction sites are enclosed in black boxes. The grey pentagons at the 5' end indicate the T7 promoter used to control the expression of the plasmids.

culture and plasmids were isolated by small scale plasmid preparation (section 2.3.9). Plasmids were examined by diagnostic restriction digestion and the presence of insert was confirmed in one plasmid. Sequence surrounding *Xho* I and *Bsu* 36I restriction sites in this plasmid was verified by Sanger dideoxy sequencing using priRSV-A10-4390+ and priHRSV-A10-8639- (Appendix 1) (section 2.3.11). Sequences were aligned with the computer clone of pHRSV^{A11}EGFP(5) using DNASTAR SeqMan Pro software and no spurious mutations were observed across the two restriction sites (data not shown). Sequence verified pHRSV^{A11}EGFP(5) (Figure 3.5B) plasmid was used to transform *E. coli* DH5α competent cells (section 2.3.8) and one colony was amplified in liquid culture containing ampicillin and plasmids were isolated by large scale plasmid preparation (section 2.3.9). Restriction digestions (section 2.3.3) were set up for the plasmid with *Ava* I, *Bam* HI, and *Spe* I enzymes and *Xho* I and *Bsu* 36I enzymes to confirm that the restriction sites are intact and that the sizes of DNA fragments generated were as expected. Sequence of the insert was verified by Sanger dideoxy sequencing (section 2.3.11) using priRSV-A10-4390+, priHRSV-A10-4426+, priRSV-A10-5305+, priRSV-A10-5761+, priHRSV-A10-5786-, priRSV-A10-6231+, and priHRSV-A10-8168+ (Appendix 1). Sequences were aligned with pHRSV^{A11}EGFP(5) computer clone using DNASTAR SeqMan Pro software and no spurious mutations were identified at the restriction sites (Figure 3.5C) or in HRSV G and F glycoprotein genes. This is important since mutations have occurred commonly when cloning plasmids

containing these HRSV sequences (data not shown). The remainder of the $HRSV^{A11}$ sequence was sequenced using the $HRSV^{A11}$ full-length genome sequencing protocol (section 2.3.14) and no spurious mutations were present.

3.3 Recovery of $rHRSV^{A11}$ and $rHRSV^{A11}EGFP(5)$

$rHRSV^{A11}$ had been previously recovered using $pHRSV^{A11}$ and plasmids expressing $HRSV^{B05}$ N, P, M2, and L proteins, but it has not been recovered using plasmids derived from $HRSV^{A11}$. The standard rHRSV rescue method (section 2.2.2) was used to recover $rHRSV^{A11}$ in HEp-2 cells and passaged four times (section 2.2.4, 2.2.5). The primary rescue and the subsequent passages were observed by phase-contrast microscopy. HRSV causes CPE *in vitro* generating multinucleated syncytia, which round up, and become non-adherent. It was difficult to identify CPE in HEp-2 cell monolayers in primary rescue, as cells became overgrown (Figure 3.6A). However, in subsequent passages when small volume of the supernatant from the primary rescue was serially passaged (section 2.2.4), it was straightforward to distinguish foci of infection (Figure 3.6B). $rHRSV^{A11}$ passage 4 (P4) stock (Figure 3.6C) was collected (section 2.2.5) and titer of $10^{6.86}$ $TCID_{50}$/ml was determined by $TCID_{50}$ assay in Vero cells (section 2.2.6). Vero cells were chosen because HRSV CPE in Vero cells were more identifiable compared to in HEp-2 cells and gave more accurate titer (data not shown).

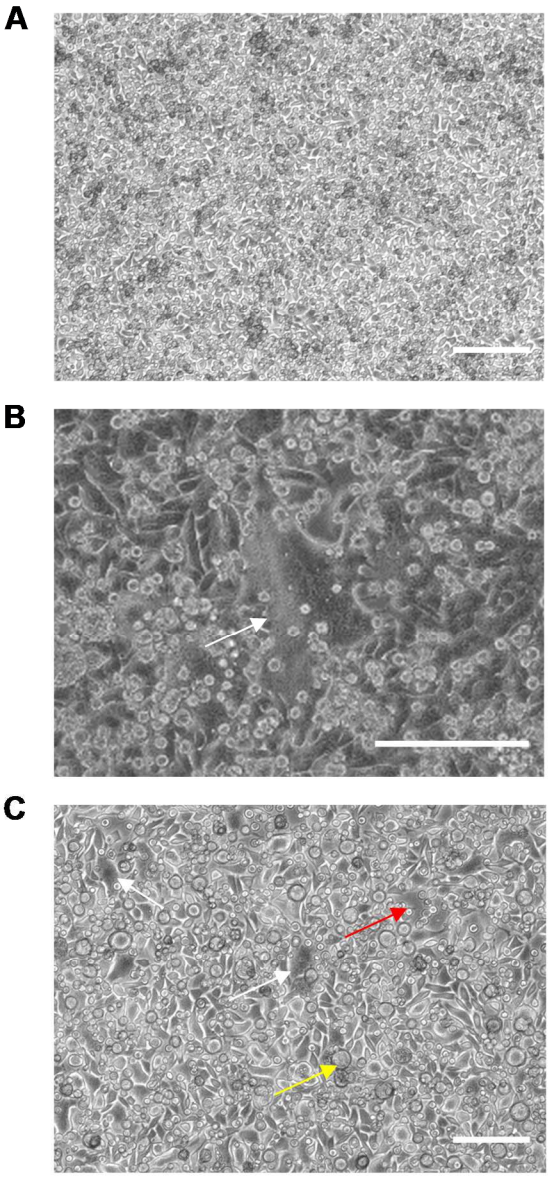

Figure 3.6: Photomicrographs of CPE caused by rHRSV^{A11}. (A) Overgrown monolayer of HEp-2 cells at 7 d.p.t. of rHRSV^{A11} primary rescue. Scale bar = 200 µm. (B) An example of CPE caused by HRSV infection. HEp-2 cells were infected with virus from rHRSV^{A11} primary rescue and this photomicrograph was obtained 7 d.p.i. Scale bar = 200 µm. (C) Various stages of CPE observed in HEp-2 cells infected with rHRSV^{A11} at P3. Photomicrograph was obtained 3 d.p.i. White arrows show multinucleated cells resulting from HRSV F glycoprotein mediated cell-to-cell fusion. Yellow arrow show rounded up large cell. Red arrow show a disruption in monolayer due to cells which became non-adherent. Scale bar = 200 µm.

Since rHRSV^{A11} recovery was successful, rHRSV^{A11}EGFP(5) was recovered with the same protocol (section 2.2.2). Expression of EGFP was observed to identify infected cells. After primary rescue (Figure 3.7A) in which all transfected wells contained virus, this virus was passaged four times to produce the stock virus for experiments (Figure 3.7B). The titer of stock virus was determined to be $10^{7.26}$ $TCID_{50}$/ml in Vero cells.

RNA was isolated (section 2.3.12) from stocks of rHRSV^{A11} and rHRSV^{A11}EGFP(5). Virus specific RNA were reverse transcribed using gene specific primers (Table 2.1) to generate cDNA. From the viral cDNA, amplicons were generated to overlap across the 15 kb full-length genome, which was sequenced to check for any spurious mutations in the viral genome (section 2.3.14). Rapid amplification of cDNA ends (RACE) protocol (section 2.3.15 and 2.3.16) was used for amplifying the termini of the genome which was sequenced using priRSV-A10-278- and priHRSV-A11-14918+. Sequences obtained by Sanger dideoxy sequencing (section 2.3.11) were aligned to rHRSV^{A11} or rHRSV^{A11}EGFP(5) sequences using DNASTAR SeqMan Pro software to identify any spurious mutations. In rHRSV^{A11} stock P4, there was a heterogenic population of sequences found at the first nucleotide of the viral genome. The expected adenine (A) was present, but approximately 30% of the population had a uracil (U) (shown as thymine (T)) at this position (Figure 3.8A). Another heterogeneous sequence was found at nucleotide 3307 of rHRSV^{A11} genome and approximately

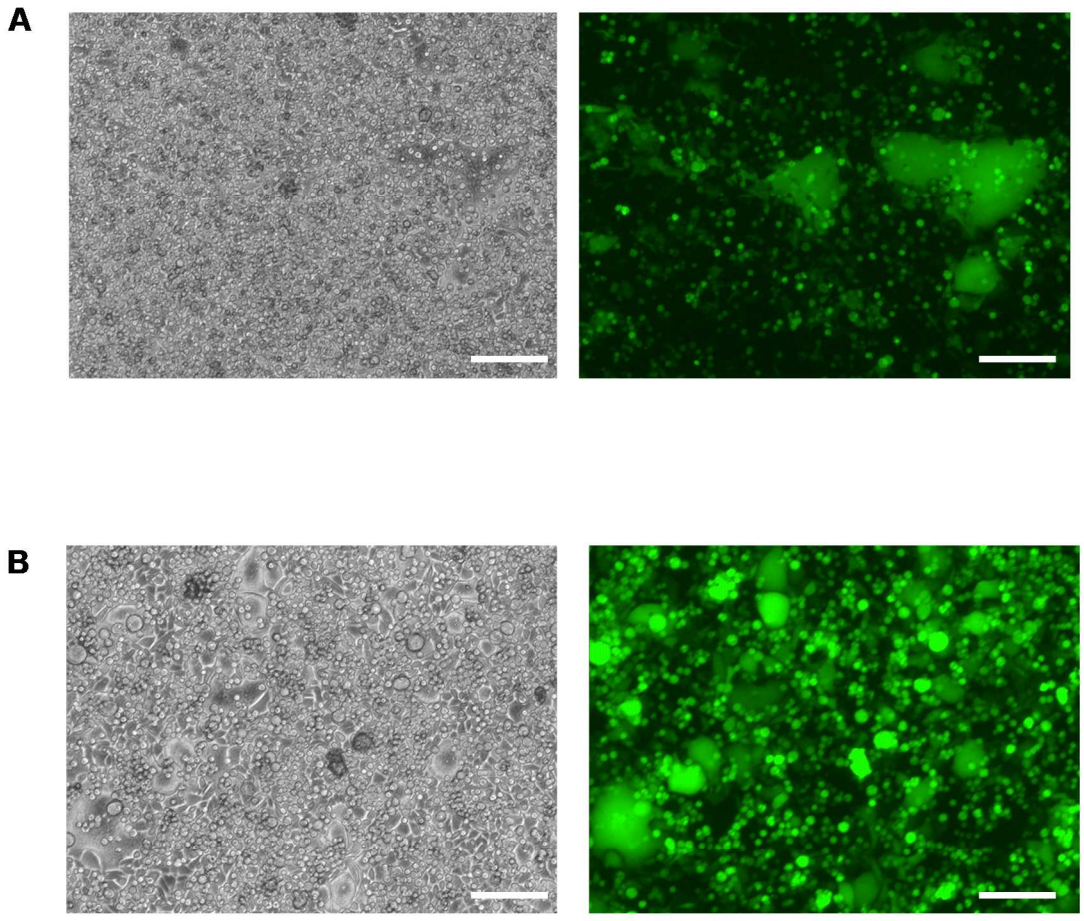

Figure 3.7: Photomicrographs of rHRSV^{A11}EGFP(5) primary rescue and passage 4 infection. (A) Primary rescue of rHRSV^{A11}EGFP(5) in HEp-2 cells. Photomicrographs were obtained 7 days after well expansion when the supernatant was collected for P0 stock. (B) HEp-2 cells were infected with rHRSV^{A11}EGFP(5) P3 and photomicrographs were obtained 4 d.p.i. The supernatant from this infection was used to generate rHRSV^{A11}EGFP(5) P4 stock. Scale bar = 200 µm.

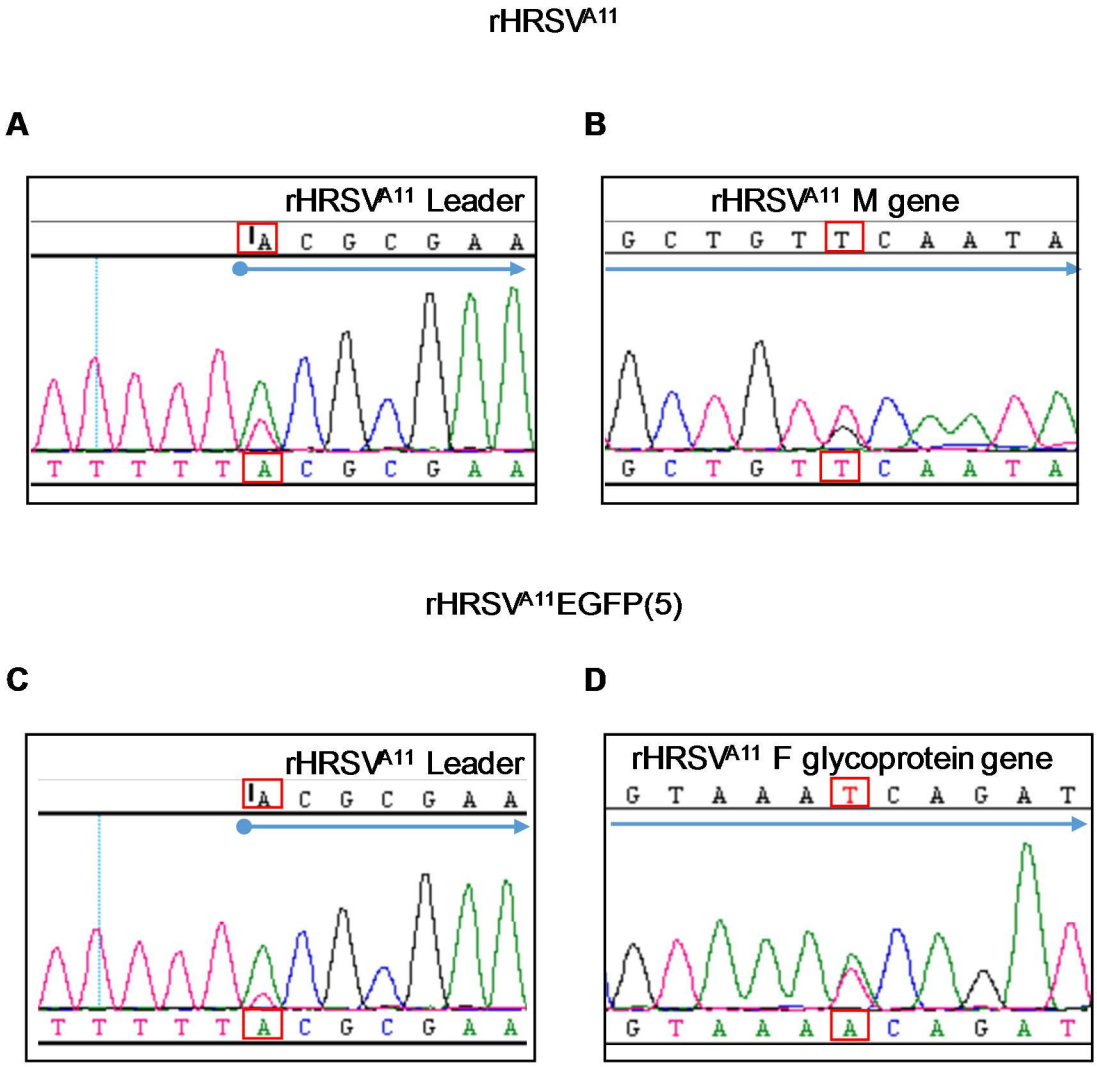

Figure 3.8: Sequence analysis for rHRSV^{A11} and rHRSV^{A11}EGFP(5). Sequences of rHRSV^{A11} cDNA and rHRSV^{A11}EGFP(5) cDNA were aligned with corresponding computer clone using DNAStar SeqMan Pro software. (A) Approximately 30% of the rHRSV^{A11} population had A1U nucleotide change in the leader region. (B) Approximately 30% of the rHRSV^{A11} population had U3307G nucleotide change in M gene which did not affect the amino acid sequence. (C) Less than 20% of the sequenced rHRSV^{A11}EGFP(5) population had A1U nucleotide change in the leader region. (D) Approximately 50% of the sequenced rHRSV^{A11}EGFP(5) population had U7176A nucleotide change in F glycoprotein gene which caused S509T mutation in F glycoprotein.

30% of the population had U to guanine (G) change at this position (Figure 3.8B). This was located in the M protein gene but did not change the amino. Two heterogeneous nucleotides were also present in rHRSV^{A11}EGFP(5) stock P4. One was located at first nucleotide of the viral genome where there was less than 25% of the population with A to U change (Figure 3.8C). Finally, there was also a U to A change at nucleotide 7176 (T in the cDNA sequence) in approximately 50% population (Figure 3.8D). This would cause S509T amino acid change in the F glycoprotein. This rHRSV^{A11}EGFP(5) stocks was used for following preliminary experiments.

3.4 Generation of pHRSV^{B05}dTom(5)

Generating two rHRSV expressing different fluorescent proteins would allow comparisons to be made in coinfection models, *in vitro* and *in vivo.* pHRSV^{B05}dTom(5) was generated to allow recovery of a rHRSV^{B05} that expresses dTom, which can be used in coinfection model with rHRSV^{A11}EGFP(5). pCG-dTom239 (Figure 3.9A) was generated by Dr. Linda Rennick (BU) to express dTom with an addition of five amino acid linker consisting of glycines and serines (GSGSG) at its terminus to adjust the protein to the length of EGFP (239 amino acids). dTom239 sequence was amplified from pCG-dTom239 by PCR (section 2.3.5) using pridTom25+BssHII, which contains a *Bss* HII site upstream of dTom sequence, and pridTom240+PacI, which contains a *Pac* I site downstream of dTom sequence (Appendix 1). The 750 bp amplicon was purified by gel extraction

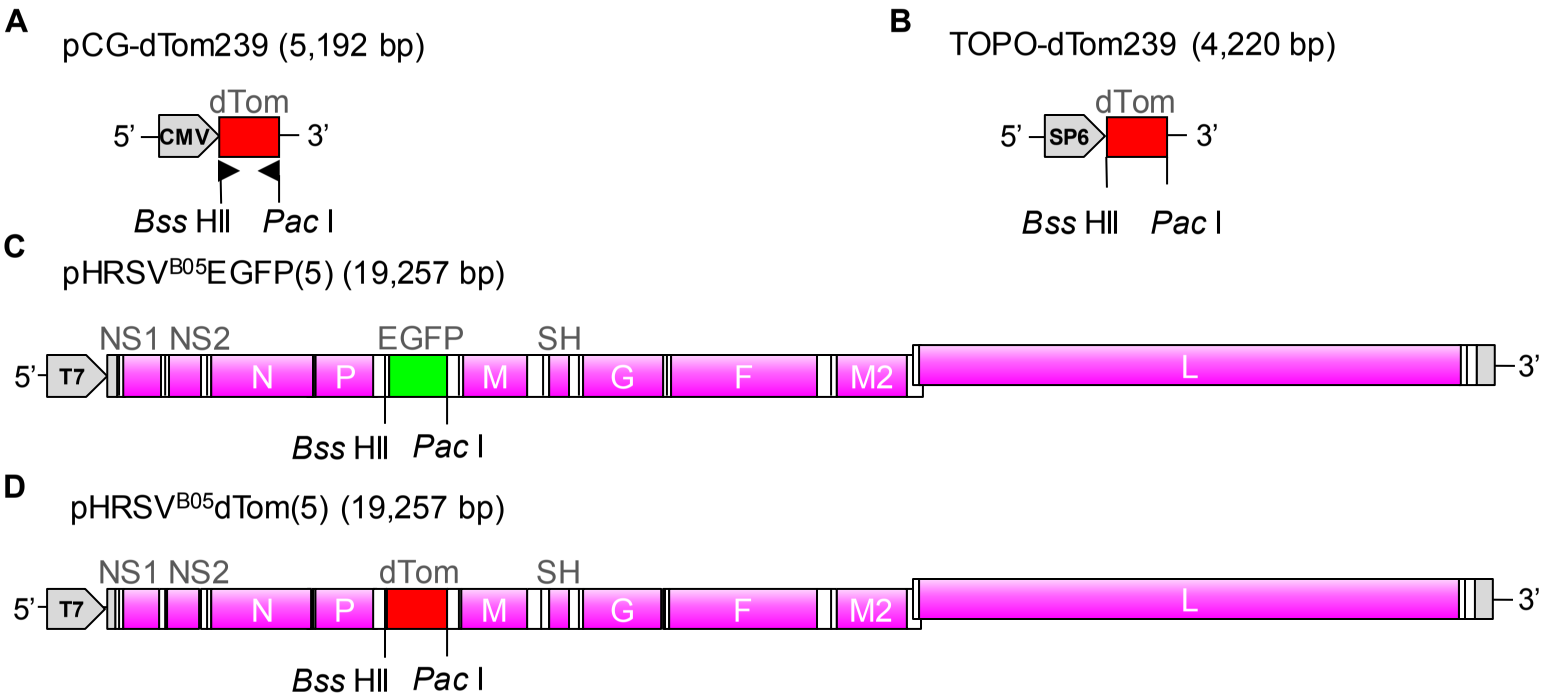

Figure 3.9: Schematic diagram of construction of pHRSV^{B05}dTom(5). (A) Two primers (►◄) were used to amplify dTom239 ORF by PCR from pCG-dTom239 and add two restriction sites. This amplicon was inserted into a TOPO clone. (B) TOPO-dTom239 was digested with *Bss* HII and *Pac* I sequentially to generate a 733 bp insert containing dTom239 ORF. (C) pHRSV^{B05}EGFP(5) was digested with *Bss* HII and *Pac* I and dephosphorylated to generate a 18,524 bp linear vector. (C) A schematic diagram of pHRSV^{B05}dTom(5). The *Bss* HII and *Pac* I restriction sites used for construction of this plasmid are shown. The grey pentagons at the 5' end indicate either the CMV, SP6, or T7 promoters used to control the expression of the plasmids.

(section 2.3.4) (Appendix 1). The 750 bp amplicon was purified by gel extraction (section 2.3.4) and cloned into a TOPO vector using ZeroBlunt TOPO kit. One third of TOPO reaction was used to transform *E. coli* DH5α competent cells (section 2.3.8) which was plated onto LB agar plates containing kanamycin. One colony was amplified in liquid culture containing ampicillin and plasmid was isolated by small scale plasmid preparation. Restriction digestion (section 2.3.3) with *Eco* RI restriction enzyme confirmed that the insert was present. TOPO-dTom239 (Figure 3.9B) was digested with *Pac* I and *Bss* HII sequentially and the 733 bp DNA fragment was gel extracted (section 2.3.4) to generate the insert. Linear vector was generated by sequentially digesting pHRSV^{B05}EGFP(5) (Figure 3.9C) with *Pac* I and *Bss* HII, gel extracting (section 2.3.4) the 18,524 bp DNA fragment, and dephosphorylating it with Antarctic phosphatase. Vector and insert were ligated using T4 DNA ligase (section 2.3.7) and *E. coli* DH5α competent cells were transformed with the ligation (section 2.3.8). Transformed cells were plated onto LB agar plates containing ampicillin. Twelve colonies were amplified in liquid culture which was used to isolate plasmids by small scale plasmid preparation. Three plasmids contained the insert when examined by diagnostic restriction digestion (section 2.3.3). These plasmids were sequence verified by Sanger dideoxy sequencing using priRSV2859F, pridTom25+BssHII, and pridTom240+PacI (Appendix 1) to check the sequence across the restriction sites used. Sequences were aligned with pHRSV^{B05}dTom(5) (Figure 3.9D) computer clone using DNASTAR SeqMan Pro software and no spurious mutations were

found (data not shown). A single bacterial clone was amplified in liquid culture containing ampicillin and was used to isolate plasmid by large scale plasmid preparation. Restriction digestion (section 2.3.3) with *Pac* I and *Bss* HII restriction enzymes and with *Bsr* GI and *Bst* XI restriction enzymes were carried out. It confirmed the presence of expected sizes of DNA fragments suggesting no large insertions or deletions that occurred during the amplification in bacterial culture (data not shown). The restriction sites (Figure 3.10) and the insert within pHRSV^{B05}dTom(5) was sequence verified by Sanger dideoxy sequencing using pridTom25+BssHII, pridTom240-PacI, priRSV-B-4476F, priRSV-B-4883F, priHRSV-B05-5385+, and priHRSV-B05-5873+ (Appendix 1). Sequences were was aligned with pHRSV^{B05}dTom(5) computer clone using DNASTAR SeqMan Pro software and no spurious mutations were identified.

3.5 Recovery of rHRSV^{B05}dTom(5)

rHRSV^{B05}dTom(5) was recovered using standard rHRSV rescue method (section 2.2.2). Four of six transfected wells during primary rescue (Figure 3.11A) showed signs of successful recovery of virus. rHRSV^{B05}dTom(5) was passaged three times (Figure 3.11B) to produce P3 stock with $10^{5.89}$ $TCID_{50}$/ml titer in Vero cells.

RNA was isolated from rHRSV^{B05}dTom(5) stock (section 2.3.12). Virus specific RNA was reverse transcribed using gene specific primers (Table 2.1) to

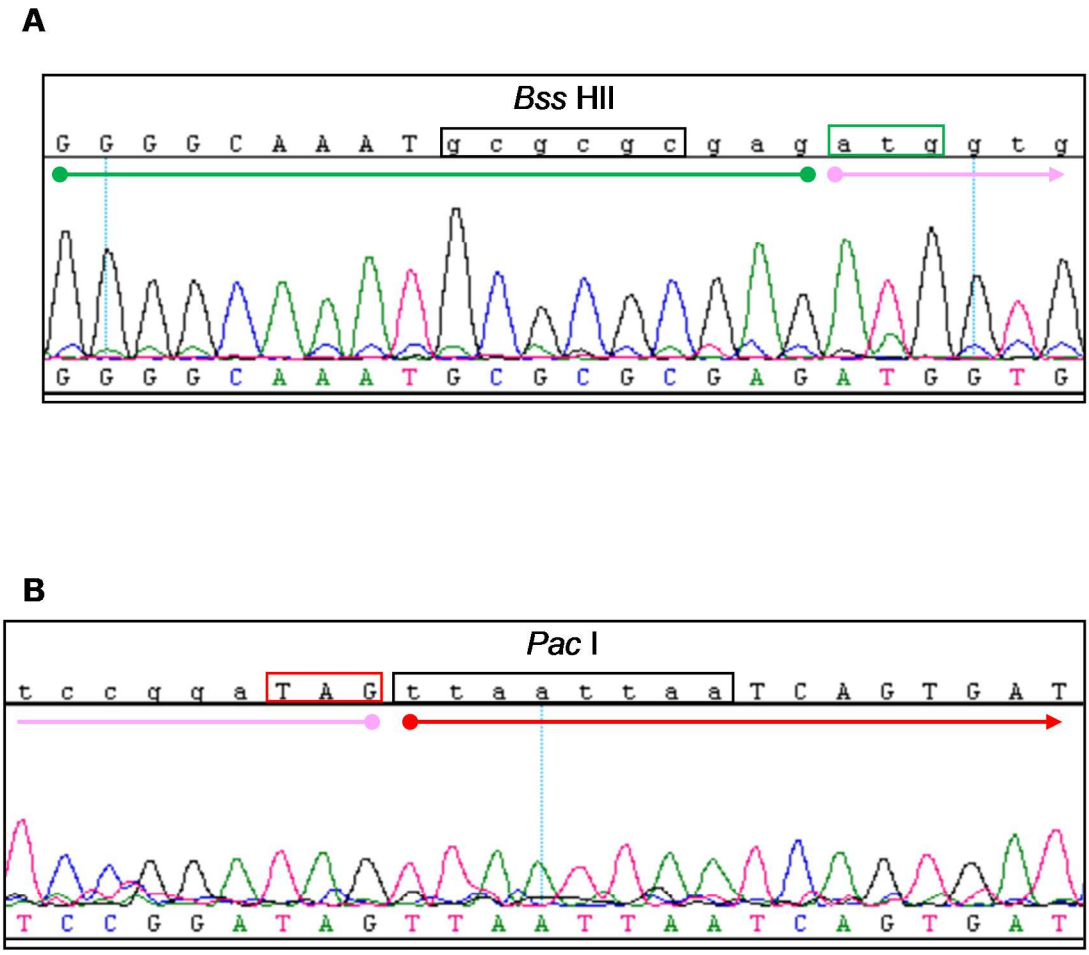

Figure 3.10: Sequence analysis of pHRSV^{B05}dTom(5) across the *Bss* HII and *Pac* I sites. (A) Sequence across the *Bss* HII site in pHRSV^{B05}dTom(5) as aligned with sequence of its computer clone. The *Bss* HII site located upstream of dTom239 gene (pink arrow) is enclosed in a black box. The start codon for dTom239 gene is enclosed in a green box. GS sequence upstream of dTom239 gene (green line) is shown. (B) Sequence across the *Pac* I site in pHRSV^{B05}dTom(5) as aligned with sequence of its computer clone. The *Pac* I site located downstream of dTom239 (pink line) is enclosed in a black box. The stop codon for dTom239 ORF is enclosed in a red box. GE sequence downstream of dTom239 gene (red arrow) is shown.

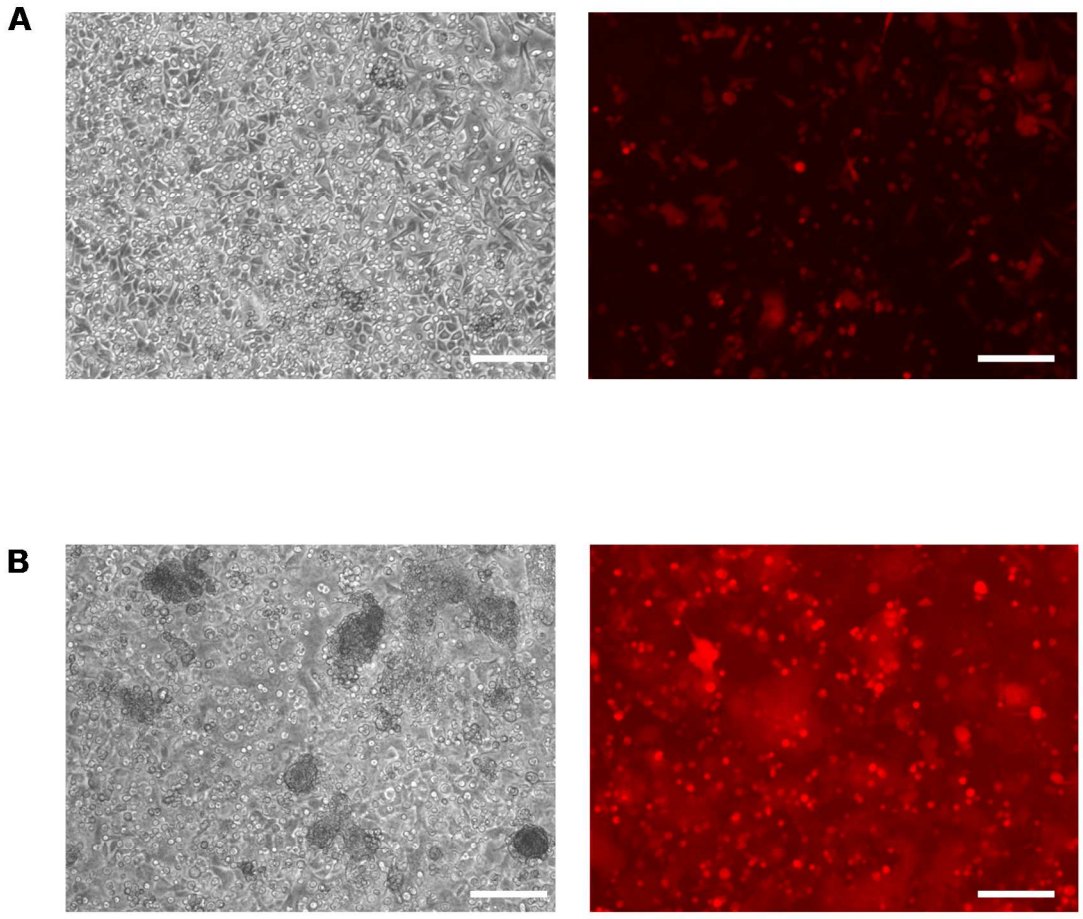

Figure 3.11: Photomicrographs of rHRSV^{B05}dTom(5) rescue and passage 3 infection. (A) Primary rescue of rHRSV^{B05}dTom(5) in HEp-2 cells. Photomicrographs were obtained 7 days after well expansion when the supernatant was collected for P0 stock. (B) HEp-2 cells were infected with rHRSV^{B05}dTom(5) P2 and photomicrographs were obtained 6 d.p.i. The supernatant from this infection was used to generate rHRSV^{B05}dTom(5) P3 stock. Scale bar = 200 µm.

generate viral cDNA. Using the cDNA generated as the template, amplicons were generated to overlap across the 15 kb full-length genome, which was sequenced (section 2.3.14). The ends of the genome were amplified by rHRSV^{B05} RACE method and sequenced (section 2.3.16) using priB05-204- and priB05-15063+. Sequences obtained by Sanger dideoxy sequencing were aligned to rHRSV^{B05}dTom(5) cDNA computer clone using DNASTAR SeqMan Pro software to identify any spurious mutations. In the leader, 50% of the population showed A to U (T in cDNA) change at first nucleotide in the viral genome (Figure 3.12A).

Minor peaks in electrochromatograms of sequences in the trailer showed a nucleotide shift of -1 after L GE (Figure 3.12B). This suggested an insertion of an A at the repeat of 6 A's at the junction of L GE and trailer in about 75% of the population. To confirm this using another method, rHRSV^{B05}dTom(5) genome ends were ligated (section 2.3.17). The ligated genome ends were reverse transcribed using priHRSV-B05-14873+ and from the cDNA, an amplicon was generated using priHRSV-B05-285- and priHRSV-B05-14966+ (Appendix 1). Sequence of the viral genome termini were verified by sanger dideoxy sequencing using priB05-204- and priB05-15063+. Sequences were aligned with rHRSV^{B05}dTom(5) computer clone using DNASTAR SeqMan Pro software and it confirmed the presence of additional A in L GE (Figure 3.12C). This virus stock was used for some preliminary experiments in this thesis.

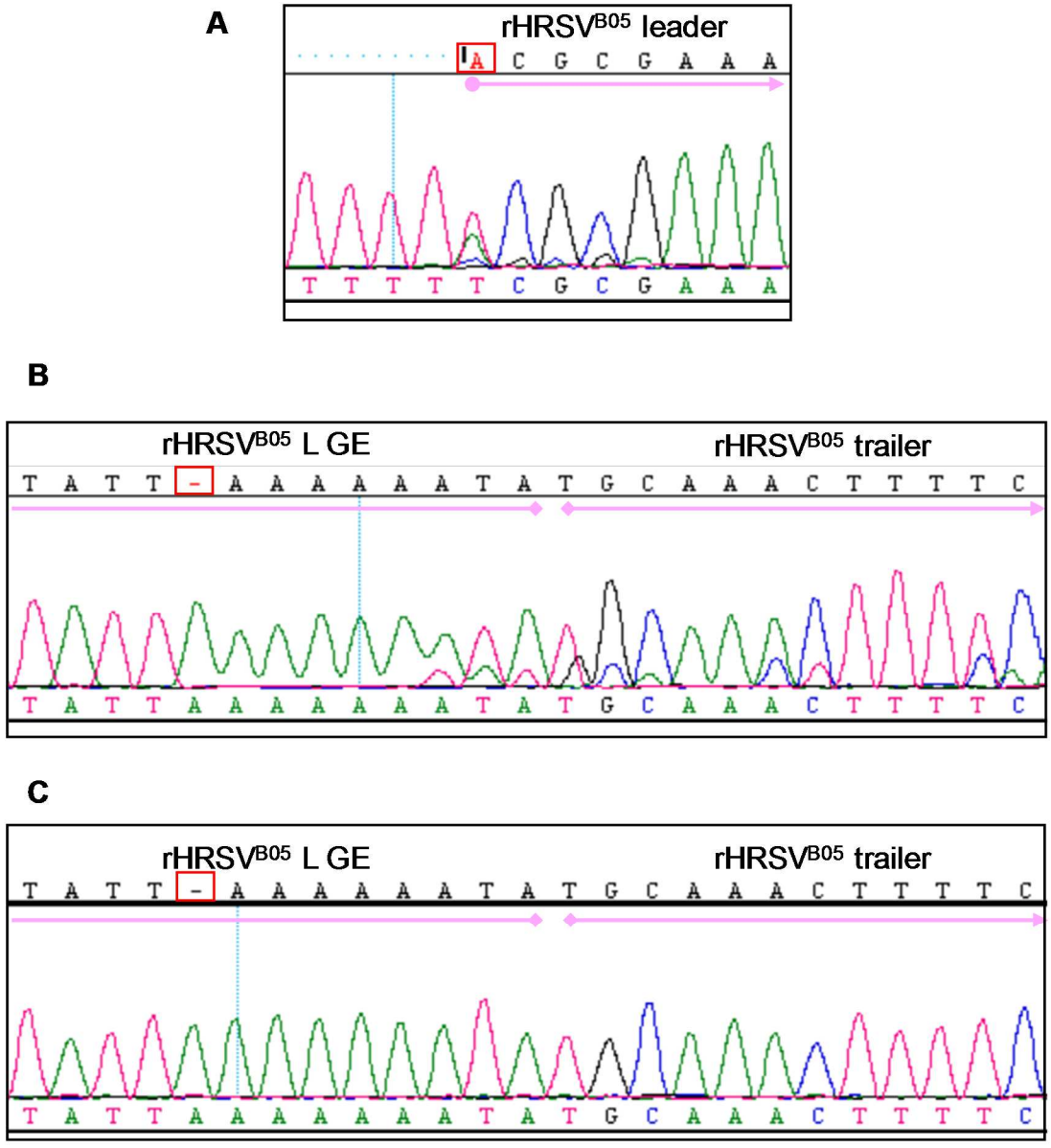

Figure 3.12: Sequencing analysis of rHRSV^{B05}dTom(5) and identification of heterogeneities in sequence. rHRSV^{B05}dTom(5) cDNA was sequenced by Sanger dideoxy sequencing. Sequences were aligned with the rHRSV^{B05}dTom(5) computer clone using DNASTAR SeqMan Pro software. (A) Over 50% of the sequenced rHRSV^{B05}dTom(5) population had A1U nucleotide change (B) Some of the sequenced rHRSV^{B05}dTom(5) population showed a shift in sequence, suggesting an A insertion at L GE. (C) This was confirmed by sequencing this region after RNA ligation.

3.6 Multi-step growth analysis of rHRSV^{B05} expressing fluorescent protein

rHRSV^{B05}dTom(5) and rHRSV^{B05}EGFP(5) growth kinetics were compared to determine if the insertion of dTom239 had an effect on virus growth. Growth kinetics was examined by multi-step growth analysis (section 2.2.8). HEp-2 cells were infected with rHRSV^{B05}EGFP(5) or rHRSV^{B05}dTom(5) at an MOI of 0.2. Supernatants from triplicate wells were collected at various time points (18 h.p.i. to 96 h.p.i.), an equal volume of 50% (w/v) sucrose was added to stabilize the virus during storage. Viral stocks were frozen at -80°C. Supernatants were thawed and the titer of virus was determined by $TCID_{50}$ assay in Vero cells (Figure 3.13). Both viruses had titers of approximately 10^3 $TCID_{50}$/ml at 24 h.p.i. The peak of infection was reached around 72 h.p.i. with titers of approximately 10^6 $TCID_{50}$/ml. These data show that rHRSV^{B05}dTom(5) grew comparably to rHRSV^{B05}EGFP(5). Published data (Lemon et al., 2015) show that rHRSV^{B05} and rHRSV^{B05}EGFP(5) have comparable replication kinetics.

3.7 Human IVIG and human serum neutralization of rHRSV^{B05}EGFP(5)

Human IVIG and human serum from plasma were used to develop a microneutralization assay for rHRSV. Three hundred p.f.u. of rHRSV^{B05}EGFP(5) were incubated with or without varying concentrations of human IVIG (1:64000 to 1:2000) or human serum (1:16000 to 1:500) for 1 hour at 37ºC in triplicate. Virus/antibody mixture was added to HEp-2 cells for 1.5 hours and growth medium

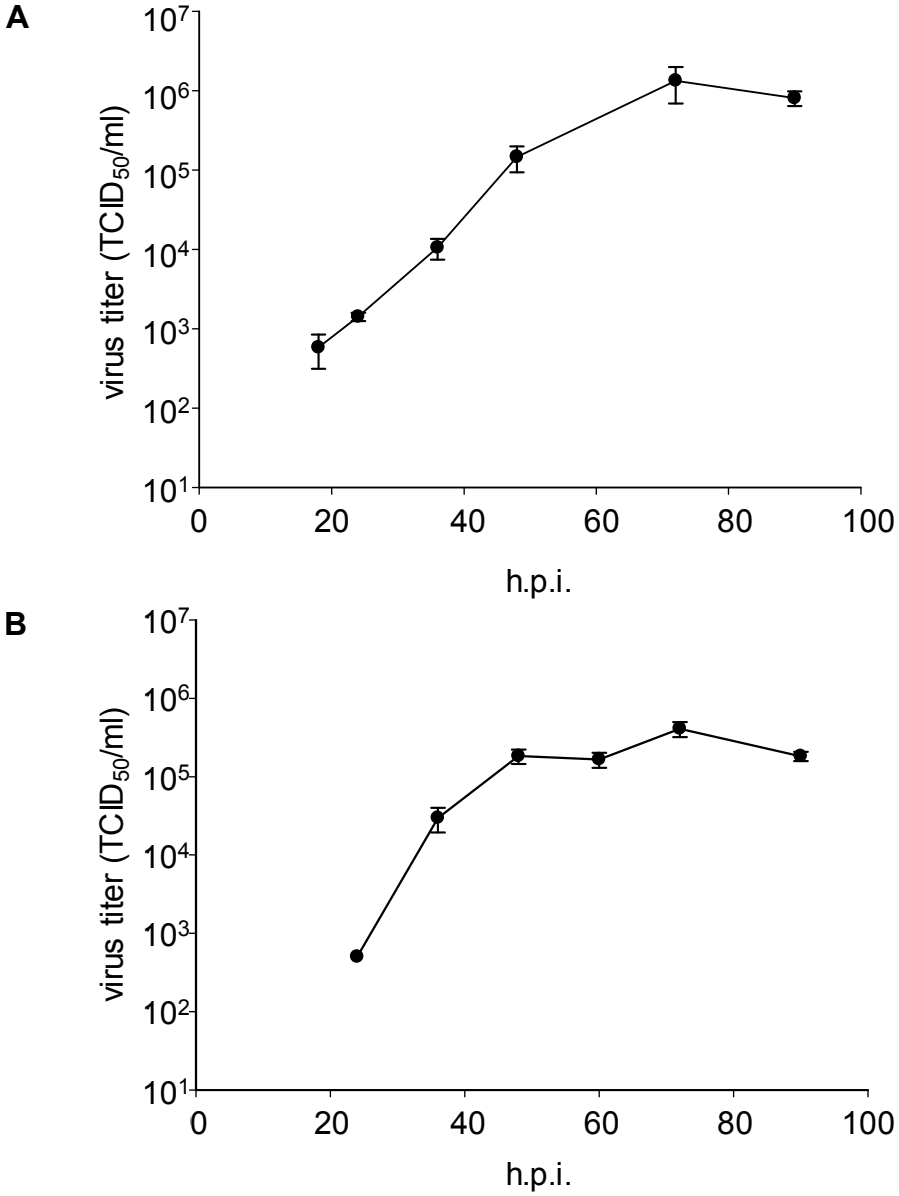

Figure 3.13: Multistep growth analysis of rHRSV^{B05}EGFP(5) and rHRSV^{B05}dTom(5). HEp-2 cells were infected with (A) rHRSV^{B05}EGFP(5) and (B) rHRSV^{B05}dTom(5) at an MOI of 0.2 in triplicate in two separate experiments. Supernatant from the triplicate wells were collected at various time points (18 h.p.i. to 96 h.p.i.) and the titer of virus in supernatant was measured by $TCID_{50}$ assay in Vero cells.

was added. Infections were observed at 1 d.p.i. by phase-contrast microscopy and UV microscopy and the foci of infection were counted by observing EGFP expression. The mean of triplicate data was plotted with standard error. There was almost 50 percent reduction in number of foci of infection when IVIG at 1:16000 dilution as compared to untreated control (Figure 3.14A). For human serum, 1:1000 dilution was needed to reach over 50 percent as compared to untreated control (Figure 3.14B).

3.8 rHRSV^{A11}EGFP(5) and rHRSV^{B05}EGFP(5) infections in vitro

Cotton rats are the gold standard *in vivo* small animal model for HRSV upper respiratory tract infection and are more susceptible to HRSV infection than mice (Bem et al., 2011; Boukhvalova et al., 2009). rHRSV^{B05}EGFP(5) has been used to infect cotton rats (Lemon et al., 2015). To confirm that rHRSV^{A11}EGFP(5) can infect cotton rat cells and to prepare for upcoming *in vivo* studies, transformed cotton rat lung cells were infected with rHRSV^{A11}EGFP(5). Control infections were carried out in HEp-2 cells because they are commonly used in HRSV research. Cells were also infected with rHRSV^{B05}EGFP(5), since it is known to be able to infect cotton rats (Lemon et al., 2015). HEp-2 cells were infected at an MOI of 0.1 in triplicate, infections were observed by UV microscopy daily, and photomicrographs were obtained (Figure 3.15AB). Cotton rat lung cells were

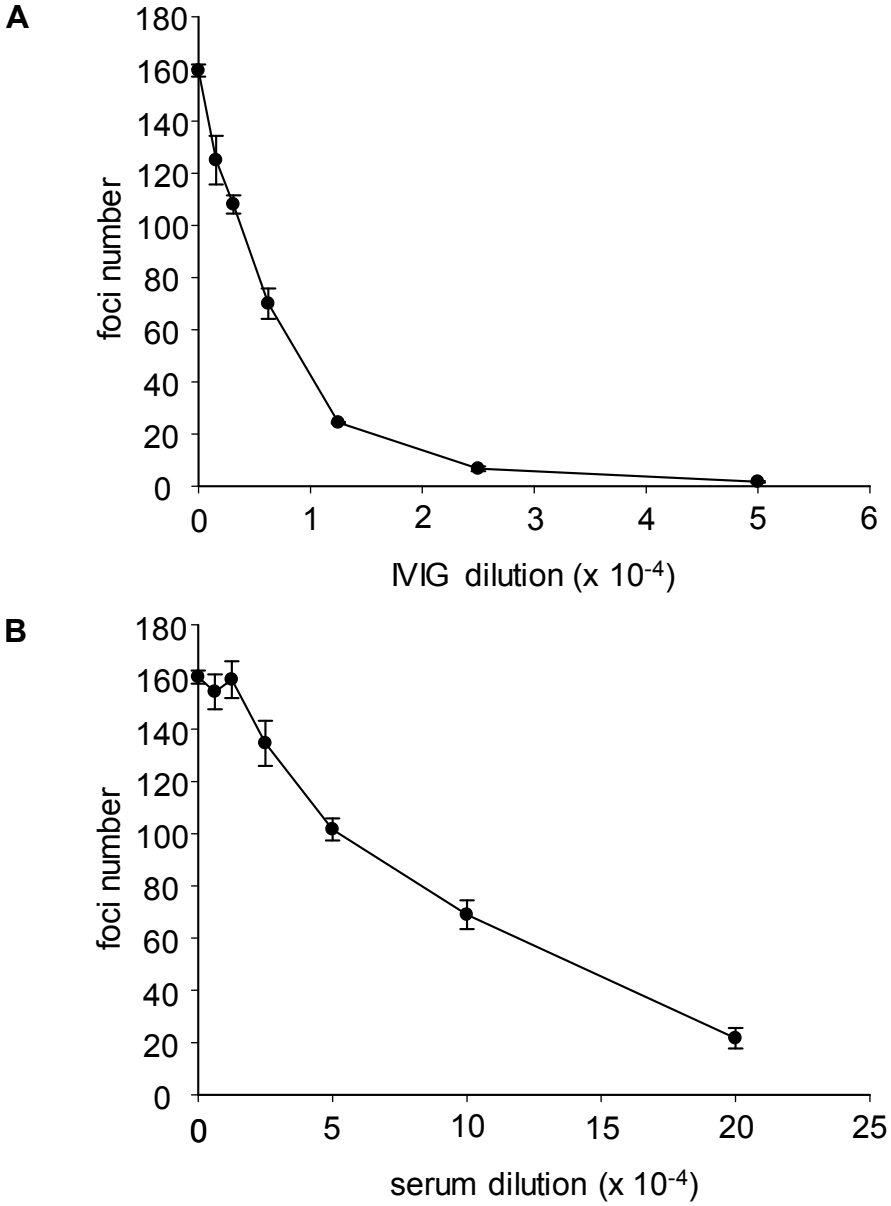

Figure 3.14: Neutralization of rHRSV^{B05}EGFP(5) by human IVIG and human serum. rHRSV^{B05}EGFP(5) was treated with increasing concentrations of (A) human IVIG and (B) human serum for 1 hour at 37ºC. HEp-2 cells were infected by 300 p.f.u. of human IVIG or human serum treated virus for 90 minutes in triplicate. Total foci of infection in each well of infected HEp-2 cells were counted at 1 d.p.i. This number reflects the extent of neutralization of rHRSV^{B05}EGFP(5) by human IVIG and human serum.

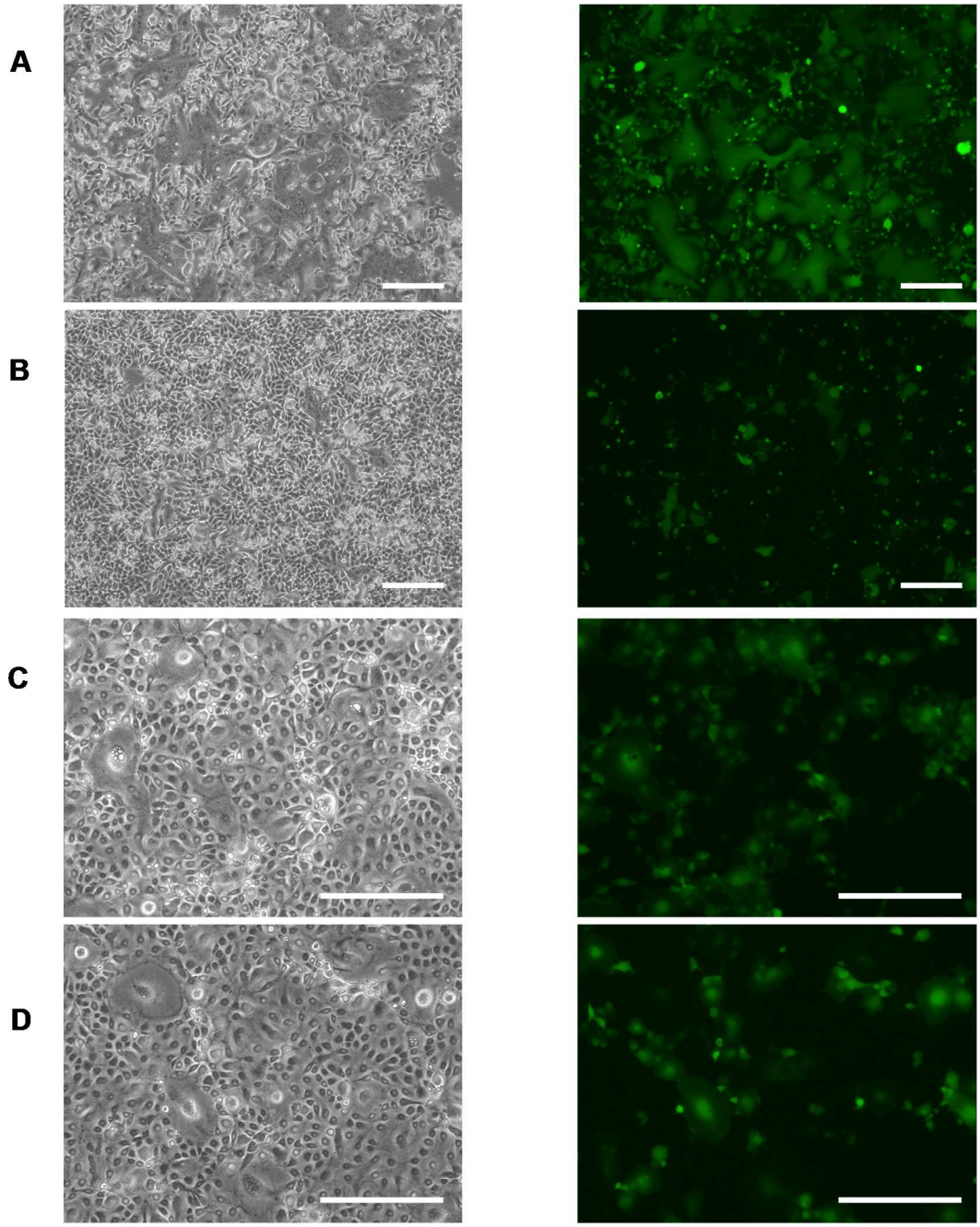

Figure 3.15: Infection of HEp-2 cells and cotton rat lung cells with rHRSV^{A11}EGFP(5) and rHRSV^{B05}EGFP(5). (A) rHRSV^{A11}EGFP(5) and (B) rHRSV^{B05}EGFP(5) infection were carried out at an MOI of 0.1 in HEp-2 cells. (C) rHRSV^{A11}EGFP(5) and (D) rHRSV^{B05}EGFP(5) infection were carried out at an MOI of 0.1 in cotton rat lung cells. All photomicrographs were obtained at 2 d.p.i. Scale bar = 400 µm.

readily infected with rHRSV^{A11}EGFP(5) or rHRSV^{B05}EGFP(5) at an MOI of 0.1 in triplicate (Figures 3.15C and 3.15D). This demonstrates both viruses infect cotton rat lung cells and the observed CPE in cotton rat lung cells is indistinguishable from that observed in HEp-2 cells.

CHAPTER 4: DUPLICATION IN HRSV^{B05} GLYCOPROTEIN GENE

4.1 Generation of pCG-HRSV^{B05}GΔ60b

HRSV^{B05} is a BA genotype virus and contains a 60 nt duplication in the G protein gene. An expression plasmid, pCG-HRSV^{B05}GΔ60b was generated to study HRSV^{B05} G protein lacking the duplication in MLD2 and the role of duplication in the successful spread of HRSV BA genotype globally. pCG-HRSV^{B05}G (Figure 4.1A) was digested with *Bmg* BI and *Pst* I (section 2.3.3) and the 4,849 bp DNA fragment was gel extracted (section 2.3.4) to generate a linear vector (section 2.3.4). A 479 bp DNA fragment (Figure 4.1B), containing the HRSV^{B05} G protein gene sequence from 30 bp upstream of the *Bmg* BI site and 22 bp downstream of *Pst* I site and with deletion of the second 60 nt of the duplication was synthesized by GeneArt. Vector and insert were assembled by Gibson assembly, a method of ligating multiple DNA fragments containing 15 to 80 bp sequence overlaps in one reaction (section 2.3.6). *E. coli DH5*α competent cells were transformed with one tenth of the total volume of the Gibson assembly reaction and plated onto LB agar plate containing ampicillin (section 2.3.8). Six colonies were amplified in liquid culture and plasmids were isolated by small scale plasmid preparation (section 2.3.9). Plasmids were verified by *Bmg* BI and *Pst* I restriction digestion (section 2.3.3) and all plasmids contained the insert. Two plasmids were sequenced by Sanger dideoxy sequencing using primers pripCG+ and pripCG-b (Appendix 1) to

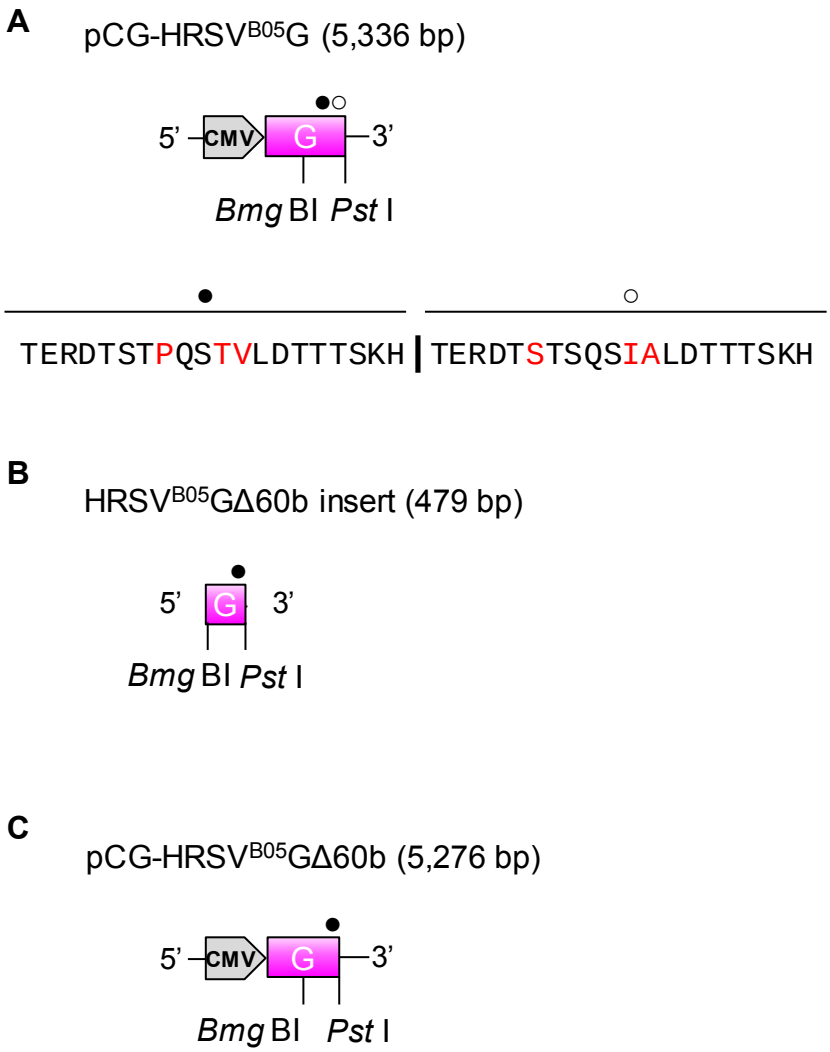

Figure 4.1: Schematic diagram of construction of pCG-HRSV^{B05}GΔ60b. (A) pCG-HRSV^{B05}G was digested with *Bmg* BI and *Pst* I to generate 4849 bp linear vector. The 40 amino acids encoded by the duplicated region is indicated with a vertical line for the separation between the tandem duplication. ● indicates the 20 amino acids encoded by first 60 nucleotides and ○ indicates those encoded by the second 60 nucleotides. The amino acid differences in the first and second half of the duplication are marked in red. (B) The insert, HRSV^{B05}GΔ60b, was synthesized by GeneArt. (C) A schematic diagram of pCG-HRSV^{B05}GΔ60b and the two restriction sites used for cloning. The grey pentagons at the 5' end indicate the CMV promoters used to control the expression of the plasmids.

sequence over the cloning sites and the insert (section 2.2.11). Sequences were aligned with pCG-HRSV^{B05}GΔ60b (Figure 4.1C) computer clone using DNASTAR SeqMan Pro software (section 2.3.1) and no spurious mutations were identified in G protein gene. The sequence across the restriction sites and near the deletion of duplication is presented in Figure 4.2. Sequence verified bacterial clone was amplified in a liquid culture containing ampicillin, which was used to isolate plasmid by large scale plasmid preparation (section 2.3.10).

4.2 Generation of pHRSV^{B05}EGFP(5)GΔ60b

A full-length antigenomic plasmid, pHRSV^{B05}EGFP(5)GΔ60b, was constructed to study the modified G protein in the context of rHRSV. This plasmid can be used to recover HRSV^{B05} virus lacking the 60 nt duplication in the HRSV G protein gene. pHRSV^{B05}EGFP(5) (Figure 4.3A) was digested with *Bmg* BI and the 16,464 bp DNA fragment was gel extracted (section 2.3.4) to generate a linear vector. A 438 bp DNA fragment containing the deletion in HRSV G protein gene was amplified from pCG-HRSV^{B05}GΔ60b (Figure 4.3B) by PCR (section 2.3.5) using priHRSV-B05-5132+ and priHRSV-B05-5586- (Appendix 1) and gel purified to generate insert 1 (I_1). The 2609 bp DNA fragment with 41 overlapping nt with I_1 and 41 overlapping nt with the second *Bmg* BI site of HRSV^{B05} genome was amplified by PCR (section 2.3.5) from pHRSV^{B05}EGFP(5) using priHRSV-B05-5588+ and priHRSV-B05-8154- (Appendix 1) and gel purified (section 2.3.4) to generate insert 2 (I_2). The 41 nt overlap was necessary for ligation of vector, I_1,

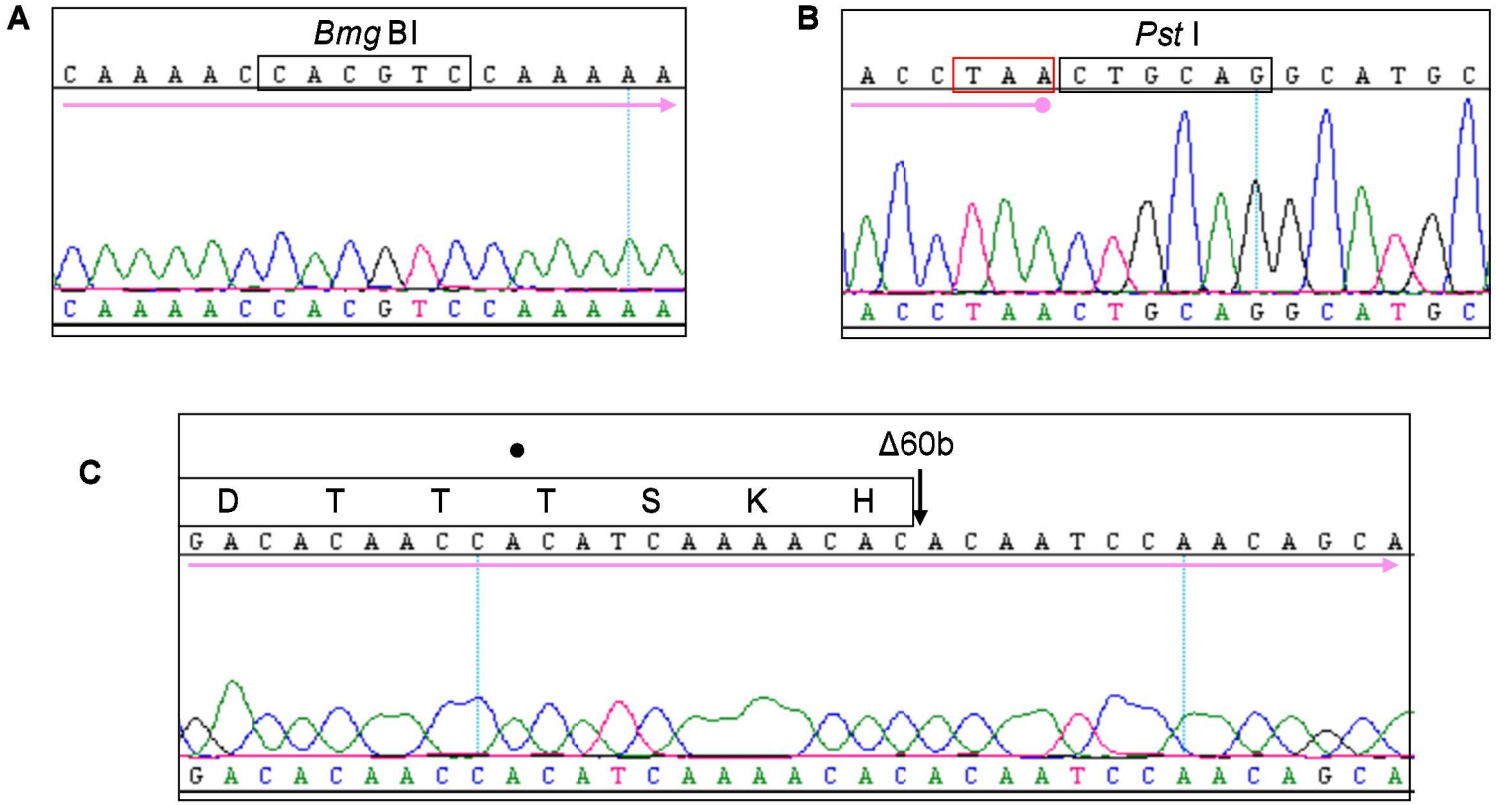

Figure 4.2: Sequence analysis of pCG-HRSV^{B05}GΔ60b across the *Bmg* BI and *Pst* I sites and the site of duplication deletion. (A) Sequence across the *Bmg* BI site in pCG-HRSV^{B05}GΔ60b was aligned with sequence of its computer clone. The *Bmg* BI site is enclosed in black box. (B) Sequence across the *Pst* I site in pCG-HRSV^{B05}GΔ60b as aligned with sequence of its computer clone. The restriction site is enclosed in black box. The stop codon for G protein gene ORF is enclosed in red box. (C) Sequence across the 60 nucleotide deletion. The amino acids encoded by first 60 nucleotides of the duplication is enclosed in a black box and marked with ●. In (A), (B), and (C) the pink line/arrow indicates the G protein gene sequence.

Figure 4.3: Schematic diagram of construction of pHRSV^{B05}EGFP(5)GΔ60b (A) pHRSV^{B05}EGFP(5) was digested with *Bmg* BI to generate the linear vector. Insert 2 (I_2) was amplified from pHRSV^{B05}EGFP(5) by PCR using primers ►◄. (B) From pCG-HRSV^{B05}GΔ60b, insert 1 (I_1) was amplified by PCR using primers ►◄ to contain 41 nucleotide overlap with the vector and insert 2 (I_2). The overlap was necessary for Gibson assembly. (C) A schematic diagram of the vector and two inserts to represent the ligation strategy. (D) A schematic diagram of pHRSV^{B05}EGFP(5)GΔ60b is shown with the two restriction sites used to generate the vector for this cloning. ● represents the first and ○ represents the second 60 nucleotides of the duplication. The grey pentagons at the 5' end indicate either the CMV or T7 promoters used to control the expression of the plasmids.

and I_2 (Figure 4.3C) by Gibson assembly (section 2.3.7). One tenth of the reaction was transformed into *E. coli DH5*α competent cells and plated onto LB agar plate containing ampicillin. Two colonies were amplified in liquid culture containing ampicillin and plasmids were isolated by small scale plasmid preparations. Plasmids were verified by restriction digests. The sequence of one plasmid containing both inserts was verified by Sanger dideoxy sequencing using priHRSV-B05-4524+, priHRSV-B05-5014+, and priHRSV-B05-5916- (Appendix 1). Sequences were aligned with pHRSV^{B05}EGFP(5)GΔ60b (Figure 4.3D) computer clone using DNASTAR SeqMan Pro software and HRSV G protein gene was confirmed to contain no spurious mutations (data not shown). Sequence verified bacterial clone was amplified in a liquid culture containing ampicillin and plasmid was isolated by large scale plasmid preparation. The sequence of the G protein gene, F glycoprotein gene, and M2-1 gene by Sanger sequencing using priHRSV-B05-4524+, priHRSV-B05-5014+, priHRSV-B05-5736+, priHRSV-B05-5916-, priHRSV-B05-6096+, priHRSV-B05-6503+, priHRSV-B0-6919+, priHRSV-B05-7435+, and priHRSV-B05-7611- (Appendix 1). Sequences were aligned with pHRSV^{B05}EGFP(5)GΔ60b computer clone using DNASTAR SeqMan Pro software and no spurious mutations were identified. The sequencing result across the two restriction sites (Figure 4.4A), the insert-insertion junctions is presented in Figure 4.4B), the deletion of 60 nt (Figure 4.5).

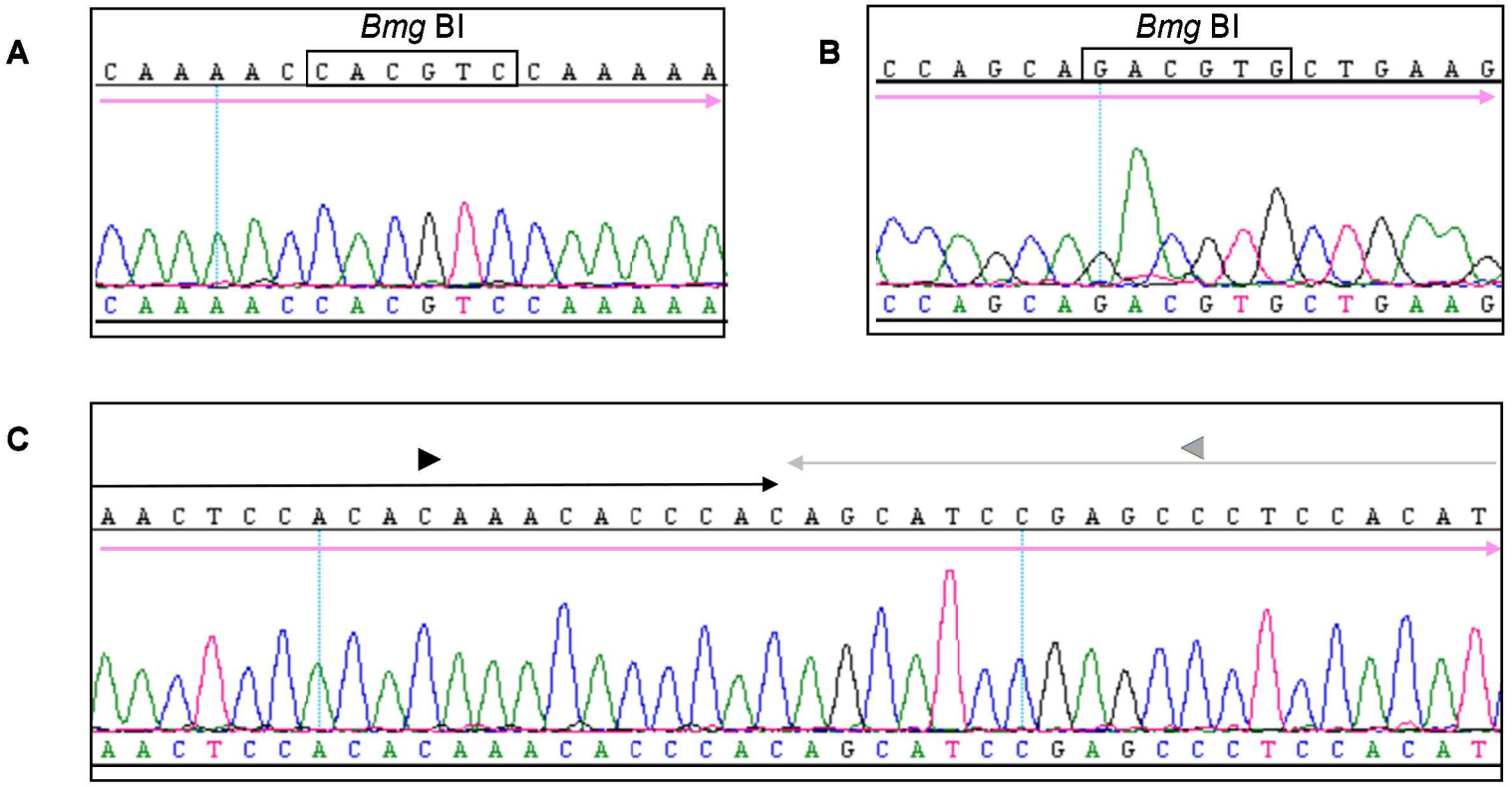

Figure 4.4 Sequence analysis of pHRSV^{B05}EGFP(5)GΔ60b across the ligation sites and I_1 and I_2 junction. (A) Sequence across the *Bmg* BI site in pHRSV^{B05}EGFP(5)GΔ60b G protein gene (pink arrow). The *Bmg* BI site is enclosed in black box. (B) Sequence across the *Bmg* BI site in pHRSV^{B05}EGFP(5)GΔ60b M2 gene (pink arrow). The *Bmg* BI site is enclosed in black box. (C) Sequence across the ligation of I_1 and I_2. The forward primer for I_2 is denoted by ▶ and the reverse primer for I_1 is denoted by ◀. G protein gene sequence is marked with pink arrow.

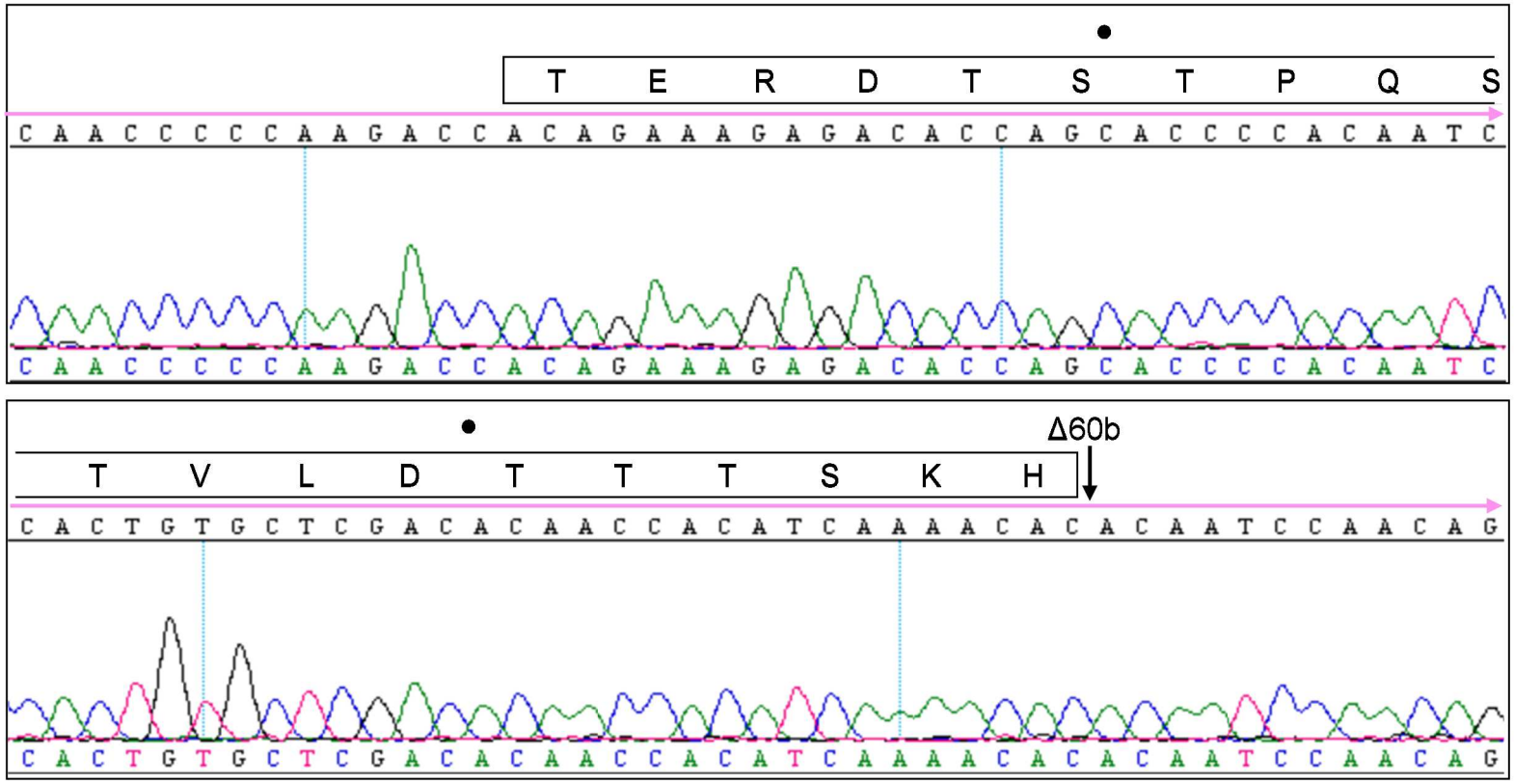

Figure 4.5 Sequence analysis of pHRSV^{B05}EGFP(5)GΔ60b across the duplication deletion. Sequence across the duplication in G protein gene of pHRSV^{B05}EGFP(5)GΔ60b. The 20 amino acids encoded by the first 60 nt of the duplication (●) is shown above the nt sequence. The site at which the deletion was introduced is denoted by the black arrow. Pink arrow indicates HRSV^{B05} G protein gene.

4.3 Recovery of rHRSV^{B05}EGFP(5)GΔ60b

rHRSV^{B05}EGFP(5)GΔ60b was recovered using the standard rHRSV rescue method (section 2.2.2) by transfecting HEp-2 cells in five wells of a 6-well plate. All five wells of transfected HEp-2 cells from primary rescue contained EGFP expressing cells and the cells in these wells were trypsinized and transferred into T75 flasks containing HEp-2 cells (section 2.2.2) (Figure 4.6A). One flask of cells from the primary rescue was passaged three times (section 2.2.3) to produce a P3 stock virus (Figure 4.6B). The titer of P3 stock was determined to be $10^{4.94}$ $TCID_{50}$/ml in Vero cells (section 2.2.6)

RNA was isolated (section 2.3.12) from rHRSV^{B05}EGFP(5)GΔ60b stock and reverse transcribed using gene specific primers (Table 2.1) to generate cDNA (section 2.3.12). From the viral cDNA, amplicons were generated to overlap across the 15 kb full-length genome, which was sequenced to check for any spurious mutations in the viral genome (section 2.3.14). Sequences were aligned with the computer clone for rHRSV^{B05}EGFP(5)GΔ60b across most of the genome using DNASTAR SeqMan Pro (section 2.3.1). However, a 638 bp gap from GE sequence of EGFP ATU to M protein gene and the genome termini have not yet been sequenced. Minor peaks were identified in the electrochromatogram at nucleotides 3234 to 3718 within the GS sequence of EGFP ATU. These minor peaks matched with one nucleotide shift in sequence which suggested an insertion of an A

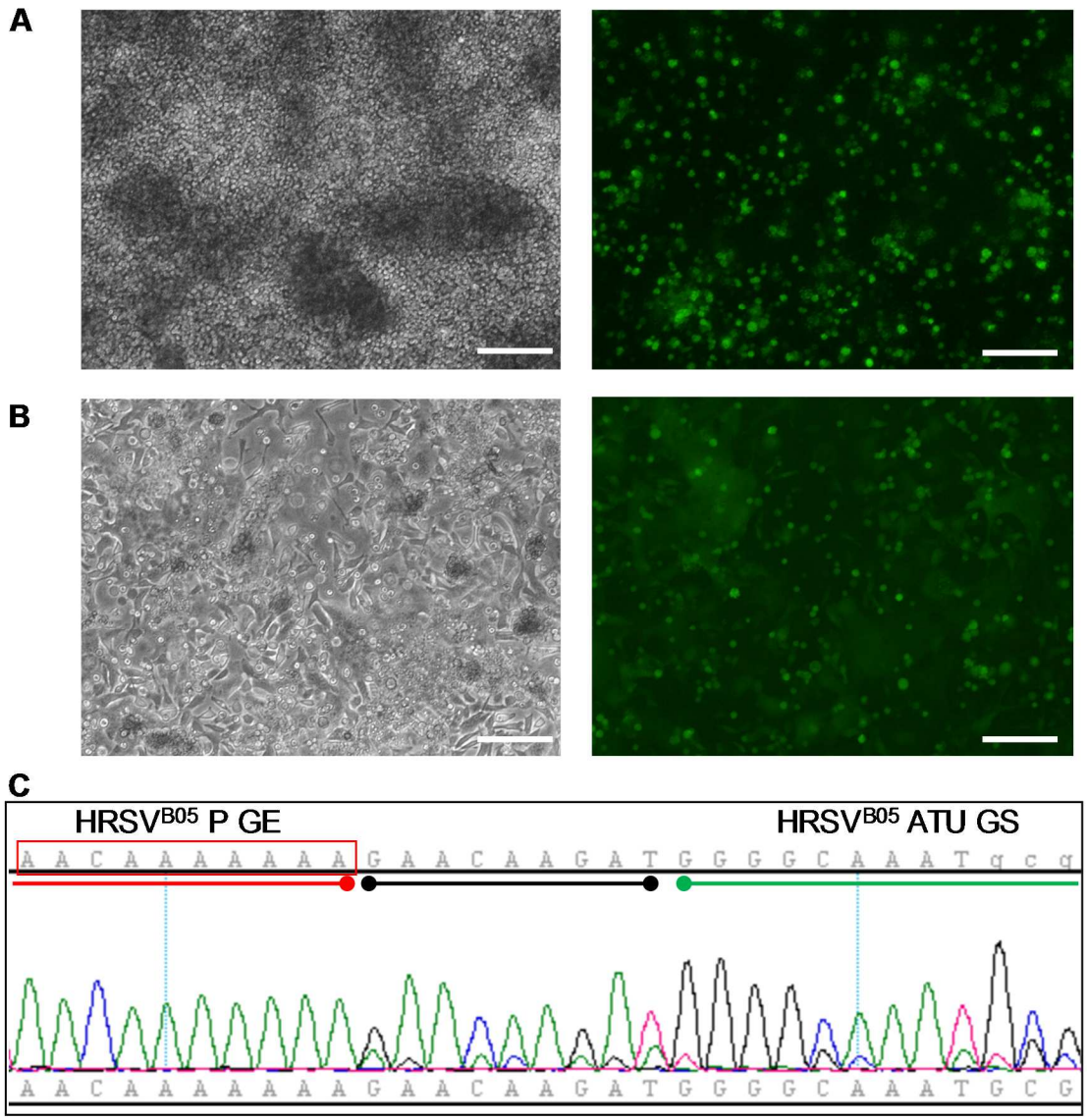

Figure 4.6: Photomicrographs of rHRSV^{B05}EGFP(5)GΔ60b and passage 3 stock generation, and passage 3 stock sequence analysis. (A) Primary rescue of rHRSV^{B05}EGFP(5)GΔ60b in HEp-2 cells. Photomicrographs were obtained 14 days after well expansion when supernatant was collected for P0 stock Scale bar = 200 µm. (B) HEp-2 cells were infected with rHRSV^{B05}EGFP(5)GΔ60b P2 and photomicrographs were obtained 4 d.p.i. The supernatant from this infection was used to generate rHRSV^{B05}EGFP(5)GΔ60b P3 stock. Scale bar = 200 µm. (C) rHRSV^{B05}EGFP(5)GΔ60b P3 sequence at P GE (red line), intergenic region (black line), and ATU GS (green line). The shift in nucleotides after P protein GE is shown. The polyadenylation signal (red box) for P protein gene may have an insertion in the repeat of 7 A nucleotides.

nucleotide in the seven repeating A's at the end of the P protein GE polyadenylation signal (Figure 4.6C) for approximately 25% of sequences.

4.4 rHRSV^{B05}EGFP(5)GΔ60b passage preliminary experiment in HEp-2 cells

A preliminary experiment was performed to study if the region containing the duplication in the G protein gene was prone to acquiring mutations during passage *in vitro*. HEp-2 cells were infected in triplicate with rHRSV^{B05}EGFP(5) P3 stock or rHRSV^{B05}EGFP(5)GΔ60b P3 stock at an MOI of 0.02. This infection was considered passage four (P4). Growth medium was replaced at 1 d.p.i. This process was repeated daily and when over 80% of cells were infected, as determined by EGFP expression, phase-contrast and UV photomicrographs were obtained (Figure 4.7). Cells were pelleted by centrifugation and the supernatant was used to infect HEp-2 cells in triplicate to set up passage five (P5) infection. Supernatant and cells were collected and stored at -80ºC for RNA isolation and subsequent sequencing of rHRSV. This process of imaging, passaging, and collecting was repeated nineteen times (Figure 4.7).

Partial sequences of the virus at passage fourteen (P14) and passage 24 (P24) were obtained to determine if there was a region in G protein gene that was more prone to occurrence of mutations. RNA was isolated from supernatants collected at P14 and P24 (section 2.3.12). RNA was used to determine the changes that arose in HRSV^{B05} G protein gene (section 2.3.14). Sequences were

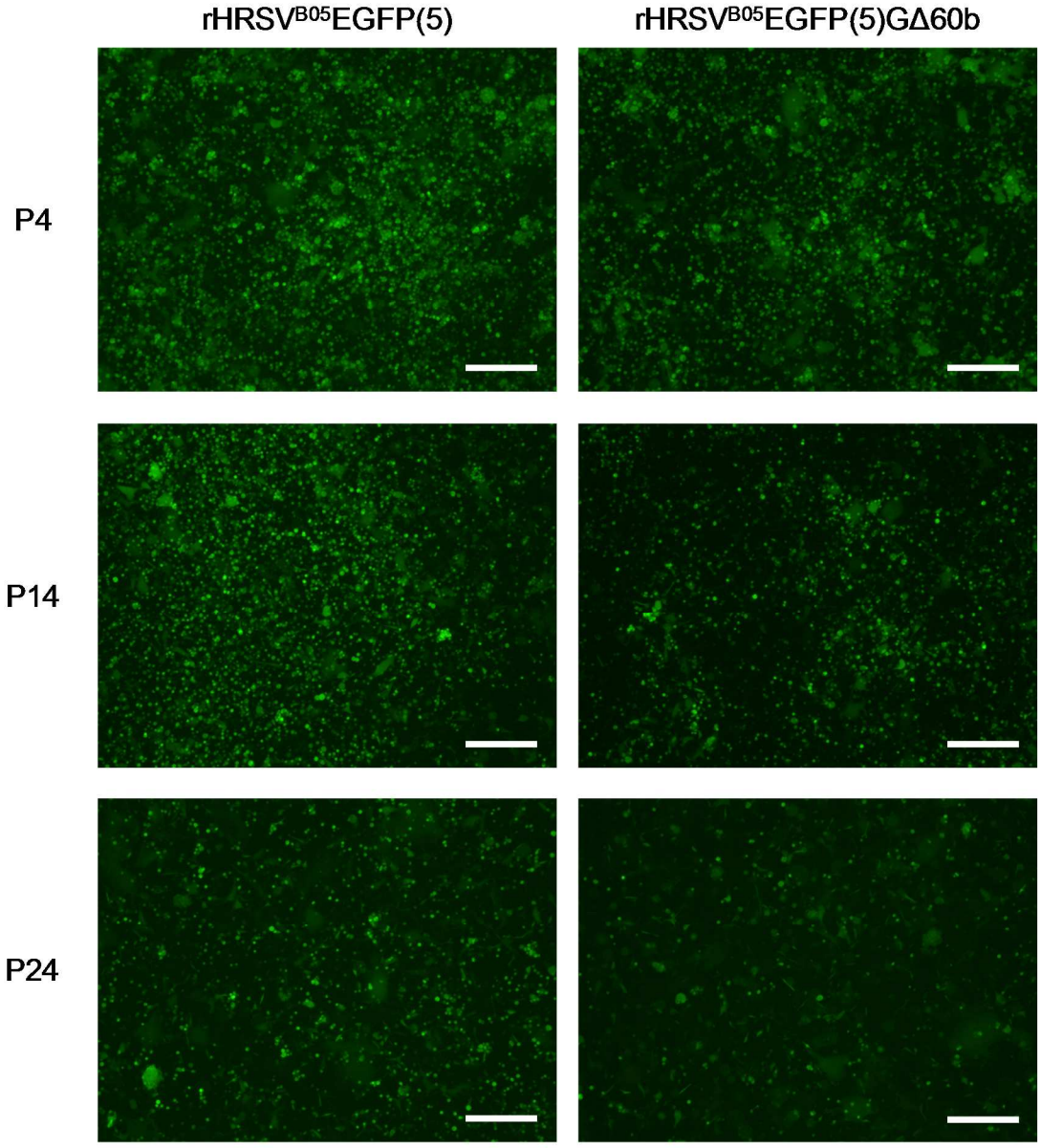

Figure 4.7: Serial passage of rHRSV^{B05}EGFP(5) and rHRSV^{B05}EGFP(5)GΔ60b in HEp-2 cells. HEp-2 cells were infected in triplicate with either rHRSV^{B05}EGFP(5) P3 stock or rHRSV^{B05}EGFP(5)GΔ60b P3 stock and supernatant was collected at the peak of infection as determined by 80% of the cells infected (passage 4). Supernatant was used to infect new cells to start passage 5 and this process was repeated until passage 24. Photomicrographs show infected cells at peak of infection as determined by CPE observation during passage 4 (P4), passage 14 (P14), and passage 24 (P24). Scale bar = 400 µm

aligned with computer clone of rHRSV^{B05}EGFP(5) or rHRSV^{B05}EGFP(5)GΔ60b, accordingly, using DNASTAR SeqMan Pro software. Although there were no complete changes in any nucleotide, heterogeneous sequence, as demonstrated by double peaks in electrochromatograms were seen. Data show mutations arise in various regions of the HRSV G protein gene during passage in HEp-2 cells and in this experiment no mutations were found in MLD2 where the duplication is located (Table 4.1).

4.5 Generation of pHRSV^{B05}EGFP(5)Gmycb and pCG-HRSV^{B05}Gmycb

pHRSV^{B05}EGFP(5)Gmycb was constructed to recover rHRSV^{B05}EGFP(5)Gmycb, which will be used to examine changes at the site where the duplication occurs in HRSV G protein gene. pHRSV^{B05}EGFP(5) (Figure 4.8A) was digested with *Bmg* BI and 16,464 bp DNA fragment was gel extracted (section 2.3.4) to generate a linear vector. pMK-HRSV^{B05}Gmycb (Figure 4.8B), plasmid containing partial HRSV^{B05} G protein gene with a c-myc epitope tag (Kolodziej and Young, 1991) encoding nucleotide sequence substituted within the second 60 nt of the duplication and partial F glycoprotein gene, was synthesized by GeneArt. The DNA fragment containing the c-myc epitope tag sequence substitution was amplified from pMK-HRSV^{B05}Gmycb by PCR (section 2.3.5) using priHRSV-B05-5132+ and priHRSV-B05-5586- (Appendix 1) to generate insert A (I_A). The DNA fragment with 41 overlapping nucleotides with I_A and 41 overlapping nucleotides with the second *Bmg* BI site of HRSV^{B05} genome was amplified by

A rHRSV^{B05}EGFP(5)

passage	nucleotide	aa	population (%)
14	U6145A	177	25
24	A6072G	153	25
24	A6073G	153	50
24	A6074G	154	25
24	A6075G	154	25
24	A6083G	157	25
24	A6084G	157	25
24	A6085G	157	25
24	A6096G	161	25
24	A6105G	164	<25
24	A6106G	164	<25
24	A6114G	167	25
24	A6141G	176	25
24	A6147G	178	<25
24	A6148G	178	<25
24	A6192G	193	25
24	C6216A	201	50

B rHRSV^{B05}EGFP(5)GΔ60b

passage	nucleotide	aa	population (%)
14	A5658G	15	75
24	A5658G	15	>75
24	U6134C	174	25

Table 4.1: Summary tables of G protein gene sequence analysis of rHRSV^{B05}EGFP(5) and rHRSV^{B05}EGFP(5)GΔ60b after serial passaging in HEp-2 cells. Sequence data have been summarized for (A) rHRSV^{B05}EGFP(5) and (B) rHRSV^{B05}EGFP(5)GΔ60b passage experiment in HEp-2 cells. RNA was isolated from P14 and P24 and reverse transcribed rHRSV cDNA was used to sequence over the G protein gene. Population column shows approximate percentage of the population contained the mutation from the electrochromatogram. For each nucleotide, corresponding amino acid (aa) position is presented.

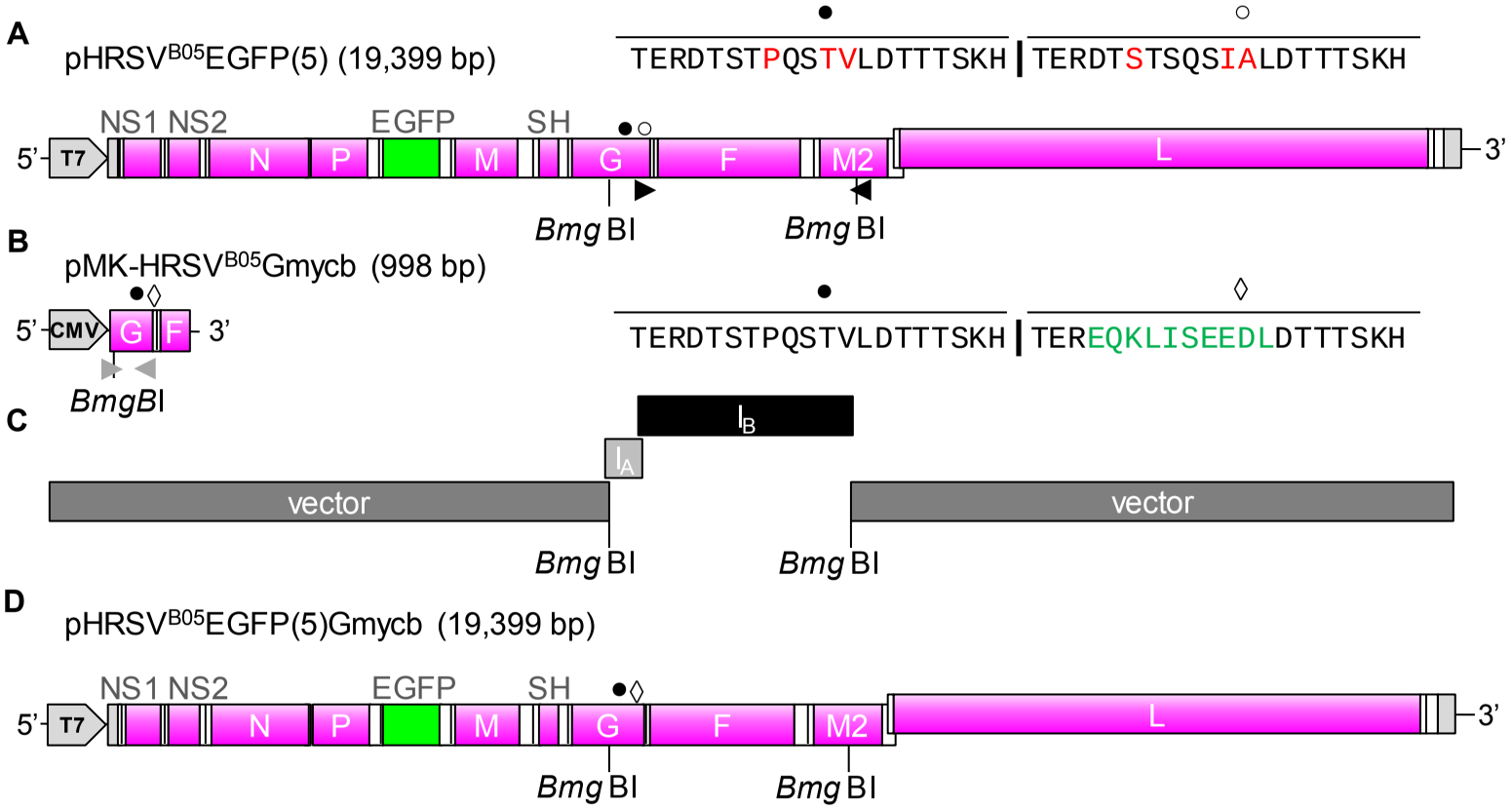

Figure 4.8: Schematic diagram of construction of pHRSV^{B05}EGFP(5)Gmycb (A) pHRSV^{B05}EGFP(5) was digested with *Bmg* BI to generate the linear vector and insert 2 (I_B) was amplified by PCR using primers (►◄). The amino acid sequence for the duplication is shown. (B) From pMK-HRSV^{B05}Gmycb, insert 1 (I_A) was amplified by PCR using primers (►◄) to contain 41 nucleotide overlap with vector and I_B. (C) Schematic diagram of the vector and two inserts to represent the ligation strategy. (D) Schematic diagram of pHRSV^{B05}EGFP(5)Gmycb and *Bmg* BI sites used for cloning is shown. The second 60 nucleotides of the duplication with c-myc epitope tag sequence insertion is denoted by ◊. The grey pentagons at the 5' end indicate either the CMV or T7 promoters used to control the expression of the plasmids.

PCR (section 2.3.5) from pHRSV^{B05}EGFP(5) using priHRSV-B05-5588+ and priHRSV-B05-8154- (Appendix 1) to generate insert 2 (I_B). Vector, I_A, and I_B were ligated by Gibson assembly (Figure 4.8C). One tenth of the reaction was transformed into *E. coli DH5*α competent cells and plated onto LB agar plate containing ampicillin. Ten colonies were amplified in liquid culture containing ampicillin and plasmids were isolated by small scale plasmid preparations.

Plasmids were examined by restriction digests and DNA gel electrophoresis confirmed that the ligation was successful for eight plasmids (data not shown). Two plasmids were sequenced by Sanger dideoxy sequencing using priHRSV-B05-5014+ and priHRSV-B05-7734+ (Appendix 1) to check the sequence across the *Bmg* BI sites. Sequences were aligned with the computer clone for pHRSV^{B05}Gmycb (Figure 4.8D) using DNASTAR SeqMan Pro software and no spurious mutations around the restriction sites were found (data not shown). A single sequence verified bacterial clone was amplified in liquid culture containing ampicillin and plasmid was isolated by large scale plasmid preparation. Sequences of the EGFP ATU, G protein gene (Figure 4.9), F glycoprotein gene, and the *Bmg* BI restriction sites used for cloning was verified by Sanger dideoxy sequencing using priEGFP-339+, priEGFP-591+, priHRSV-B05-2916+, priHRSV-B05-3153+, priHRSV-3767-, priHRSV-B05-4109-, priHRSV-B05-4524+, priHRSV-B05-5014+, priHRSV-B05-5555+, priHRSV-5599-, priHRSV-B05-6251+, priHRSV-6743+, and priHRSV-B05-7435+ (Appendix 1). Sequences were aligned with the computer

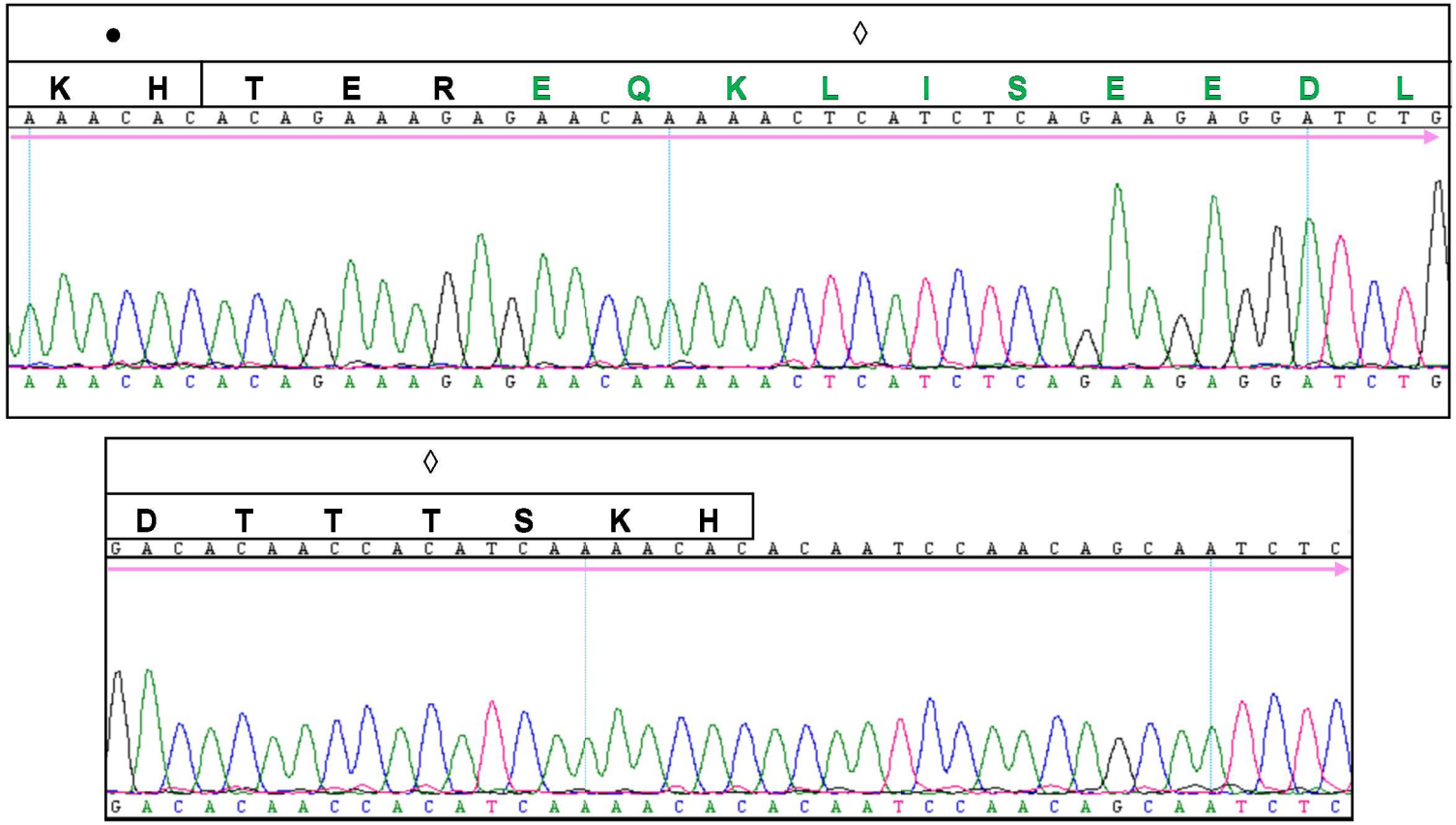

Figure 4.9: Sequence analysis of modification of the duplication in HRSV G protein gene. pHRSV^{B05}EGFP(5)Gmycb was sequenced by Sanger dideoxy sequencing to verify the sequence at the c-myc epitope tag encoding sequence substitution at the duplication in G protein gene. Sequences were aligned with the computer clone of pHRSV^{B05}Gmycb. The aligned sequence at the duplication modification within the HRSV G protein gene is shown. The duplication is indicated by boxes around the amino acid sequence and c-myc epitope tag amino acid sequence is denoted in green. G protein gene sequence is marked by pink arrow.

clone for pHRSV^{B05}EGFP(5)Gmycb using DNASTAR SeqMan Pro software and no spurious mutations were identified in the ATU and the G protein gene. The aligned sequence data for the duplication in G protein gene is presented in Figure 4.9. One point mutation (A8033C), which would result in E463D amino acid change in the F glycoprotein was identified (Figure 4.10).

pCG-HRSV^{B05}Gmycb was constructed using Gmycb sequence from pHRSV^{B05}EGFP(5)Gmycb. pCG-HRSV^{B05}GΔ60b (Figure 4.11A) was digested with *Mlu* I and *Pst* I (section 2.3.3) and the 4387 bp DNA fragment was gel extracted to produce a linear vector (section 2.3.4). An amplicon containing HRSV^{B05} G protein gene from pHRSV^{B05}EGFP(5)Gmycb (Figure 4.11B) was generated by PCR (section 2.3.5) using priRSV-B05-GORF+MluI and priRSV-B05-GORF-PstI (Appendix 1). These primers were used to add *Mlu* I restriction site upstream of the G protein gene sequences and *Pst* I restriction site downstream of the G protein gene sequences. The amplicon was purified and digested with *Mlu* I and *Pst* I (section 2.3.3). The 933 bp DNA fragment from the digestion was gel extracted to generate the insert (section 2.3.4). Vector and insert were ligated using T4 DNA ligase (section 2.3.7), one fourth of the ligation was transformed into *E. coli* DH5α competent cells, and transformations were plated onto LB agar plates containing ampicillin (section 2.3.8). Six colonies were amplified in liquid culture containing ampicillin and plasmids were isolated by small scale plasmid preparation (section 2.3.9). All plasmids were contained the insert

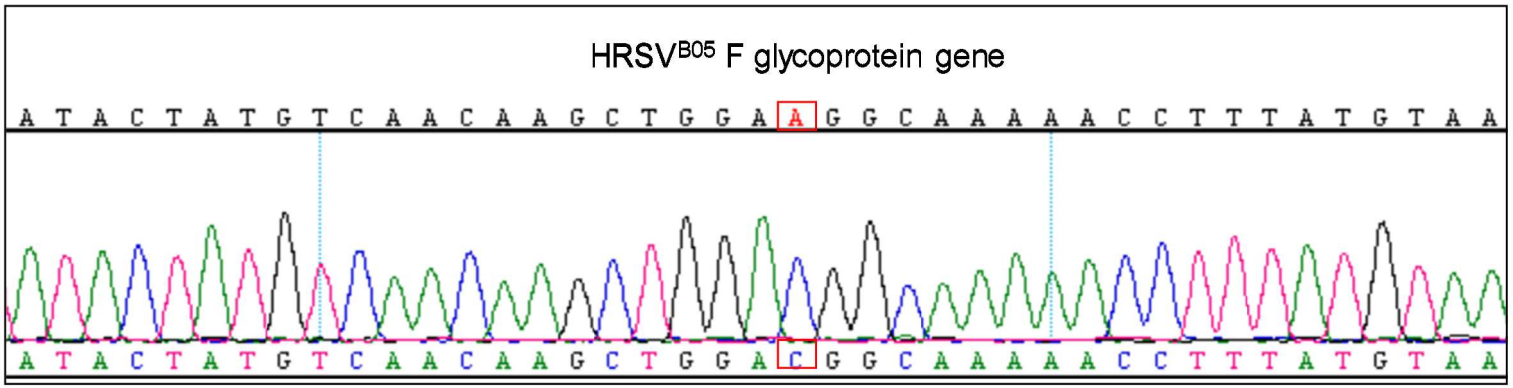

Figure 4.10: Sequence analysis of a single nucleotide mutation in F glycoprotein gene of pHRSV^{B05}EGFP(5)Gmycb.pHRSV^{B05}EGFP(5)Gmycb was sequenced by Sanger dideoxy sequencing to verify the sequence at the F glycoprotein gene. Sequences were aligned with the computer clone of pHRSV^{B05}Gmycb. The aligned sequence at the single nucleotide mutation in the HRSV F glycoprotein gene is shown. A8033C mutation shown in red here would result in E463D amino acid change in the F glycoprotein.

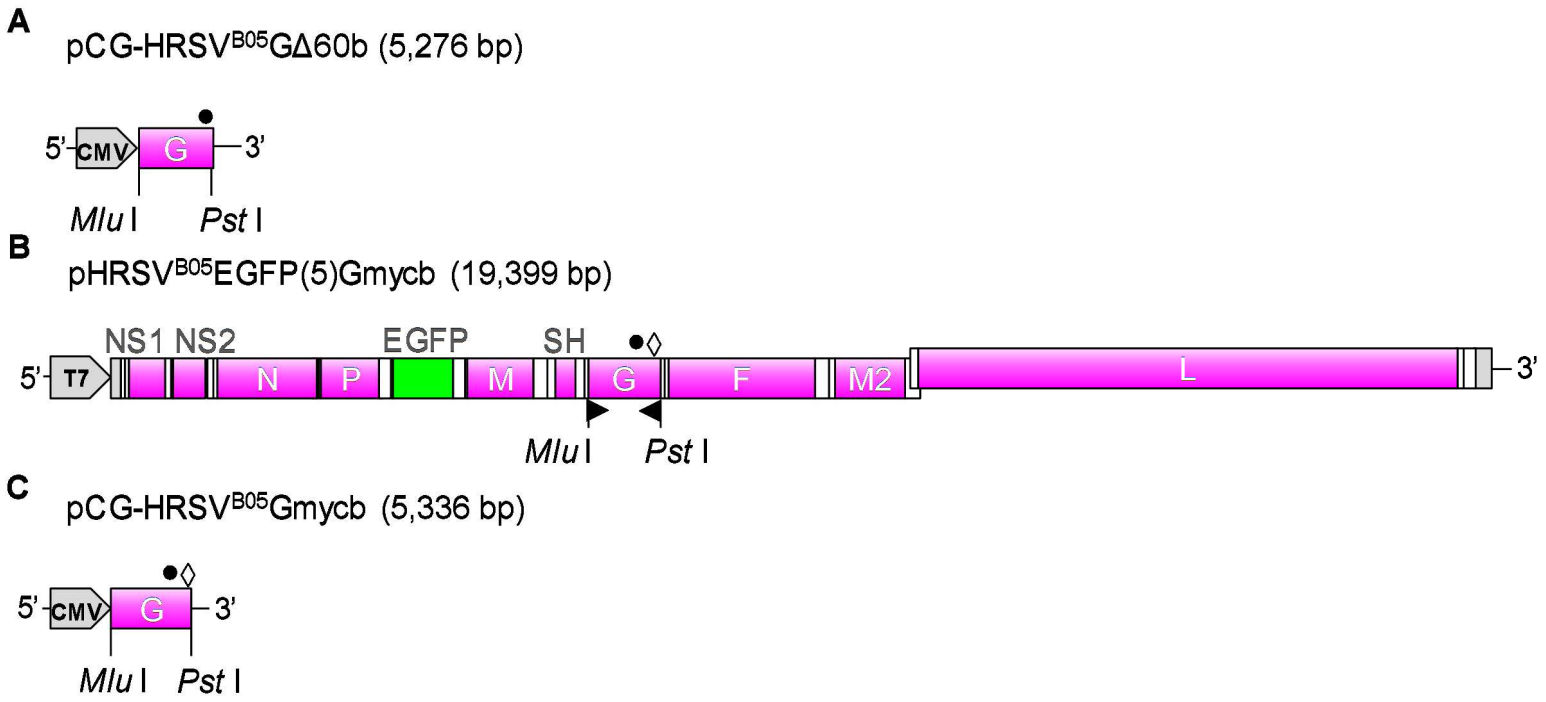

Figure 4.11: Schematic diagram of construction of pCG-HRSV^{B05}Gmycb. (A) pCG-HRSV^{B05}GΔ60b was digested with *Mlu* I and *Pst* I to generate the linear vector. (B) The G protein gene ORF of pHRSV^{B05}Gmycb was amplified by PCR using primer ► to add *Mlu* I restriction site upstream of G protein gene ORF and primer ◄ to add *Pst* I restriction sites downstream of the G protein gene ORF. The purified PCR product was digested with *Mlu* I and *Pst* I to generate the insert. (C) Schematic diagram of pCG-HRSV^{B05}Gmycb showing the two restriction sites used for cloning. The grey pentagons at the 5' end indicate either the CMV or T7 promoters used to control the expression of the plasmids.

when verified by restriction digest. A single bacterial clone was used for a large scale liquid culture containing ampicillin and plasmid was isolated by large scale plasmid preparation (section 2.3.10). Sequences of the plasmid at the restriction sites were verified by Sanger dideoxy sequencing (section 2.3.11) using pri-pCG+ and pri-pCG-b (Appendix 1). Sequences were aligned with the computer clone for pCG-HRSV^{B05}Gmycb (Figure 4.11C) using DNASTAR SeqMan Pro (section 2.3.1) and no spurious mutations were identified at the cloning sites (Figure 4.12).

4.6 Recovery of rHRSV^{B05}EGFP(5)Gmycb

rHRSV^{B05}EGFP(5)Gmycb was recovered using pHRSV^{B05}EGFP(5)Gmycb, which contained a point mutation in the F glycoprotein gene (section 2.2.2) (Figure 4.9). Five days after transfection of the antigenomic plasmid and the HRSV^{B05} expression plasmids (Figure 4.13A), six syncytia containing over thirty infected cells as determined by EGFP expression were picked and passaged onto HEp-2 cells (section 2.2.3). This virus was passaged twice to generate a rHRSV^{B05}EGFP(5)Gmycb P3 stock (Figure 4.13B). The titer determined to be $10^{5.81}$ $TCID_{50}$/ml by $TCID_{50}$ assay in Vero cells.

Following rHRSV rescue, passage, and sequencing, many spurious mutations and heterogeneity were seen in the ATU, G protein gene, and F glycoprotein gene. Therefore, those regions of rHRSV^{B05}EGFP(5)Gmycb P3 were sequenced first before sequencing the full-length genome. RNA was extracted

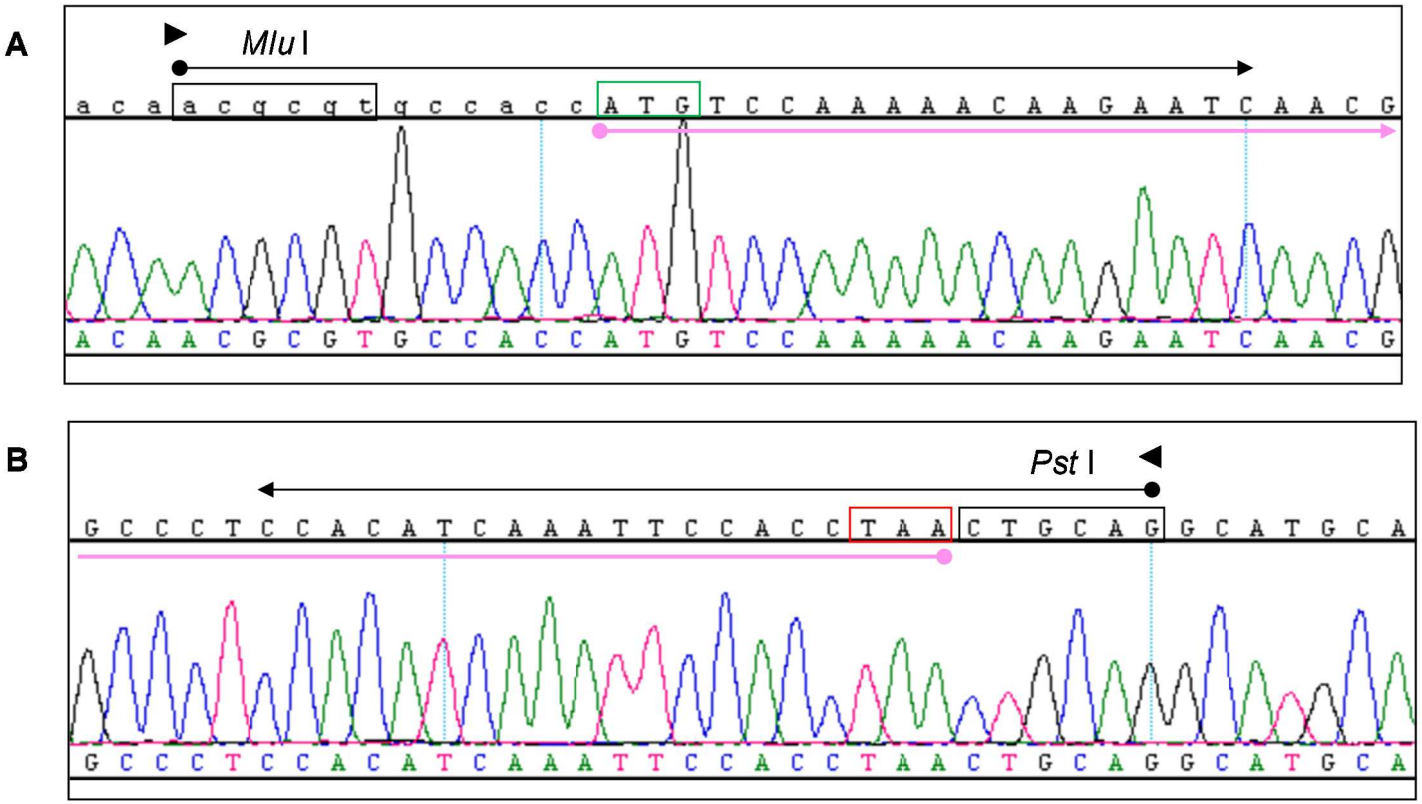

Figure 4.12: Sequence analysis of pCG-HRSV^{B05}Gmycb over the ligation sites. Sequence of pCG-HRSV^{B05}Gmycb was verified by Sanger dideoxy sequencing. Sequences were aligned with sequence of its computer clone for pCG-HRSV^{B05}Gmycb and the electrochromatogram across the restriction sites used are shown here. (A) *Mlu* I site upstream of HRSV^{B05} G protein gene (pink arrow) is enclosed in black box and the start codon for G protein gene is enclosed in a green box. The primer used to insert in the *Mlu* I site for cloning is marked by ►. (B) *Pst* I site downstream of HRSV^{B05} G protein gene (pink line) is enclosed in black box and the G protein gene stop codon is enclosed in a red box. The primer used to insert in the *Pst* I site for cloning is marked by ◄.

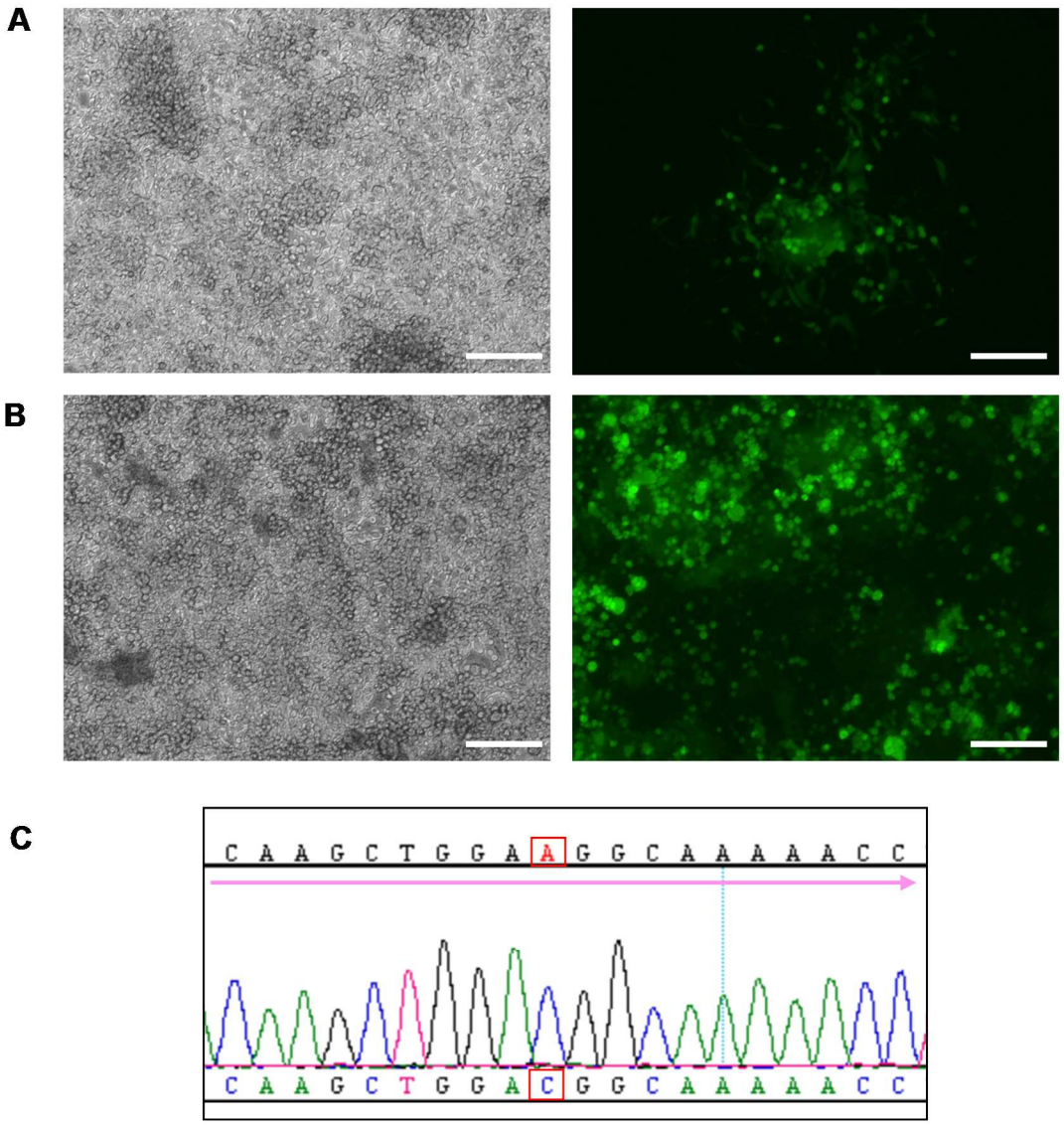

Figure 4.13: Photomicrographs of rHRSV^{B05}EGFP(5)Gmycb recovery, P3 stock generation, and stock sequence analysis. (A) Primary rescue of rHRSV^{B05}EGFP(5)Gmycb in HEp-2 cells. Photomicrographs were obtained 5 d.p.t. when the plaque shown was used for passage 1 infection. (B) HEp-2 cells were infected with rHRSV^{B05}EGFP(5)Gmycb P2 and photomicrographs were obtained 4 d.p.i. The supernatant from this infection was used to generate rHRSV^{B05}EGFP(5)Gmycb P3 stock. Scale bar = 200 µm. (C) Electrochromatogram showing the A8033C mutation in F glycoprotein gene (pink arrow) that was observed in rHRSV^{B05}Gmycb P3 stock. This mutation was present in the pHRSV^{B05}EGFP(5)Gmycb used for the recovery of the rHRSV.

from rHRSV^{B05}EGFP(5)Gmycb P3 (section 2.3.12) and cDNA containing rHRSV^{B05} ATU, G protein gene, F glycoprotein gene were reverse transcribed using priHRSV-B05-2554+ (section 2.3.14) (Appendix 1). Three overlapping amplicons were generated (section 2.3.14) and they were sequenced by Sanger dideoxy sequencing (section 2.3.11) Sequences were aligned with the computer clone of rHRSV^{B05}EGFP(5)Gmycb using DNASTAR SeqMan Pro software (section 2.3.1). No spurious mutations were identified from the ATU and G protein gene sequences. As expected, the mutation (A8033C) was present in the virus stock (Figure 4.13C).

4.7 Characterization of rHRSV^{B05}EGFP(5)Gmycb

Immunoblot analysis was performed to examine HRSV^{B05} Gmycb protein expression in rHRSV^{B05}EGFP(5)Gmycb P3 infected HEp-2 cells in MLD2. Uninfected HEp-2 cells were used as a control. To generate positive control sample for anti-myc antibody, HEp-2 cells were transfected with pCG-Venus-cmyc, expressing a Venus/c-myc fusion protein. Venus is a 26.4 kDa yellow fluorescent protein derivative. HEp-2 cells were either transfected with pCG-HRSV^{B05}Gmycb or infected with rHRSV^{B05}EGFP(5)Gmycb at an MOI of 0.1. Lysates were prepared and samples were used for immunoblot analysis (section 2.2.10). The c-myc epitope tag was detected using a mouse anti-c-myc antibody and human β-actin was detected by mouse anti-β-actin antibody. Primary antibodies were detected using an anti-mouse IRDye 800CW secondary antibody. An image of the exposed

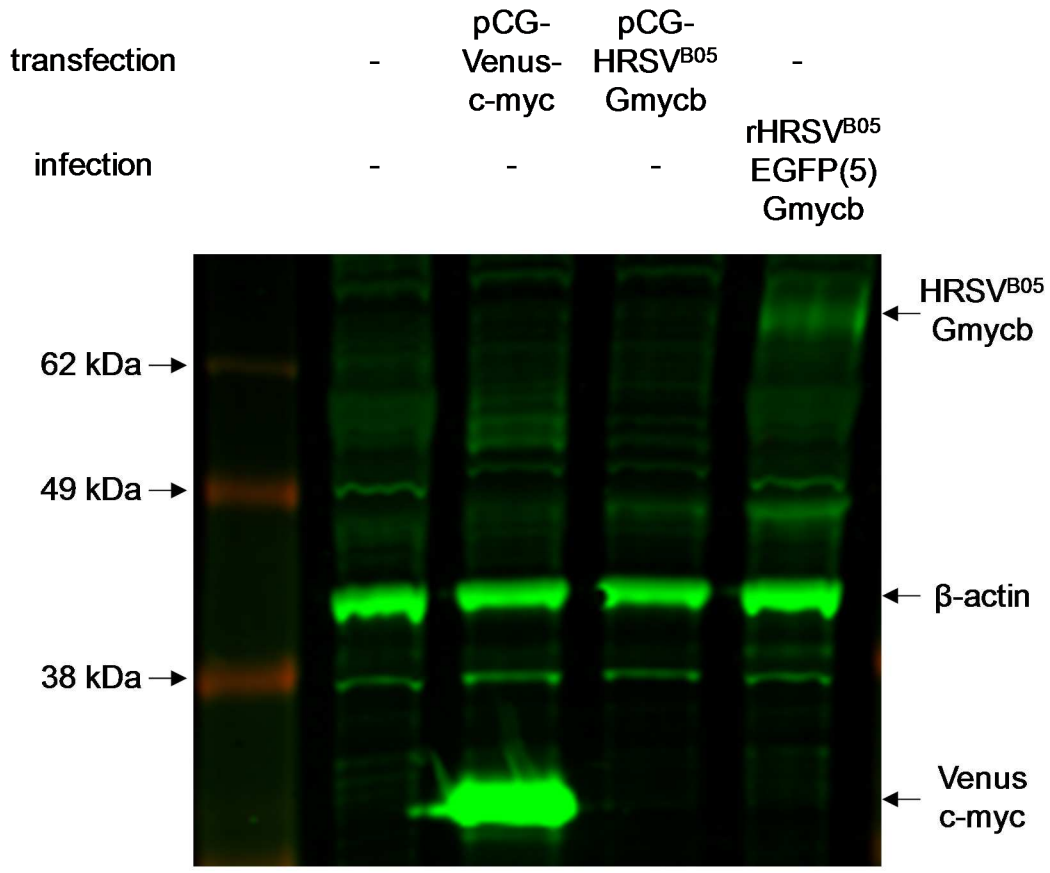

Figure 4.14: Detection of HRSV Gmycb protein by immunoblot analysis. HEp-2 cells were transfected with pCG-Venus-cmyc, transfected with pCG-HRSV^{B05}Gmycb, or infected with rHRSV^{B05}EGFP(5)Gmycb. At 3 d.p.t./d.p.i., cells lysates were used for immunoblot analysis. c-myc tagged proteins were detected with mouse anti-myc antibody. Human β-actin was detected in all samples by mouse anti-β-actin antibody. Both of the primary antibodies were detected using anti-mouse IRDye 800CW secondary antibody.

blot was obtained using an Odyssey CLx Imaging System (Figure 4.14). Specific binding of c-myc epitope tag by the anti-myc antibody was confirmed by Venus/c-myc fusion protein. There was a signal at approximately 30 kDa in cell lysates prepared from the pCG-Venus-cmyc transfected sample which corresponded to Venus/c-myc fusion protein. A protein was detected at approximately 90 kDa corresponding to $HRSV^{B05}$ Gmycb protein in $rHRSV^{B05}$EGFP(5)Gmycb infected lysates. $HRSV^{B05}$ Gmycb protein was not detected in the lysates obtained from HEp-2 cells transfected with pCG-$HRSV^{B05}$Gmycb. However, loading control β-actin was detected in all samples.

Indirect immunofluorescence was used to examine $HRSV^{B05}$ Gmycb localization in $rHRSV^{B05}$EGFP(5)Gmyc infected cells. HEp-2 cells, grown on glass coverslips in a 6 well plate, were infected with $rHRSV^{B05}$EGFP(5)Gmycb at an MOI of 0.1. Growth medium was changed at 1 d.p.i., cells were rinsed with DPBS, fixed with 4% (w/v) paraformaldehyde, and permeabilized with 0.5% (v/v) Triton-X100. Cells were treated with non-specific binding blocking reagents and $HRSV^{B05}$ Gmycb proteins were detected using mouse anti-myc epitope tag primary antibody and anti-mouse AlexaFluor 647 secondary antibody (section 2.2.11). Coverslips were mounted onto glass microscope slides using VECTASHIELD HardSet DAPI mounting solution. Cells were observed by UV microscopy and photomicrographs

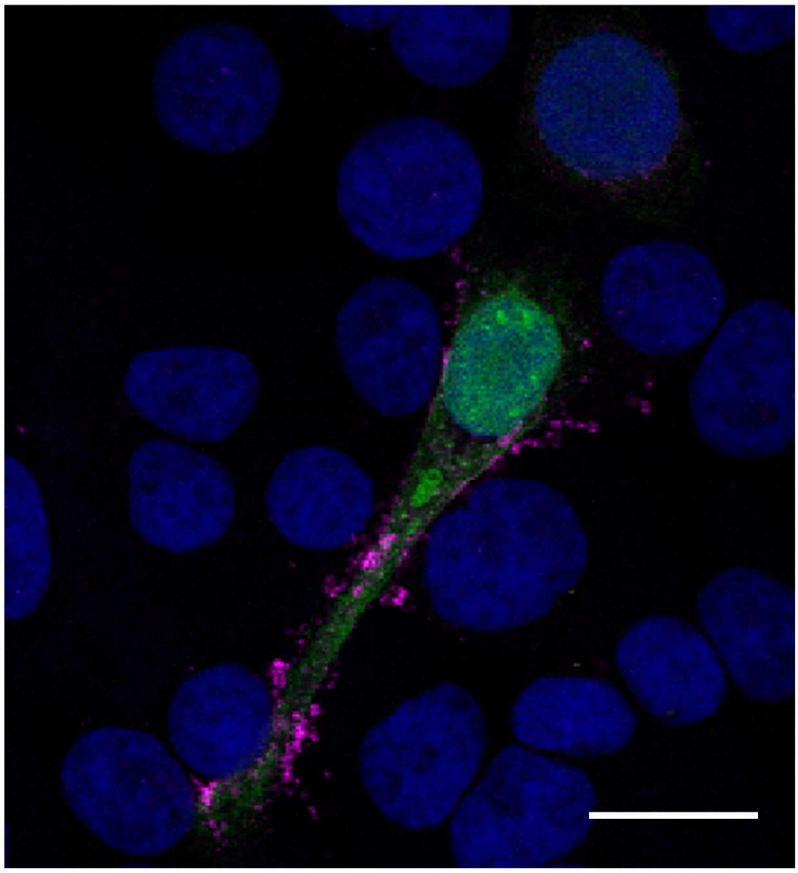

Figure 4.15: Examination of HRSV^{B05} Gmycb protein expression by indirect immunofluorescence. HEp-2 cells grown on coverslips were infected with rHRSV^{B05}EGFP(5) at an MOI of 0.1 and at 1 d.p.i. the cells were fixed and permeabilized. c-myc epitope tag was detected using mouse anti-myc primary antibody and anti-mouse AlexaFluor 647 secondary antibody. Cells on coverslips were mounted onto a glass slide using DAPI mounting medium and were photomicrographs were obtained by confocal laser scanning microscopy. In this photomicrograph, infected cell can be identified by EGFP expression (green), nuclei by DAPI stain (blue), and HRSV Gmycb protein by AlexaFluor647 (magenta). Scale bar = 20 µm.

were obtained using CLSM (Figure 4.15). Photomicrograph showed that rHRSV^{B05}EGFP(5)Gmycb infected cells express EGFP in the cytoplasm and Gmycb proteins seem to be localized to the area surrounding the cytoplasm. Further investigation using a membrane stain will be necessary to confirm membrane expression of Gmycb proteins.

CHAPTER 5: SUB-CELLULAR LOCALIZATION OF HRSV POLYMERASE

5.1 Generation of an expression plasmid for modified HRSV L protein

pCG-HRSV^{B05}LVenus, a plasmid expressing LVenus, was generated to study the effects of insertion of a fluorescent protein ORF into the VR between CRV and CRVI of the L gene of HRSV. The plasmid was constructed using pCG-HRSV^{B05}L and pHRSV^{B05}LVenus (Dr. Ken Lemon, QUB and Dr. Linda Rennick, BU). pCG-HRSV^{B05}L (Figure 5.1A) was digested with *Cla* I (section 2.3.3), the 7,733 bp DNA fragment was gel extracted (section 2.3.4), and dephosphorylated using Antarctic phosphatase to generate a linear vector (section 2.3.7). pHRSV^{B05}LVenus (Figure 5.1B) was digested with *Cla* I (section 2.3.3) and the 3,954 bp DNA fragment was gel extracted to generate the insert (section 2.3.4). Vector and insert were ligated using T4 DNA ligase (section 2.3.7) and one fourth of the ligation was used to transform *E. coli* DH5α competent cells. Transformed cells were plated onto LB agar plates containing ampicillin. Eight colonies were amplified in liquid culture containing ampicillin and plasmids were isolated by small scale plasmid preparation (section 2.3.9). Plasmids were verified by restriction digestion (section 2.3.3), and three plasmids contained the insert (data not shown). Two of the plasmids were sequenced across the *Cla* I restriction sites by Sanger dideoxy sequencing (section 2.3.11) using pri-pCG-b, and priRSV-B-11038+ (Appendix 1). Sequences were aligned to the computer clone of pCG-HRSV^{B05}LVenus (Figure 5.1C) using DNASTAR SeqMan Pro software (section 2.3.1) and no spurious

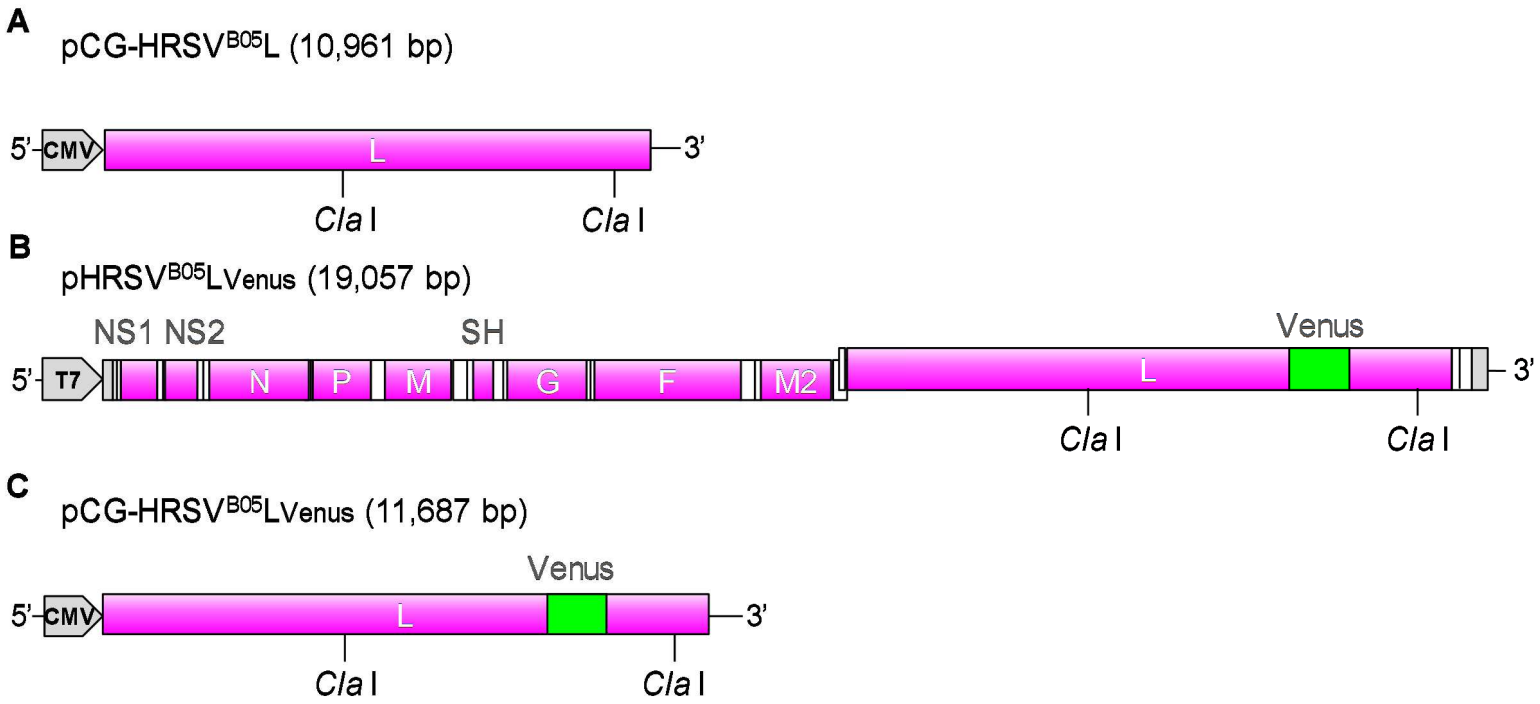

Figure 5.1: Schematic diagram of construction of pCG-HRSV^{B05}LVenus. (A) pCG-HRSV^{B05}L was digested with *Cla* I to generate the 7733 bp linear vector. (B) pHRSV^{B05}LVenus was digested with *Cla* I to generate the 3954 bp insert. (C) A schematic diagram of pCG-HRSV^{B05}LVenus and the *Cla* I sites used for cloning. The grey pentagons at the 5' end indicate either the CMV or T7 promoters used to control the expression of the plasmids.

mutations were found across the *Cla* I sites (Figure 5.2). A single clone was amplified in large liquid culture containing ampicillin and plasmids was isolated by large scale plasmid preparation (section 2.3.10).

5.2 Modified HRSV L protein retains polymerase activity in mini-genome assay

A mini-genome replication-transcription assay was performed to compare the RdRp activity of HRSV^{B05} L protein and HRSV^{B05} LVenus protein. RdRp activity of unmodified and modified HRSV^{B05} L proteins are similar in minigenome replication-transcription assay independent of the amount of L protein expression plasmid added (Figure 5.3). Data provided by Dr. Linda Rennick (BU).

5.3 Characterization of rHRSV^{B05}LVenus recombinant virus

rHRSV^{B05}LVenus was recovered from a full-length cDNA clone by Dr. Linda Rennick (BU). The growth kinetics of this virus was compared with rHRSV^{B05}EGFP(5) by multi-step growth analysis. HEp-2 cells were infected with rHRSV^{B05}EGFP(5) or rHRSV^{B05}LVenus viruses at an MOI of 0.2. Supernatants from triplicate wells were collected, mixed with 50% (w/v) sucrose solution, and frozen at -80°C from 18 h.p.i. to 96 h.p.i., The virus titer in the supernatant at each time point was measured by $TCID_{50}$ assay in Vero cells. The two viruses had similar growth kinetics with titer of less than 10^3 $TCID_{50}$/ml at 18 h.p.i. and reaching peak titer at 72 h.p.i. with titer of about 10^6 $TCID_{50}$/ml (Figure 5.4). This suggests

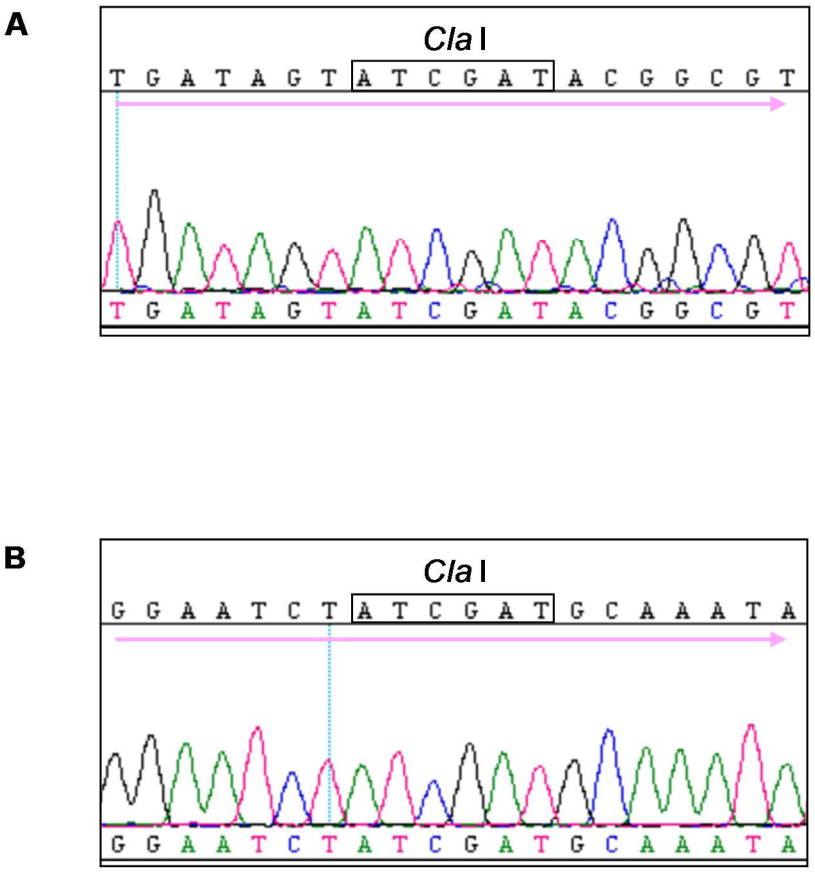

Figure 5.2: Sequence analysis of pCG-HRSV^{B05}LVenus across the cloning restriction sites. Sequences were aligned with the computer clone of pCG-HRSV^{B05}LVenus using DNASTAR SeqMan Pro software (A) Sequence across the first *Cla* I site (black box) in pCG-HRSV^{B05}LVenus L protein gene (pink arrow) (B) Sequence across the second *Cla* I site (black box) in pCG-HRSV^{B05}LVenus L protein gene (pink arrow).

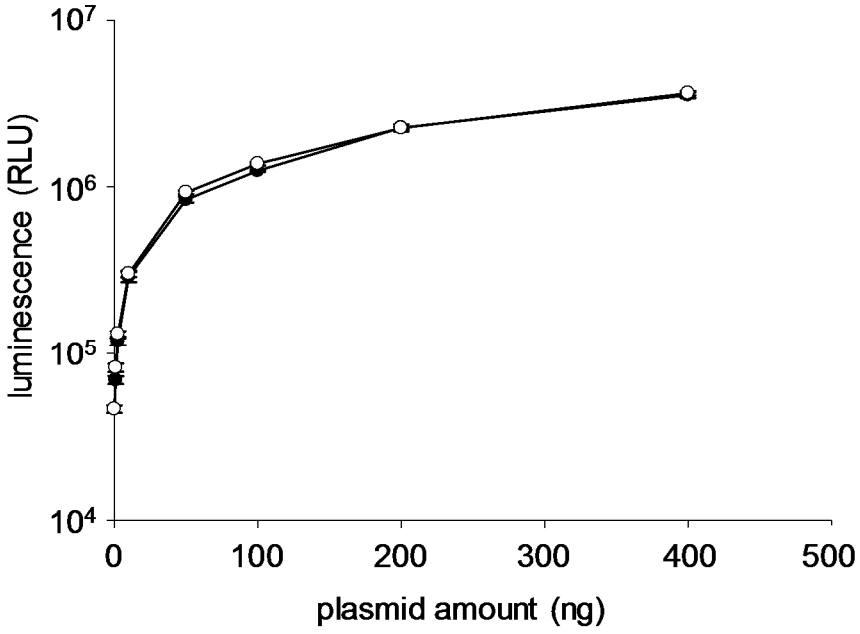

Figure 5.3: Minigenome replication-transcription assay to compare the RdRp acitivty of HRSV^{B05} L protein and HRSV^{B05} LVenus protein. HRSV^{B05} L protein (●) and HRSV^{B05} LVenus protein (○) were used in a minigenome replication-transcription assay. Plasmids expressing HRSV^{B05} N (1.6 µg), P (1.2 µg), and M2-1 (0.8 µg), and L (0.4 µg) proteins and HRSV^{B05} minigenome (1 µg) expressing *Gaussia* luciferase were transfected into HEp-2 cells infected with MVA-T7 in triplicate. Luciferase expression was measured 48 h.p.t. by detecting luminescence as measured in relative light unit (RLU). Data provided by Dr. Linda Rennick, BU.

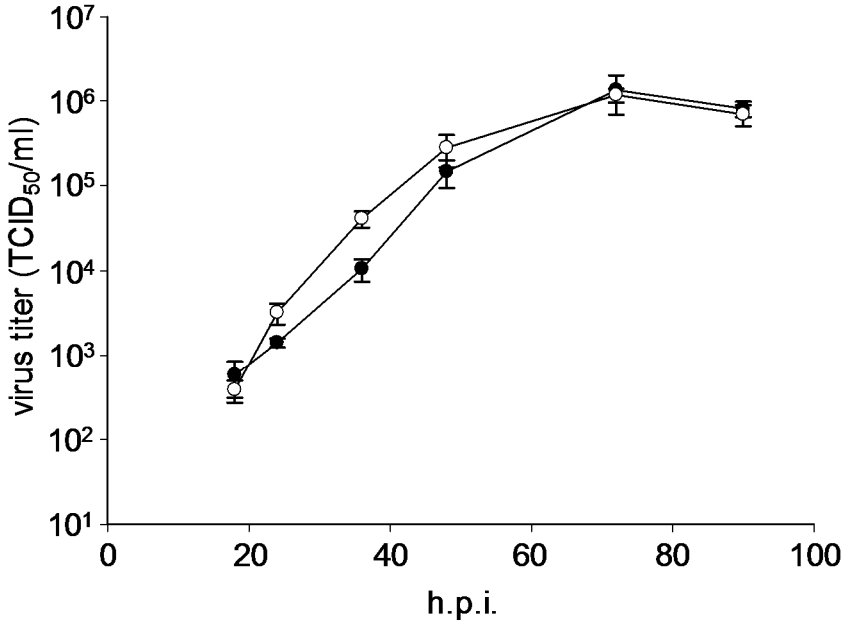

Figure 5.4: Multi-step growth analysis of rHRSV^{B05}EGFP(5) and rHRSV^{B05}LVenus. HEp-2 cells were infected with either rHRSV^{B05}EGFP(5) (●) or rHRSV^{B05}LVenus (○) at MOI of 0.2 in triplicate. Supernatant from the triplicate wells were collected at 18, 24, 36, 48, 72, and 90 h.p.i. and used for $TCID_{50}$ assay in Vero cells to determine virus titer at each timepoint. The rHRSV^{B05}EGFP(5) data is presented in Figure 3.13, but is compared with the rHRSV^{B05}LVenus data, because the two growth kinetics assays were set up simultaneously under identical conditions.

modification of HRSV L protein by insertion of Venus protein in its VR did not affect virus replication *in vitro* in HEp-2 cells.

HEp-2 cells, grown in glass-bottom dishes, were infected with rHRSV^{B05}LVenus at an MOI of 0.02 to examine the expression and localization of LVenus protein (section 2.2.12). Infected cells were observed by UV microscopy 17 h.p.i. Cellular membranes were detected with wheat germ agglutinin conjugated to AlexaFluor 594 and nuclei were detected with NucBlue Live ReadyProbes. Cells were supplemented with VectaCell Trolox Antifade Reagent in Leibovitz L-15 medium with 20% (v/v) FBS and 100 U/ml of penicillin-streptomycin (section 2.2.12). Leibovitz L-15 medium supports cell maintenance in the absence of 5% (v/v) CO_2 and penicillin-streptomycin was used to prevent contamination. Living cells were imaged by CLSM with Leica TCS SP5 at 48 h.p.i. This demonstrated that the HRSV LVenus proteins were expressed and localized in inclusion bodies of various sizes, which are marked with white arrows (Figure 5.5).

5.4 Modified HRSV L protein is equally sensitive to ribavirin

Presence of Venus in the L protein of HRSV^{B05} had no effect on function and virus infectivity was equivalent to that of parental virus, rHRSV^{B05}, *in vitro*. Ribavirin is a guanosine analog, which is the only FDA approved antiviral for HRSV. It was used to examine if HRSV^{B05} LVenus protein and rHRSV^{B05}LVenus could be used to study

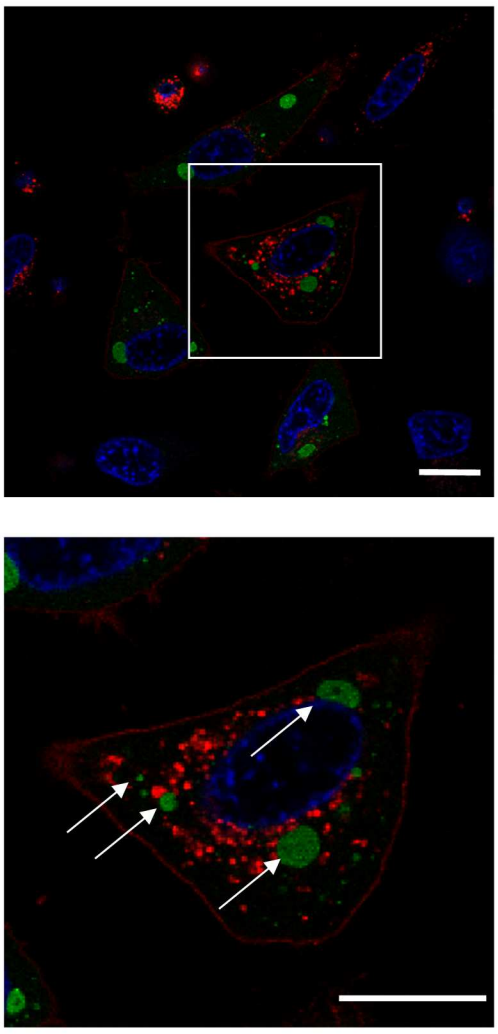

Figure 5.5: Confocal laser scanning microscopy live-cell photomicrographs of HEp-2 cells infected with rHRSV^{B05}LVenus. HEp-2 cells, infected with rHRSV^{B05}LVenus (green) at an MOI of 0.02, were stained for cell membrane with wheat germ agglutinin AlexaFluor 594 (red), and for nuclei with NucBlue ReadyProbe (blue) at 16 h.p.i. Photomicrograph was taken at 48 h.p.i. using Leica SP5 CLSM. Photomigrograph above shows a square inset which is magnified below. Arrows show the inclusion bodies containing LVenus proteins. Scale bar = 20 µm.

the effects of antiviral compounds on RdRp function and intracellular localization of the polymerase.

A mini-genome replication-transcription assay was carried out in the absence or presence of varying amounts of ribavirin to compare its inhibitory effect on modified and unmodified HRSV^{B05} L protein (Dr. Linda Rennick, BU). A mini-genome replication-transcription assay was performed in the presence or absence of various concentrations of ribavirin (1 μM, 5 μM, 10 μM, and 40 μM). RdRp activity of unmodified and modified HRSV^{B05} L protein were similar in each ribavirin treatment, with samples with luminescence of over 10^6 RLU when untreated and luminescence of under 10^4 RLU with 40 μM ribavirin treatment (Figure 5.6). This demonstrates that the HRSV^{B05} L protein activity in the presence of ribavirin was not affected by the presence of Venus in HRSV^{B05} L protein *in vitro* mini-genome replication-transcription assay.

The effects of ribavirin on the replication and transcription in the context of a virus infection was examined. HEp-2 cells, plated in 96-well plates, were infected with rHRSV^{B05}EGFP(5) or rHRSV^{B05}LVenus at an MOI of 0.2. Infected cells were treated with 0.1 μM, 1 μM, 5 μM, 7.5 μM, 15 μM, 30 μM, or 40 μM of ribavirin or left untreated. Phase-contrast and UV photomicrographs were obtained at 46 h.p.i. A decrease in fluorescence as the concentration of ribavirin increased was observed (Figure 5.7). In rHRSV^{B05}LVenus infected cells, Venus expression was

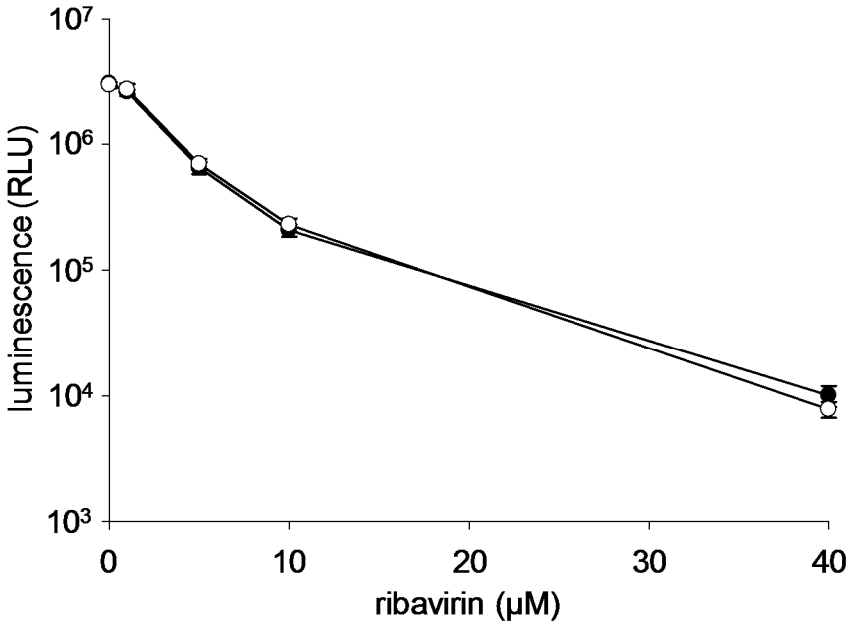

Figure 5.6: Minigenome replication-transcription assay to assess HRSV L protein and HRSV LVenus protein RdRp activity in the presence of ribavirin. Plasmids expressing HRSV^{B05} L protein (●) and HRSV^{B05} LVenus protein (○) were used in a minigenome replication-transcription assay. Plasmids expressing HRSV^{B05} N (1.6 μg), P (1.2 μg), and M2-1 (0.8 μg), and L (0.4 μg) proteins and HRSV^{B05} minigenome (1 μg) expressing *Gaussia* luciferase were transfected into HEp-2 cells infected with MVA-T7 and treated with ribavirin in triplicate. Luciferase expression was measured 48 h.p.t. by detecting luminescence as measured in relative light unit (RLU). Data provided by Dr. Linda Rennick, BU.

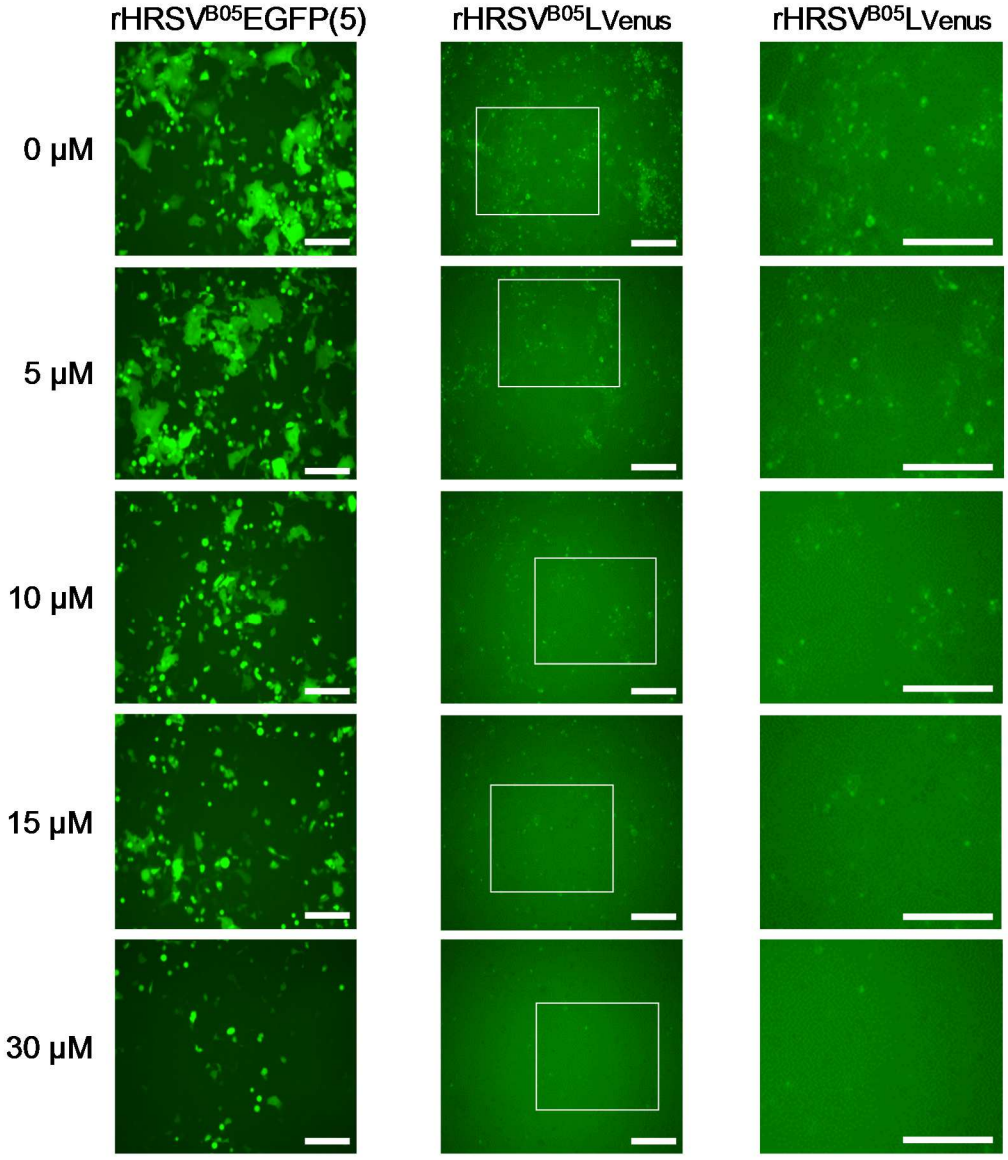

Figure 5.7: Photomicrographs of HEp-2 cells infected with rHRSV^{B05}EGFP(5) and rHRSV^{B05}LVenus in the presence of varying concentrations of ribavirin. HEp-2 cells treated with varying concentration of ribavirin were infected with rHRSV^{B05}EGFP(5) or rHRSV^{B05}LVenus at an MOI of 0.2 in triplicate. At 46 h.p.i. the infected cells were observed by UV microscopy and photomicrographs were obtained. The brightness and contrast were increased to make the inclusion bodies more visible in rHRSV^{B05}LVenus. The third column shows x2 magnification of the white boxes in photomicrographs from column 2. Scale bar = 100 µm.

localized to inclusion bodies. In rHRSV^{B05}EGFP(5) infected cells, EGFP expression was diffuse throughout the cytoplasm. Supernatants from infected cells were collected and the titers were measured by $TCID_{50}$ assay in Vero cells (section 2.2.6). These were similar for the two viruses indicating that they were equally sensitive to ribavirin (Figure 5.8). Untreated samples contained 10^5 to $10^{5.4}$ $TCID_{50}$/ml of virus and 40 µM ribavirin treatment decreased the titer to around 10^4 to $10^{3.3}$ $TCID_{50}$/ml for both viruses. Cells were collected and lysed with Laemmli buffer and used for immunoblot analysis (section 2.2.10). HRSV^{B05} proteins were detected using goat polyclonal anti-HRSV primary antibody and anti-goat IRDye 680RD secondary antibody. Images of immunoblot was obtained using LI-COR Oddyssey CLx imaging system and the N protein expression was quantified using LI-COR Image Studio software. Expression of N protein relative to untreated rHRSV^{B05}EGFP(5) infection and untreated rHRSV^{B05}LVenus infection was plotted for each ribavirin concentration. The N protein expression decreased equivalently for both viruses in the presence of increasing concentration of ribavirin (Figure 5.9).

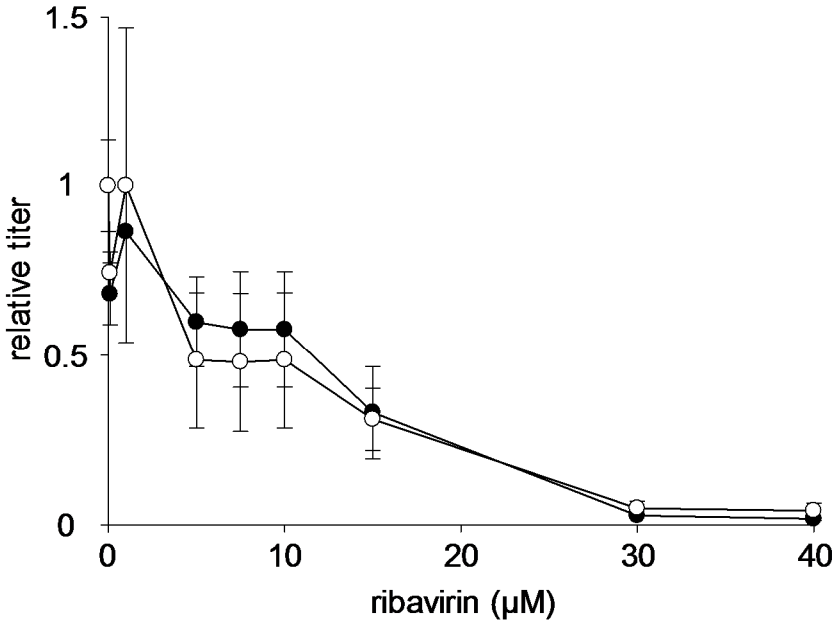

Figure 5.8: Comparison of the ribavirin sensitivity of rHRSV^{B05}EGFP(5) and rHRSV^{B05}LVenus. HEp-2 cells were treated with varying concentration of ribavirin and infected with rHRSV^{B05}EGFP(5) (●) or rHRSV^{B05}LVenus (○) at an MOI of 0.2 in triplicate. Supernatant from infected cells were taken at 46 h.p.i. and the titer was determined by $TCID_{50}$ assay in Vero cells. Data is presented as titer with each ribavirin treatment relative to the untreated HEp-2 cell control.

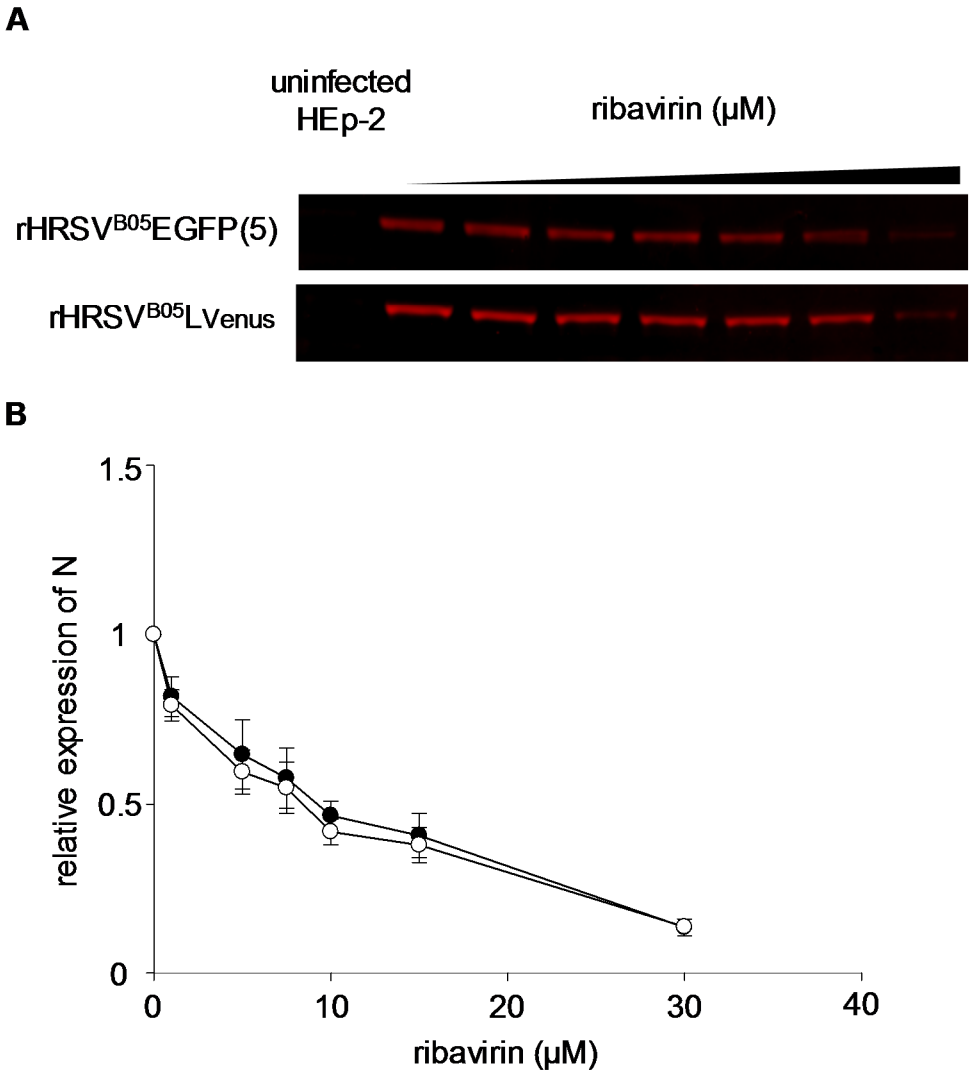

Figure 5.9: Western blot analysis to compare ribavirin sensitivity of rHRSV^{B05}EGFP(5) and rHRSV^{B05}LVenus. HEp-2 cells were treated with varying concentration of ribavirin and infected with rHRSV^{B05}EGFP(5) (●) or rHRSV^{B05}LVenus (○) at an MOI of 0.2 in triplicate. Cell lysates were used for Western blot analysis at 46 h.p.i. A polyclonal anti-HRSV primary antibody and IRDye 680RD secondary antibody (red) were used to detect HRSV proteins. (A) An image of the blots showing bands corresponding to HRSV N protein. (B) HRSV N protein expression was quantified using LI-COR Image Studio. Relative expression of N in each treatment group to the N protein expression in the untreated sample is shown.

CHAPTER 6: DISCUSSION

6.1 Generation of rHRSV to study A and B antigenic subtypes

Molecular characterization of HRSV antigenic subtypes A and B suggests a role of immune pressure in the prevalence of one subtype over another in a geographical region during a HRSV season (Melero and Moore, 2013). Short-lived subtype specific immunity has been described as the cause for this phenomenon from sequence analysis of circulating HRSV strains in various geographical regions (Agoti et al., 2015; Bose et al., 2015; Botosso et al., 2009; Tan et al., 2012). Understanding the basic differences in fitness of the two HRSV subgroups, comparing the pathology caused by each subgroup, and investigating the interplay between host immunity to strains of each subgroup is crucial in understanding the HRSV circulation patterns and development of vaccines (Coggins et al., 1998; Papadopoulos et al., 2004; Peret et al., 2000; Sullender, 2000).

Chapter 3 of this thesis describes generation of multiple rHRSVs, to be used in functional assays *in vitro* and *in vivo* to compare the antigenic subtypes of HRSV and the host immunity to strains of each subgroup. $HRSV^{A11}$, HRSV isolated in 2011, was chosen as the representative strain for HRSV antigenic subtype A. pCG-$HRSV^{A11}$L was generated to recover $rHRSV^{A11}$ using $HRSV^{A11}$ helper plasmids (section 3.1). p$HRSV^{A11}$EGFP(5) was constructed (section 3.2) and used to recover r$HRSV^{A11}$EGFP(5) (section 3.3). Identification of infected cells were

easier in rHRSV^{A11}EGFP(5) infection *in vitro* (Figure 3.7) as compared to rHRSV^{A11} infection (Figure 3.6) due to the expression of EGFP. This will be valuable in visualizing infected cells and identifying rHRSV^{A11}EGFP(5) infection in co-infection models. pHRSV^{B05}dTom(5) was constructed (section 3.4) to be used in recovery of rHRSV^{B05}dTom(5) (section 3.5). This HRSV B subtype virus demonstrated similar growth kinetics as a rHRSV^{B05}EGFP(5) (Lemon et al., 2015) (section 3.6). When the RNA genome ends of the three rHRSVs generated, rHRSV^{A11}, rHRSV^{A11}EGFP(5), rHRSV^{B05}dTom(5), were analyzed by RACE (section 2.3.16), a heterogeneity at nucleotide 1 was observed for all (figures 3.8 and 3.12). Further analysis is necessary to determine whether this heterogeneity is due to a population of viruses which contain a uracil at the first nucleotide. Alternatively, this could be due to a population of viruses in which the first nucleotide was deleted and thymine appears in the electrochromatogram as an artifact due to the RACE protocol involving polyA tail step. Few other single nucleotide heterogeneity was observed for each of the rHRSV generated, but they were not identical between different rHRSVs (Figure 3.8, Figure 3.12).

Using the two viruses generated in this chapter, an *in vivo* study in cotton rats was planned. To confirm that rHRSV^{A11}EGFP(5) is able to infect cotton rat cells, cotton rat lung cells were infected (section 3.8). Similar to HEp-2 cell infection, infected cotton rat lung cells showed cell-to-cell fusion (Figure 3.15). HRSV microneutralization assay was optimized using human IVIG and human

serum (section 3.7) to develop a method to determine the presence of neutralizing antibodies in immunized cotton rats. A cotton rat co-infection study (Dr. Linda Rennick, BU) using rHRSV^{A11}EGFP(5) and rHRSV^{B05}dTom(5) confirmed that they can be visualized within the tissues of the infected cotton rats by UV microscopy (figure 6.1). This experiment confirms that the tools developed in this chapter can be used to study the differences between HRSV of subtype A and B not only *in vitro*, but also *in vivo.*

6.2 Generation of rHRSV to study the 60 nucleotide duplication in G protein gene

BA genotype of HRSV, containing 60 nt duplication that was first described in Buenos Aires in 1998, is now found circulating globally as a predominant HRSV B genotype (Trento et al., 2003, 2010). It has been hypothesized that this duplication confers an advantage to the virus, but the role of the duplication has not been investigated until recently (Hotard et al., 2015). A study published in 2015 characterized few functional differences of viruses with and without the 60 nt duplication (Hotard et al., 2015). A chimeric rHRSV containing the genome of A subgroup with a consensus G protein gene sequence from BA genotype viruses was used and a mutant of this rHRSV without duplication in G protein gene was generated. Data suggested that with the duplication, the virus binds to cells better *in vitro*, but there was no viral load difference in infection in mice with virus with and without duplication. We hypothesized that in addition to improved attachment, the duplication may also play a role in HRSV evasion of host's adaptive immune

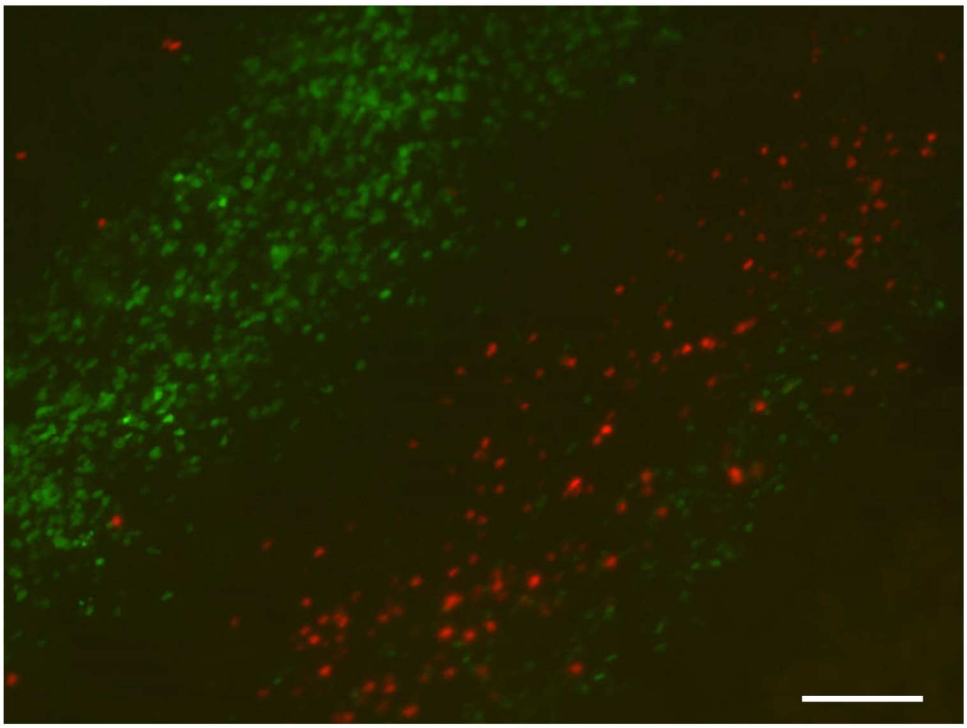

Figure 6.1: Photomicrograph of cotton rat septum after rHRSV^{A11}EGFP(5) and rHRSV^{B05}dTom(5) infection. Cotton rat was infected intranasally with equal amount of rHRSV^{A11}EGFP(5) and rHRSV^{B05}EGFP(5) and the nasal septum was observed at 4 d.p.i. using Leica DMI3000B inverted microscope. Data provided by Dr. Linda Rennick, BU. Scale bar = 200 µm

system. To limit the possible confounding factors resulting from using chimeric viruses, we used various rHRSVs generated from sequences of clinical isolates.

In Chapter 4, multiple rHRSV were generated for investigating the role of duplication within MLD2 in success of BA genotypes. rHRSV^{B05}EGFP(5) has been previously generated using a BA isolate from 2005 and it has been characterized (Lemon et al., 2015). Using pHRSV^{B05}EGFP(5), pCG-HRSV^{B05}GΔ60b and pHRSV^{B05}EGFP(5)GΔ60b were constructed (section 4.1 and 4.2). rHRSV^{B05}EGFP(5)GΔ60b was recovered using pHRSV^{B05}EGFP(5)GΔ60b in which the 60 nucleotides in the duplication has been deleted (section 4.3). Having rHRSV^{B05}EGFP(5) and rHRSV^{B05}EGFP(5)GΔ60b allowed study of two viruses in which the only differences are in the presence duplication in the G protein gene. A preliminary serial passaging experiment was developed with rHRSV^{B05}EGFP(5) and pHRSV^{B05}EGFP(5)GΔ60b in the absence of immune pressure (section 4.3) to prepare for future studies looking at the changes that accrue in the HRSV G protein gene in the presence of immune pressure. HEp-2 cells were infected with either virus and the supernatant at each infection was passaged for 20 passages. The sequence analysis of viruses collected at two different passages suggested that even in the absence of immune pressure there are many random mutations that arise throughout the G protein genes and that most are accumulated in MLD1 and CD (table 4.1). Further studies are needed to determine if the differences in the number of mutations that arise in the passaging of rHRSV^{B05}EGFP(5) and

pHRSV^{B05}EGFP(5)GΔ60b are significant and if MLD2 accumulates mutations as readily as MLD1 and CD. rHRSV^{B05}EGFP(5)Gmycb was recovered (section 4.5) using pHRSV^{B05}Gmycb (section 4.4) to study the changes at the site of duplication in HRSV G protein and to provide a method of detection of HRSV^{B05} G protein. Gmycb expression in rHRSV^{B05}EGFP(5)Gmycb infection was confirmed by immunoblot assay and indirect immunofluorescence (section 4.6).

The recombinant viruses generated in this chapter not only provides tools to study the duplication in G protein gene and the mutation that occur in the duplicated region, but also basic HRSV G protein biology. The localization of G protein and expression level in various conditions can be studied using rHRSV^{B05}EGFP(5)Gmycb, because Gmycb can be detected by c-myc antibodies that have been well characterized. Also, the serial passaging assay that was developed in chapter 4 can be modified by addition of immune pressure in the form of human IVIG, which has been shown to neutralize rHRSV^{B05}EGFP(5) (section 3.7). This experiment will investigate the number of mutations that accumulate in the HRSV G protein gene in the presence and absence of duplication, the location of mutations that arise, and the advantage conferred by the 60 nt duplication in the presence of immune pressure.

6.3 Generation of rHRSV to study L protein

HRSV L protein has been difficult to study due to its large size, problems with purifying the protein, and lack of good antibodies against the protein for analyzing expression and localization (Fearns and Plemper, 2017). One way to overcome some of these problems would be to generate an L-reporter fusion protein. This method of inserting reporter protein sequence into L protein sequence of other NNS virus has provided us with insights into localization and tolerance of the L protein to modification (Brown et al., 2005; Hoenen et al., 2012; Ruedas and Perrault, 2009). Many NNS viruses tolerate insertion of reporter protein sequence into VR between CR V and CR VI in L protein (Figure 1.2B). However, it also attenuates the virus (Brown et al., 2005; Duprex et al., 2002; Ruedas and Perrault, 2009; Silin et al., 2007). Investigators have inserted EGFP and mCherry sequences into the HRSV L expression plasmid at the sequence corresponding to VR. The resulting protein showed that there was downmodulation of RdRp activity of modified L protein in minigenome replication transcription assay (Fix et al., 2011).

In chapter 5, modified HRSV L protein fused with a yellow fluorescent protein derivative, L$_{Venus}$, and rHRSV^{B05} which expresses L$_{Venus}$ protein is presented. pCG-HRSV^{B05}L$_{Venus}$ (section 5.1), with the modification in the HRSV L gene, was generated. L$_{Venus}$ protein expressed by pCG-HRSV^{B05}L$_{Venus}$ retained RdRp activity in minigenome assay (section 5.2) and rHRSV^{B05}L$_{Venus}$ growth was

not affected by L protein modification as compared to the growth of rHRSV^{B05}EGFP(5) (section 5.3). CLSM analysis of rHRSV^{B05}LVenus infected cells show that LVenus can be visualized in infected cells (figure 5.5). In the future, with optimization of live-cell imaging protocol, formation of inclusion bodies containing HRSV RdRp in rHRSV^{B05}LVenus infected cells could be observed and trafficking of LVenus could be studied in living cells. Even with a lack of good HRSV L protein antibody, analysis of colocalization of LVenus with other HRSV proteins and host proteins becomes possible using rHRSV^{B05}LVenus as a tool.

rHRSV^{B05}EGFP(5) and rHRSV^{B05}LVenus are equally inhibited by ribavirin, a FDA approved treatment for HRSV infection. This is shown by the comparable virus titer and viral protein expression level in an infection in the presence of various concentrations of ribavirin (section 5.4). In the future, effects of novel HRSV inhibitors on HRSV L protein expression and localization could be studied using rHRSV^{B05}LVenus. This is important as more emphasis is put on finding HRSV inhibitors targeting HRSV L protein due to its essential role in HRSV infection (Fearns and Deval, 2016).

APPENDIX 1: PRIMER SEQUENCES

Primer name	**Sequence (5' - 3')**
priB05-15063+	ACCTTCCTAATGAACAGTAAC
priB05-204-	GCTAATGCATTAGTCAGAAG
pridTom240+PacI	TCACTGATTAATTAACTATCCGGATCCGGATCCCTTG
pridTom25+BssHII	GCAAATGCGCGCGAGATGGTGAGCAAGGGCGAGGAGGTC
priEGFP-339+	GAAGTTCGAGGGCGACAC
priEGFP-591+	CGACAACCACTACCTGAG
priEGFP-685+	GGGATCACTCTCGGCATG
priHRSV-A10-10076+	AGTTTCGGTTGCCTAAAAA
priHRSV-A10-10150-	TGTGTGACGGCATATAATTT
priHRSV-A10-103+	GCAGCAACTCATTGAGTG
priHRSV-A10-10401+	GTTCAAATATTAGCAGAG
priHRSV-A10-10771-	ATCCACTTTGCTCATCTACA
priHRSV-A10-11023+	AAGAGTATGCAGGAATAG
priHRSV-A10-11648+	CGTTACATTGATGAGAGATC
priHRSV-A10-12273+	GTTGGTTCATCTACACAAG
priHRSV-A10-12600+	ACTAGCCCTATTAATCGCATA
priHRSV-A10-12910+	ATTTAATATTGGCGCATAAG
priHRSV-A10-13291-	AGTTTGAAGCTATGACATCCT
priHRSV-A10-13537+	CTCATCTATTAACTAAAC

priHRSV-A10-14144+	ACCAATTGAGTTTTTAAG
priHRSV-A10-14854+	CATTTATATATGGTAGAATC
priHRSV-A10-15171-	AAAGTGTCAAAAACTAATATCTCG
priHRSV-A10-1569+	CCAGAATACAGGCATGACTC
priHRSV-A10-15838+	CGGCTTTCCCCGTCAAGCTC
priHRSV-A10-1946+	CATTATGTTAGGACACG
priHRSV-A10-2558+	CCCAATAAATGAGACAGATGA
priHRSV-A10-2576+	CAATTATCAAAGAAAGC
priHRSV-A10-2617-	AAGGATTATCACTTGGCGTA
priHRSV-A10-278-	AGGGCAAATATCACTACTTGT
priHRSV-A10-2803+	ACTAGGAATGCTTCACACATTAG
priHRSV-A10-2924-	CTTTTGCCATCTTTTCAC
priHRSV-A10-3203+	AGCCACCCAGAAAAAATC
priHRSV-A10-3285-	GCAGCTGTGTATGTGGAG
priHRSV-A10-3845+	TCAGGATTACTGTTAGTC
priHRSV-A10-42+	AAACTTGCGTAAACCAAAAA
priHRSV-A10-4390+	ATAATCTCCATCATGATTG
priHRSV-A10-4426+	GATTGCAATATTAAACAAACTC
priHRSV-A10-5046+	TTCAACAATACCAAGTGCTG
priHRSV-A10-5095-	GGTTTGCTAGGTGGTATTTG
priHRSV-A10-5305+	CAAAAAAACCAACCATCAAG
priHRSV-A10-5786-	CAACCAGTTCTTAGAGCACT

priHRSV-A10-6231+	TTAACCAGCAAAGTGTTAG
priHRSV-A10-6707+	GGATCAGTATCCTTTTTC
priHRSV-A10-7158+	AGAAAATTAATCAGAGTC
priHRSV-A10-7577+	CCAAATTAACTTACTATTTGTGAAA
priHRSV-A10-7607-	ATTTCGAATTTGCAAGGAT
priHRSV-A10-8168+	ACCATGCCAAAAATAATG
priHRSV-A10-8281-	CCGGTGGGTATATATAGTTA
priHRSV-A10-8617+	ATGGTCCTTATCTCAAAAATG
priHRSV-A10-8639-	GTGTTCTATTAATGGATTTTG
priHRSV-A10-9102+	CATTGGTTTAACTTATAC
priHRSV-A10-913+	GCACTTTCCCTATGCCAATA
priHRSV-A10-9781+	CAATGGTAGATGAAAGAC
priHRSV-A11-14918+	GAATTGTTAAACAGCTTGAC
priHRSV-A10-42+	AAACTTGCGTAAACCAAAAA
priHRSV-B05-10127+	TATCAGGATTGCGGTTCTAT
priHRSV-B05-10145-	TCATTTCAAGATCCACTTTTT
priHRSV-B05-10309+	AGCGACAGATCAAGAAGAGTACT
priHRSV-B05-10581-	TGACTTGTTGCTTATTCCTGCT
priHRSV-B05-10747+	ACTGCATGGGGTACAATCTCT
priHRSV-B05-11757+	GGATCCACAGGCTTTAGGGT
priHRSV-B05-12230+	AGTAGGAGTAACATCGCCAAGT
priHRSV-B05-12609+	CTGCCTCAATACCAGCTTAT

priHRSV-B05-1262+	ACACTCCCAATTATGATGTGCA
priHRSV-B05-12687-	TGTCGATATCTTCATCTCCA
priHRSV-B05-12815+	TCTCATACCGAAGCTGAATGAG
priHRSV-B05-13104-	ACCCCTCTCCCCAATCTTTT
priHRSV-B05-13598+	CTCTTTTACATTAGTTATAAC
priHRSV-B05-14176+	GTAGAACTTCATCCTGACATAAG
priHRSV-B05-14604+	CCTTACAATAGGCCCTGCAA
priHRSV-B05-15214-	AATGCACATGTGTGATTGTT
priHRSV-B05-169+	TTATTTGACAATGACGAAGTAGCA
priHRSV-B05-1745+	CGCTACAAGGGCCTAATACC
priHRSV-B05-2225+	GAGCAACTCAAAGAAAATGGAGT
priHRSV-B05-2554+	ATCAATCCAACAAGTGAAGC
priHRSV-B05-2579-	TAGGGGTTTTCTTGGGTAGT
priHRSV-B05-2916+	GAGCAGAAGCATTAATGACCAATG
priHRSV-B05-3084-	GTTGTTGATTGCTGAGTGAG
priHRSV-B05-33+	TGCGTACTACAAACTTGCACA
priHRSV-B05-3698+	CCACTCATGAGATCATTGCT
priHRSV-B05-3767-	GTTCAGGTCCTTGTTTTTGA
priHRSV-B05-3936+	GCCACAGAGTCAATTTATAGTGG
priHRSV-B05-4109-	TGTGATGAAGTGTGTAGTGT
priHRSV-B05-4524+	TCTCCCATTATGCTGTGTCAA
priHRSV-B05-5014+	CAAACAACCCACAACCACAC

priHRSV-B05-5087+	CACCATACAACAGCACAAAC
priHRSV-B05-5132+	CACAGAACAACAAGCCAAGCAC
priHRSV-B05-5555+	TCTCTCTACTCAACCACCCC
priHRSV-B05-5586-	ATGTGGAGGGCTCGGATGCTG
priHRSV-B05-5588+	CAACTCCACACAAACACCCAC
priHRSV-B05-5599-	AGGTGGAATTTGATGTGGAG
priHRSV-B05-5650-	GGTTCTCTGCTAAGATGTAGTTT
priHRSV-B05-5736+	ACCATGGAGTTGCTGATCCA
priHRSV-B05-5916-	TCAGTTCCATTGCATTTGGT
priHRSV-B05-6096+	TCTGGGCTTCTTGTTAGGTG
priHRSV-B05-6251+	TGCTGTCTACAAACAAAGCTG
priHRSV-B05-6503+	TAATGTCAAGCAATGTTCAG
priHRSV-B05-6743+	ACAAGGACTGATAGAGGATGGT
priHRSV-B05-6919+	GCTATAGTGTCATGCTATGG
priHRSV-B05-739+	CACCAAAGAAATCATCACACACA
priHRSV-B05-7435+	GAATCAATAATATTGCATTC
priHRSV-B05-7574+	TCATGCTACCCACACAACTA
priHRSV-B05-7609-	TTTAGTGTTGATTGCGATATTT
priHRSV-B05-7611-	GCAGGGATTTCTTCGCGAC
priHRSV-B05-7788+	TGCATTACTAGTGAGGCAAA
priHRSV-B05-7870-	AGAGCATATTCTTCTGTTCT
priHRSV-B05-8154-	TTGTGGATATCTAATGTGTTC

priHRSV-B05-8230+	ACCGTAAGTGATCAAAATGACCA
priHRSV-B05-8734+	ACAAAGCCCACTACTAGAGCA
priHRSV-B05-9476+	CTTAGGGTTGAGATGCGGATTC
pripCG+	CAGCTCCTGGGCAACGTG
pripCG-b	TTATTAGCCAGAAGTCAG
priRSV-A10-10401+	GTTCAAATATTAGCAGAG
priRSV-A10-11023+	AAGAGTATGCAGGAATAG
priRSV-A10-11648+	CGTTACATTGATGAGAGATC
priRSV-A10-12273+	GTTGGTTCATCTACACAAG
priRSV-A10-12910+	ATTTAATATTGGCGCATAAG
priRSV-A10-13537+	CTCATCTATTAACTAAAC
priRSV-A10-14144+	ACCAATTGAGTTTTTAAG
priRSV-A10-2576+	CAATTATCAAAGAAAGC
priRSV-A10-278-	AGGGCAAATATCACTACTTGT
priRSV-A10-4390+	ATAATCTCCATCATGATTG
priRSV-A10-5305+	CAAAAAAACCAACCATCAAG
priRSV-A10-5761+	ATTTTATCAATCAACATG
priRSV-A10-6231+	TTAACCAGCAAAGTGTTAG
priRSV-A10-8489+	CAAGCTATGGGACAAAATG
priRSV-A10-9102+	CATTGGTTTAACTTATAC
priRSV-A-14854+	CATTTATATATGGTAGAATC
priRSV-A-2637+	CTATACAAAGAAACCATAG

priRSV-A-3528+	GTGTCCTTGGATGAAAGAAGC
priRSV-A-9051-	CCATGATGGAGGATGTTGC
priRSV-B05-GORF+MluI	ACGCGTGCCACCATGTCCAAAAACAAGAATC
priRSV-B05-GORF-PstI	TATATACTGCAGTTAGGTGGAATTTGATGTG
priRSV-B-285R	GTTATCAGGGCACACTTCAC
priRSV-B-3267+	ACAAGATGGGGCAAATATGG
priXFP-22+	ATGGTGAGCAAGGGCGAGGAG
priXFP-698-	CTTGTACAGCTCGTCCATG

APPENDIX 2: ANTIBODIES

Antibody	**Source (product)**	**Working dilution**
Anti-c-myc	GenScript (A00704-40)	1:1000 (IB); 1:500 (IF)
Anti-goat IRDye 680RD	LI-COR (925-68074)	1:10,000 (IB)
Anti-mouse IRDye CW800	LI-COR (925-32212)	1:10,000 (IB)
Anti-respiratory syncytial virus	Abcam (ab20745)	1:500 (IB)
Human IVIG	CSL Behring (Privigen)	
Human serum	Atlanta Biologicals (S40190)	
Wheat germ agglutinin AlexaFluor 594	Invitrogen (W11262)	1mg/ml (IF)
Anti-human β-actin	Abcam (ab8226)	1:2000 (IB)

IB: immunoblot *IF: immunofluorescence*

REFERENCES

Afonso, C.L., Amarasinghe, G.K., Bányai, K., Bào, Y., Basler, C.F., Bavari, S., Bejerman, N., Blasdell, K.R., Briand, F.-X., Briese, T., Bukreyev A, Calisher CH, Chandran K, Chéng J, Clawson AN, Collins PL, Dietzgen RG, Dolnik O, Domier LL, Dürrwald R, Dye JM, Easton AJ, Ebihara H, Farkas SL, Freitas-Astúa J, Formenty P, Fouchier RA, Fù Y, Ghedin E, Goodin MM, Hewson R, Horie M, Hyndman TH, Jiāng D, Kitajima EW, Kobinger GP, Kondo H, Kurath G, Lamb RA, Lenardon S, Leroy EM, Li CX, Lin XD, Liú L, Longdon B, Marton S, Maisner A, Mühlberger E, Netesov SV, Nowotny N, Patterson JL, Payne SL, Paweska JT, Randall RE, Rima BK, Rota P, Rubbenstroth D, Schwemmle M, Shi M, Smither SJ, Stenglein MD, Stone DM, Takada A, Terregino C, Tesh RB, Tian JH, Tomonaga K, Tordo N, Towner JS, Vasilakis N, Verbeek M, Volchkov VE, Wahl-Jensen V, Walsh JA, Walker PJ, Wang D, Wang LF, Wetzel T, Whitfield AE, Xiè JT, Yuen KY, Zhang YZ, Kuhn JH. (2016). Taxonomy of the order Mononegavirales: update 2016. Archives of Virology *161*, 2351–2360.

Agoti, C.N., Gitahi, C.W., Medley, G.F., Cane, P.A., and Nokes, D.J. (2013). Identification of group B respiratory syncytial viruses that lack the 60-nucleotide duplication after six consecutive epidemics of total BA dominance at coastal Kenya. Influenza and Other Respiratory Viruses *7*, 1008–1012.

Agoti, C.N., Otieno, J.R., Munywoki, P.K., Mwihuri, A.G., Cane, P.A., Nokes, D.J., Kellam, P., and Cotten, M. (2015). Local evolutionary patterns of human respiratory syncytial virus derived from whole-genome sequencing. Journal of Virology. *89*, 3444.

American Academy of Pediatrics Committee on Infectious Diseases, and American Academy of Pediatrics Bronchiolitis Guidelines Committee (2014). Updated guidance for palivizumab prophylaxis among infants and young children at increased risk of hospitalization for respiratory syncytial virus infection. Pediatrics *134*, 415–420.

Anderson, L.J., Hierholzer, J.C., Tsou, C., Hendry, R.M., Fernie, B.F., Stone, Y., and McIntosh, K. (1985). Antigenic characterization of respiratory syncytial virus strains with monoclonal antibodies. The Journal of Infectious Diseases. *151*, 626–633.

Bajorek, M., Caly, L., Tran, K.C., Maertens, G.N., Tripp, R.A., Bacharach, E., Teng, M.N., Ghildyal, R., and Jans, D.A. (2014). The Thr205 phosphorylation site within respiratory syncytial virus matrix (M) protein modulates M oligomerization and virus production. Journal of Virology. *88*, 6380–6393.

Barik, S. (1992). Transcription of human respiratory syncytial virus genome RNA *in vitro*: requirement of cellular factor(s). Journal of Virology. *66*, 6813–6818.

Been, M.D., and Wickham, G.S. (1997). Self-cleaving ribozymes of hepatitis delta virus RNA. European Journal of Biochemistry. *247*, 741–753.

Bem, R.A., Domachowske, J.B., and Rosenberg, H.F. (2011). Animal models of human respiratory syncytial virus disease. The American Journal of Physiology Lung Cellular Molecular Physiology. *301*, L148–L156.

Bermingham, A., and Collins, P.L. (1999). The M2-2 protein of human respiratory syncytial virus is a regulatory factor involved in the balance between RNA replication and transcription. Proceedings of the National Academy of Sciences of the United States of America. *96*, 11259–11264.

Bose, M.E., He, J., Shrivastava, S., Nelson, M.I., Bera, J., Halpin, R.A., Town, C.D., Lorenzi, H.A., Noyola, D.E., Falcone, V., Gerna, G., De Beenhouwer, H., Videla, C., Kok, T., Venter, M., Williams, J., Henrickson, K. (2015). Sequencing and analysis of globally obtained human respiratory syncytial virus A and B genomes. PLoS ONE *10*, e0120098.

Botosso, V.F., Zanotto, P.M. de A., Ueda, M., Arruda, E., Gilio, A.E., Vieira, S.E., Stewien, K.E., Peret, T.C.T., Jamal, L.F., Pardini, M.I. de M.C., et al. (2009). Positive selection results in frequent reversible amino acid replacements in the G protein gene of human respiratory syncytial virus. PLoS Pathog. *5*, e1000254.

Boukhvalova, M.S., Prince, G.A., and Blanco, J.C.G. (2009). The cotton rat model of respiratory viral infections. Biologicals *37*, 152–159.

Bridgen, A. (2012). Reverse Genetics of RNA Viruses: Applications and Perspectives (John Wiley & Sons).

Brown, D.D., Rima, B.K., Allen, I.V., Baron, M.D., Banyard, A.C., Barrett, T., and Duprex, W.P. (2005). Rational attenuation of a morbillivirus by modulating the activity of the RNA-dependent RNA polymerase. Journal of Virology. *79*, 14330–14338.

Bukreyev, A., Camargo, E., and Collins, P.L. (1996). Recovery of infectious respiratory syncytial virus expressing an additional, foreign gene. Journal of Virology. *70*, 6634–6641.

Byington, C.L., Wilkes, J., Korgenski, K., and Sheng, X. (2015). Respiratory syncytial virus–associated mortality in hospitalized infants and young children. Pediatrics *135*, e24–e31.

Carter, S.D., Dent, K.C., Atkins, E., Foster, T.L., Verow, M., Gorny, P., Harris, M., Hiscox, J.A., Ranson, N.A., Griffin, S., Barr, J. N. (2010). Direct visualization of the small hydrophobic protein of human respiratory syncytial virus reveals the structural basis for membrane permeability. FEBS Letters. *584*, 2786–2790.

Castagné, N., Barbier, A., Bernard, J., Rezaei, H., Huet, J.-C., Henry, C., Da Costa, B., and Eléouët, J.-F. (2004). Biochemical characterization of the respiratory syncytial virus P-P and P-N protein complexes and localization of the P protein oligomerization domain. Journal of General Virology. *85*, 1643–1653.

Chanock, R., Roizman, B., and Myers, R. (1957). Recovery from infants with respiratory illness of a virus related to chimpanzee coryza agent (CCA). I. Isolation, properties and characterization. American Journal of Hygiene. *66*, 281–290.

Coggins, W.B., Lefkowitz, E.J., and Sullender, W.M. (1998). Genetic variability among group A and group B respiratory syncytial viruses in a children's hospital. Journal of Clinical Microbiology. *36*, 3552–3557.

Collins, P.L., Dickens, L.E., Buckler-White, A., Olmsted, R.A., Spriggs, M.K., Camargo, E., and Coelingh, K.V. (1986). Nucleotide sequences for the gene junctions of human respiratory syncytial virus reveal distinctive features of intergenic structure and gene order. Proceedings of the National Academy of Sciences of the United States of America. *83*, 4594–4598.

Collins, P.L., Hill, M.G., Camargo, E., Grosfeld, H., Chanock, R.M., and Murphy, B.R. (1995). Production of infectious human respiratory syncytial virus from cloned cDNA confirms an essential role for the transcription elongation factor from the 5' proximal open reading frame of the M2 mRNA in gene expression and provides a capability for vaccine development. Proceedings of the National Academy of Sciences of the United States of America. *92*, 11563.

Collins, P.L., Hill, M.G., Cristina, J., and Grosfeld, H. (1996). Transcription elongation factor of respiratory syncytial virus, a nonsegmented negative-strand RNA virus. Proceedings of the National Academy of Sciences of the United States of America. *93*, 81–85.

Collins, P.L., Fearns, R., and Graham, B.S. (2013). Respiratory Syncytial Virus: Virology, Reverse Genetics, and Pathogenesis of Disease. In Challenges and Opportunities for Respiratory Syncytial Virus Vaccines, L.J. Anderson, and B.S. Graham, eds. (Berlin, Heidelberg: Springer Berlin Heidelberg), pp. 3–38.

Committee on Infectious Diseases (1993). Use of ribavirin in the treatment of respiratory syncytial virus infection. Pediatrics 92, 501–504.

Conrad, D.A., Christenson, J.C., Waner, J.L., and Marks, M.I. (1987). Aerosolized ribavirin treatment of respiratory syncytial virus infection in infants hospitalized during an epidemic. The Pediatric Infectious Disease Journal. J. *6*, 152–158.

Conzelmann, K.K. (2004). Reverse genetics of mononegavirales. Current Topics in Microbiology and Immunology. Journal of Immunology. *283*, 1–41.

Corry, J., Johnson, S.M., Cornwell, J., and Peeples, M.E. (2015). Preventing cleavage of the respiratory syncytial virus attachment protein in vero cells rescues the infectivity of progeny virus for primary human airway cultures. Journal of Virology. *90*, 1311–1320.

Cox, R., and Plemper, R.K. (2015). The paramyxovirus polymerase complex as a target for next-generation anti-paramyxovirus therapeutics. Frontiers in Microbiology. *6*.

De Clercq, E., and Li, G. (2016). Approved antiviral drugs over the past 50 years. Clinical Microbiology Reviews. *29*, 695–747.

Devincenzo, J.P. (2004). Natural infection of infants with respiratory syncytial virus subgroups A and B: a study of frequency, disease severity, and viral load. Pediatric Research. *56*, 914–917.

DeVincenzo, J.P., El Saleeby, C.M., and Bush, A.J. (2005). Respiratory syncytial virus load predicts disease severity in previously healthy infants. The Journal of Infectious Diseases. *191*, 1861–1868.

Duprex, W.P., McQuaid, S., Hangartner, L., Billeter, M.A., and Rima, B.K. (1999). Observation of measles virus cell-to-cell spread in astrocytoma cells by using a green fluorescent protein-expressing recombinant virus. Journal of Virology. *73*, 9568–9575.

Duprex, W.P., Collins, F.M., and Rima, B.K. (2002). Modulating the function of the measles virus RNA-dependent RNA polymerase by insertion of green fluorescent protein into the open reading frame. Journal of Virology. *76*, 7322–7328.

Dupuy, L.C., Dobson, S., Bitko, V., and Barik, S. (1999). Casein kinase 2-mediated phosphorylation of respiratory syncytial virus phosphoprotein P is essential for the transcription elongation activity of the viral polymerase; phosphorylation by casein kinase 1 occurs mainly at Ser(215) and is without effect. Journal of Virology. *73*, 8384–8392.

Eshaghi, A., Duvvuri, V.R., Lai, R., Nadarajah, J.T., Li, A., Patel, S.N., Low, D.E., and Gubbay, J.B. (2012). Genetic variability of human respiratory syncytial virus A strains circulating in Ontario: a novel genotype with a 72 nucleotide G gene duplication. PloS One *7*, e32807.

Farrag, M.A., and Almajhdi, F.N. (2015). Human respiratory syncytial virus: role of innate immunity in clearance and disease progression. Viral Immunology. *26,* 11-26.

Fearns, R., and Collins, P.L. (1999). Role of the M2-1 transcription antitermination protein of respiratory syncytial virus in sequential transcription. Journal of Virology. *73*, 5852–5864.

Fearns, R., and Deval, J. (2016). New antiviral approaches for respiratory syncytial virus and other mononegaviruses: Inhibiting the RNA polymerase. Antiviral Research *134*, 63–76.

Fearns, R., and Plemper, R.K. (2017). Polymerases of paramyxoviruses and pneumoviruses. Virus Research. *234*, 87–102.

Fearns, R., Peeples, M.E., and Collins, P.L. (1997). Increased expression of the N protein of respiratory syncytial virus stimulates minigenome replication but does not alter the balance between the synthesis of mRNA and antigenome. Virology *236*, 188–201.

Fearns, R., Collins, P.L., and Peeples, M.E. (2000). Functional analysis of the genomic and antigenomic promoters of human respiratory syncytial virus. Journal of Virology. *74*, 6006–6014.

Fearns, R., Peeples, M.E., and Collins, P.L. (2002). Mapping the transcription and replication promoters of respiratory syncytial virus. Journal of Virology. *76*, 1663–1672.

Feldman, S.A., Hendry, R.M., and Beeler, J.A. (1999). Identification of a linear heparin binding domain for human respiratory syncytial virus attachment glycoprotein G. Journal of Virology. *73*, 6610–6617.

Fix, J., Galloux, M., Blondot, M.-L., and Eléouët, J.-F. (2011). The insertion of fluorescent proteins in a variable region of respiratory syncytial virus L polymerase results in fluorescent and functional enzymes but with reduced activities. The Open Virology Journal. J. *5*, 103–108.

Gan, S.-W., Tan, E., Lin, X., Yu, D., Wang, J., Tan, G.M.-Y., Vararattanavech, A., Yeo, C.Y., Soon, C.H., Soong, T.W., Pervushin, K., Torres, J. (2012). The small

hydrophobic protein of the human respiratory syncytial virus forms pentameric ion channels. The Journal of Biological Chemistry. *287*, 24671–24689.

García-Barreno, B., Portela, A., Delgado, T., López, J.A., and Melero, J.A. (1990). Frame shift mutations as a novel mechanism for the generation of neutralization resistant mutants of human respiratory syncytial virus. The EMBO Journal. *9*, 4181–4187.

García-Beato, R., Martínez, I., Francí, C., Real, F.X., García-Barreno, B., and Melero, J.A. (1996). Host cell effect upon glycosylation and antigenicity of human respiratory syncytial virus G glycoprotein. Virology *221*, 301–309.

Ghildyal, R., Ho, A., and Jans, D.A. (2006). Central role of the respiratory syncytial virus matrix protein in infection. FEMS Microbiology Reviews. *30*, 692–705.

Gorman, J.J., Ferguson, B.L., Speelman, D., and Mills, J. (1997). Determination of the disulfide bond arrangement of human respiratory syncytial virus attachment (G) protein by matrix-assisted laser desorption/ionization time-of-flight mass spectrometry. Protein Science: A Publication of the Protein Society. *6*, 1308–1315.

Graham, B.S. (2011). Biological challenges and technological opportunities for respiratory syncytial virus vaccine development: RSV vaccine development. Immunological Reviews. *239*, 149–166.

Gross, A.E., and Bryson, M.L. (2015). Oral ribavirin for the treatment of noninfluenza respiratory viral infections: A systematic review. Annals of Pharmacotherapy. *49*, 1125–1135.

Habibi, M.S., Jozwik, A., Makris, S., Dunning, J., Paras, A., DeVincenzo, J.P., de Haan, C.A.M., Wrammert, J., Openshaw, P.J.M., Chiu, C., et al. (2015). Impaired antibody-mediated protection and defective IgA B-cell memory in experimental infection of adults with respiratory syncytial virus. American Journal of Respiratory and Critical Care Medicine. *191*, 1040–1049.

Hall, C.B., Walsh, E.E., Schnabel, K.C., Long, C.E., McConnochie, K.M., Hildreth, S.W., and Anderson, L.J. (1990). Occurrence of groups A and B of respiratory syncytial virus over 15 years: associated epidemiologic and clinical characteristics in hospitalized and ambulatory children. The Journal of Infectious Diseases. *162*, 1283–1290.

Hall, C.B., Walsh, E.E., Long, C.E., and Schnabel, K.C. (1991). Immunity to and frequency of reinfection with respiratory syncytial virus. The Journal of Infectious Diseases. *163*, 693–698.

Hall, C.B., Weinberg, G.A., Iwane, M.K., Blumkin, A.K., Edwards, K.M., Staat, M.A., Auinger, P., Griffin, M.R., Poehling, K.A., Erdman, D., Grijalva, C.G., Zhu, Y., Szilagyi, P. (2009). The burden of respiratory syncytial virus infection in young children. The New England Journal of Medicine. *360*, 588–598.

Hall, C.B., Simőes, E.A.F., and Anderson, L.J. (2013). Clinical and epidemiologic features of respiratory syncytial virus. Current Topics in Microbiology and Immunology. *372*, 39–57.

Hardy, R.W., Harmon, S.B., and Wertz, G.W. (1999). Diverse gene junctions of respiratory syncytial virus modulate the efficiency of transcription termination and respond differently to M2-mediated antitermination. Journal of Virology. *73*, 170–176.

Henderson, G., Murray, J., and Yeo, R.P. (2002). Sorting of the respiratory syncytial virus matrix protein into detergent-resistant structures is dependent on cell-surface expression of the glycoproteins. Virology *300*, 244–254.

Hendricks, D.A., Baradaran, K., McIntosh, K., and Patterson, J.L. (1987). Appearance of a soluble form of the G protein of respiratory syncytial virus in fluids of infected cells. Journal of General Virology. *68*, 1705–1714.

Hendricks, D.A., McIntosh, K., and Patterson, J.L. (1988). Further characterization of the soluble form of the G glycoprotein of respiratory syncytial virus. Journal of Virology. *62*, 2228–2233.

Hickling, T.P., Malhotra, R., Bright, H., McDowell, W., Blair, E.D., and Sim, R.B. (2000). Lung surfactant protein A provides a route of entry for respiratory syncytial virus into host cells. Viral Immunology. *13*, 125–135.

Hoenen, T., Shabman, R.S., Groseth, A., Herwig, A., Weber, M., Schudt, G., Dolnik, O., Basler, C.F., Becker, S., and Feldmann, H. (2012). Inclusion bodies are a site of ebolavirus replication. Journal of Virology. *86*, 11779–11788.

Hotard, A.L., Shaikh, F.Y., Lee, S., Yan, D., Teng, M.N., Plemper, R.K., Crowe, J.E., and Moore, M.L. (2012). A stabilized respiratory syncytial virus reverse genetics system amenable to recombination-mediated mutagenesis. Virology *434*, 129–136.

Hotard, A.L., Laikhter, E., Brooks, K., Hartert, T.V., and Moore, M.L. (2015). Functional analysis of the 60-nucleotide duplication in the respiratory syncytial virus Buenos Aires strain attachment glycoprotein. Journal of Virology. *89*, 8258–8266.

Huong, T.N., Iyer Ravi, L., Tan, B.H., and Sugrue, R.J. (2016). Evidence for a biphasic mode of respiratory syncytial virus transmission in permissive HEp2 cell monolayers. Virology. J. *13*, 12.

Jafri, H.S., Wu, X., Makari, D., and Henrickson, K.J. (2013). Distribution of respiratory syncytial virus subtypes A and B among infants presenting to the emergency department with lower respiratory tract infection or apnea. The Pediatric Infectious Disease Journal. *32*, 335–340.

Johnson, T.R., and Graham, B.S. (1999). Secreted respiratory syncytial virus G glycoprotein induces interleukin-5 (IL-5), IL-13, and eosinophilia by an IL-4-independent mechanism. Journal of Virology. *73*, 8485–8495.

Johnson, P.R., Spriggs, M.K., Olmsted, R.A., and Collins, P.L. (1987). The G glycoprotein of human respiratory syncytial viruses of subgroups A and B: extensive sequence divergence between antigenically related proteins. Proceedings of the National Academy of Sciences of the United States of America. *84*, 5625–5629.

Johnson, S.M., McNally, B.A., Ioannidis, I., Flano, E., Teng, M.N., Oomens, A.G., Walsh, E.E., and Peeples, M.E. (2015). Respiratory syncytial virus uses CX3CR1 as a receptor on primary human airway epithelial cultures. PLoS Pathogen. *11*, e1005318.

Johnson, T.R., McLellan, J.S., and Graham, B.S. (2012). Respiratory syncytial virus glycoprotein G interacts with DC-SIGN and L-SIGN to activate ERK1 and ERK2. Journal of Virology. *86*, 1339–1347.

Kim, H.W., Canchola, J.G., Brandt, C.D., Pyles, G., Chanock, R.M., Jensen, K., and Parrott, R.H. (1969). Respiratory syncytial virus disease in infants despite prior administration of antigenic inactivated vaccine. American Journal of Epidemiology. *89*, 422–434.

Kim, Y.-I., Murphy, R., Majumdar, S., Harrison, L.G., Aitken, J., and DeVincenzo, J.P. (2015). Relating plaque morphology to respiratory syncytial virus subgroup, viral load, and disease severity in children. Pediatric Research. *78*, 380–388.

Kolodziej, P.A., and Young, R.A. (1991). Epitope tagging and protein surveillance. Methods in Enzymology. *194*, 508–519.

Krzyzaniak, M.A., Zumstein, M.T., Gerez, J.A., Picotti, P., and Helenius, A. (2013). Host cell entry of respiratory syncytial virus involves macropinocytosis followed by proteolytic activation of the F protein. PLoS Pathog. *9*, e1003309.

Kumaria, R., Iyer, L.R., Hibberd, M.L., Simões, E.A.F., and Sugrue, R.J. (2011). Whole genome characterization of non-tissue culture adapted HRSV strains in severely infected children. Virology Journal. *8*, 372.

Kuo, L., Fearns, R., and Collins, P.L. (1997). Analysis of the gene start and gene end signals of human respiratory syncytial virus: quasi-templated initiation at position 1 of the encoded mRNA. Journal of Virology. *71*, 4944–4953.

Kwilas, S., Liesman, R.M., Zhang, L., Walsh, E., Pickles, R.J., and Peeples, M.E. (2009). Respiratory syncytial virus grown in Vero cells contains a truncated attachment protein that alters its infectivity and dependence on glycosaminoglycans. Journal of Virology. *83*, 10710–10718.

Le Nouën, C., McCarty, T., Brown, M., Smith, M.L., Lleras, R., Dolan, M.A., Mehedi, M., Yang, L., Luongo, C., Liang, B., Munir, S., DiNapoli, J., Wimmer, E., Collins, P., Buchholz, U. (2017). Genetic stability of genome-scale deoptimized RNA virus vaccine candidates under selective pressure. Proceedings of the National Academy of Sciences of the United States of America. *114*, E386–E395.

Lemon, K., Nguyen, D.T., Ludlow, M., Rennick, L.J., Yüksel, S., van Amerongen, G., McQuaid, S., Rima, B.K., de Swart, R.L., and Duprex, W.P. (2015). Recombinant subgroup B human respiratory syncytial virus expressing enhanced green fluorescent protein efficiently replicates in primary human cells and is virulent in cotton rats. Journal of Virology. *89*, 2849–2856.

Levine, S., Klaiber-Franco, R., and Paradiso, P.R. (1987). Demonstration that glycoprotein G is the attachment protein of respiratory syncytial virus. Journal of General Virology. *68*, 2521–2524.

Liuzzi, M., Mason, S.W., Cartier, M., Lawetz, C., McCollum, R.S., Dansereau, N., Bolger, G., Lapeyre, N., Gaudette, Y., Lagacé, L., Massariol, M., Dô, F., Whitehead, P., Lamarre, L., Scouten, E., Bordeleau, J., Landry, S., Rancourt, J., Fazal, G., Simoneau, B. (2005). Inhibitors of respiratory syncytial virus replication target cotranscriptional mRNA guanylylation by viral RNA-dependent RNA polymerase. Journal of Virology. *79*, 13105–13115.

Ludlow, M., Nguyen, D.T., Silin, D., Lyubomska, O., de Vries, R.D., von Messling, V., McQuaid, S., De Swart, R.L., and Duprex, W.P. (2012). Recombinant canine distemper virus strain Snyder Hill expressing green or red fluorescent proteins causes meningoencephalitis in the ferret. Journal of Virology. *86*, 7508–7519.

Malhotra, R., Ward, M., Bright, H., Priest, R., Foster, M.R., Hurle, M., Blair, E., and Bird, M. (2003). Isolation and characterisation of potential respiratory syncytial virus receptor(s) on epithelial cells. Microbes and Infection. *5*, 123–133.

Martínez, I., Dopazo, J., and Melero, J.A. (1997). Antigenic structure of the human respiratory syncytial virus G glycoprotein and relevance of hypermutation events for the generation of antigenic variants. Journal of General Virology. *78*, 2419–2429.

Marty, A., Meanger, J., Mills, J., Shields, B., and Ghildyal, R. (2004). Association of matrix protein of respiratory syncytial virus with the host cell membrane of infected cells. Archives of Virology. *149*, 199–210.

McConnochie, K.M., Hall, C.B., Walsh, E.E., and Roghmann, K.J. (1990). Variation in severity of respiratory syncytial virus infections with subtype. Journal of Pediatrics. *117*, 52–62.

McLellan, J.S., Ray, W.C., and Peeples, M.E. (2013). Structure and Function of Respiratory Syncytial Virus Surface Glycoproteins. In Challenges and Opportunities for Respiratory Syncytial Virus Vaccines, L.J. Anderson, and B.S. Graham, eds. (Berlin, Heidelberg: Springer Berlin Heidelberg), pp. 83–104.

Melero, J.A., and Moore, M.L. (2013). Influence of Respiratory Syncytial Virus Strain Differences on Pathogenesis and Immunity. In Challenges and Opportunities for Respiratory Syncytial Virus Vaccines, L.J. Anderson, and B.S. Graham, eds. (Berlin, Heidelberg: Springer Berlin Heidelberg), pp. 59–82.

Melero, J.A., García-Barreno, B., Martínez, I., Pringle, C.R., and Cane, P.A. (1997). Antigenic structure, evolution and immunobiology of human respiratory syncytial virus attachment (G) protein. Journal of General Virology. *78*, 2411–2418.

Meshram, C.D., Baviskar, P.S., Ognibene, C.M., and Oomens, A.G.P. (2016). The respiratory syncytial virus phosphoprotein, matrix protein, and fusion protein carboxy-terminal domain drive efficient filamentous virus-like particle formation. Journal of Virology. *90*, 10612–10628.

Mink, M.A., Stec, D.S., and Collins, P.L. (1991). Nucleotide sequences of the 3' leader and 5' trailer regions of human respiratory syncytial virus genomic RNA. Virology *185*, 615–624.

Mitra, R., Baviskar, P., Duncan-Decocq, R.R., Patel, D., and Oomens, A.G.P. (2012). The human respiratory syncytial virus matrix protein is required for maturation of viral filaments. Journal of Virology. *86*, 4432–4443.

Mochizuki, H., Kusuda, S., Okada, K., Yoshihara, S., Furuya, H., and Simões, E.A.F. (2017). Palivizumab prophylaxis in preterm infants and subsequent recurrent wheezing: 6 year follow up study. American Journal of Respiratory and Critical Care Medicine. *196.* 29-38.

Moore, E.C., Barber, J., and Tripp, R.A. (2008). Respiratory syncytial virus (RSV) attachment and nonstructural proteins modify the type I interferon response associated with suppressor of cytokine signaling (SOCS) proteins and IFN-stimulated gene-15 (ISG15). Virology Journal. *5*, 116.

Moore, M.L., Chi, M.H., Luongo, C., Lukacs, N.W., Polosukhin, V.V., Huckabee, M.M., Newcomb, D.C., Buchholz, U.J., Crowe, J.E., Goleniewska, K., et al. (2009). A chimeric A2 strain of respiratory syncytial virus (RSV) with the fusion protein of RSV strain line 19 exhibits enhanced viral load, mucus, and airway dysfunction. Journal of Virology. *83*, 4185–4194.

Moudy, R.M., Sullender, W.M., and Wertz, G.W. (2004). Variations in intergenic region sequences of Human respiratory syncytial virus clinical isolates: analysis of effects on transcriptional regulation. Virology *327*, 121–133.

Mufson, M.A., Orvell, C., Rafnar, B., and Norrby, E. (1985). Two distinct subtypes of human respiratory syncytial virus. Journal of General Virology. *66*, 2111–2124.

Nair, H., Nokes, D.J., Gessner, B.D., Dherani, M., Madhi, S.A., Singleton, R.J., O'Brien, K.L., Roca, A., Wright, P.F., Bruce, N., Chandran, A., Theodoratou, E., Sutanto, A., Sedyaningsih, E.R., Ngama, M., Munywoki, P.K., Kartasasmita, C., Simões, E.A., Rudan, I., Weber, M.W., Campbell, H. (2010). Global burden of acute lower respiratory infections due to respiratory syncytial virus in young children: a systematic review and meta-analysis. The Lancet *375*, 1545–1555.

Neuzil, K.M. (2016). Progress toward a respiratory syncytial virus vaccine. Clinical and Vaccine Immunology. *23*, 186–188.

Noton, S.L., and Fearns, R. (2011). The first two nucleotides of the respiratory syncytial virus antigenome RNA replication product can be selected independently of the promoter terminus. RNA *17*, 1895–1906.

Openshaw, P.J.M., Chiu, C., Culley, F.J., and Johansson, C. (2017). Protective and harmful immunity to RSV infection. Annual Review of Immunology. *35*, 501-532.

Papadopoulos, N.G., Gourgiotis, D., Javadyan, A., Bossios, A., Kallergi, K., Psarras, S., Tsolia, M.N., and Kafetzis, D. (2004). Does respiratory syncytial virus subtype influences the severity of acute bronchiolitis in hospitalized infants? Respiratory Medicine. *98*, 879–882.

Peeples, M.E., and Collins, P.L. (2000). Mutations in the 5' trailer region of a respiratory syncytial virus minigenome which limit RNA replication to one step. Journal of Virology. *74*, 146–155.

Peret, T.C., Hall, C.B., Schnabel, K.C., Golub, J.A., and Anderson, L.J. (1998). Circulation patterns of genetically distinct group A and B strains of human respiratory syncytial virus in a community. Journal of General Virology. *79*, 2221–2229.

Peret, T.C.T., Hall, C.B., Hammond, G.W., Piedra, P.A., Storch, G.A., Sullender, W.M., Tsou, C., and Anderson, L.J. (2000). Circulation patterns of group A and B human respiratory syncytial virus genotypes in 5 communities in North America. The Journal of Infectious Diseases. *181*, 1891–1896.

Poch, O., Blumberg, B.M., Bougueleret, L., and Tordo, N. (1990). Sequence comparison of five polymerases (L proteins) of unsegmented negative-strand RNA viruses: theoretical assignment of functional domains. Journal of General Virology. *71*, 1153–1162.

Power, U.F. (2008). Respiratory syncytial virus (RSV) vaccines--two steps back for one leap forward. Journal of Clinical Virology: the Official Publication of the Pan American Society of Virology. *41*, 38–44.

Prince, G.A., Horswood, R.L., Camargo, E., Koenig, D., and Chanock, R.M. (1983). Mechanisms of immunity to respiratory syncytial virus in cotton rats. Infection and Immunity. *42*, 81–87.

Ramirez, J.A. (2008). RSV infection in the adult population. Managed Care (Langhorne, Pa.) Journal *17*, 13–15.

Reed, L.J., and Muench, H. (1938). A simple method of estimating fifty per cent endpoints. American Journal of Epidemiology. *27*, 493–497.

Roberts, S.R., Compans, R.W., and Wertz, G.W. (1995). Respiratory syncytial virus matures at the apical surfaces of polarized epithelial cells. Journal of Virology. *69*, 2667–2673.

Rostad, C.A., Stobart, C.C., Gilbert, B.E., Pickles, R.J., Hotard, A.L., Meng, J., Blanco, J.C.G., Moin, S.M., Graham, B.S., Piedra, P.A., Moore, M.L. (2016). A recombinant respiratory syncytial virus vaccine candidate attenuated by a low-fusion F protein is immunogenic and protective against challenge in cotton rats. Journal of Virology. *90*, 7508–7518.

Ruedas, J.B., and Perrault, J. (2009). Insertion of enhanced green fluorescent protein in a hinge region of vesicular stomatitis virus L polymerase protein creates a temperature-sensitive virus that displays no virion-associated polymerase activity *in vitro*. Journal of Virology. *83*, 12241–12252.

Ruedas, J.B., and Perrault, J. (2014). Putative domain-domain interactions in the vesicular stomatitis virus L polymerase protein appendage region. Journal of Virology. *88*, 14458–14466.

Sa, C., D, Y., and S, H. (2010). The use of a neonatal mouse model to study respiratory syncytial virus infections., The use of a neonatal mouse model to study respiratory syncytial virus infections. Expert Review of Anti-infective Therapy. *8*, 1371–1380.

Sacco, R.E., Durbin, R.K., and Durbin, J.E. (2015). Animal models of respiratory syncytial virus infection and disease. Current Opinion in Virology. *13*, 117–122.

Schmidt, K.M., Schümann, M., Olejnik, J., Krähling, V., and Mühlberger, E. (2011). Recombinant Marburg virus expressing EGFP allows rapid screening of virus growth and real-time visualization of virus spread. The Journal of Infectious Diseases. *204 Suppl 3*, S861-870.

Schmidt, M.R., McGinnes, L.W., Kenward, S.A., Willems, K.N., Woodland, R.T., and Morrison, T.G. (2012). Long-term and memory immune responses in mice against Newcastle disease virus-like particles containing respiratory syncytial virus glycoprotein ectodomains. Journal of Virology. *86*, 11654–11662.

Schmidt, M.R., McGinnes-Cullen, L.W., Kenward, S.A., Willems, K.N., Woodland, R.T., and Morrison, T.G. (2014). Modification of the respiratory syncytial virus f protein in virus-like particles impacts generation of B cell memory. Journal of Virology. *88*, 10165–10176.

Schnell, M.J., Buonocore, L., Whitt, M.A., and Rose, J.K. (1996). The minimal conserved transcription stop-start signal promotes stable expression of a foreign gene in vesicular stomatitis virus. Journal of Virology. *70*, 2318–2323.

Schobel, S.A., Stucker, K.M., Moore, M.L., Anderson, L.J., Larkin, E.K., Shankar, J., Bera, J., Puri, V., Shilts, M.H., Rosas-Salazar, C., Halpin, R.A., Fedorova, N., Shrivastava, S., Stockwell, T.B., Peebles, R.S., Hartert, T.V., Das, S.R. (2016). Respiratory Syncytial Virus whole-genome sequencing identifies convergent evolution of sequence duplication in the C-terminus of the G gene. Scientific Reports. *6*, 26311.

Silin, D., Lyubomska, O., Ludlow, M., Duprex, W.P., and Rima, B.K. (2007). Development of a challenge-protective vaccine concept by modification of the viral RNA-dependent RNA polymerase of canine distemper virus. Journal of Virology. *81*, 13649–13658.

Simões, E.A.F., DeVincenzo, J.P., Boeckh, M., Bont, L., Crowe, J.E., Griffiths, P., Hayden, F.G., Hodinka, R.L., Smyth, R.L., Spencer, K., Thirstrup, S., Walsh,

E.E., Whitley, R.J. (2015). Challenges and opportunities in developing respiratory syncytial virus therapeutics. The Journal of Infectious Diseases. *211*, S1–S20.

Smith, D.W., Frankel, L.R., Mathers, L.H., Tang, A.T., Ariagno, R.L., and Prober, C.G. (1991). A controlled trial of aerosolized ribavirin in infants receiving mechanical ventilation for severe respiratory syncytial virus infection. The New England Journal of Medicine. *325*, 24–29.

Spann, K.M., Tran, K.C., and Collins, P.L. (2005). Effects of nonstructural proteins NS1 and NS2 of human respiratory syncytial virus on interferon regulatory factor 3, NF-kappaB, and proinflammatory cytokines. Journal of Virology. *79*, 5353–5362.

Stark, J.M., McDowell, S.A., Koenigsknecht, V., Prows, D.R., Leikauf, J.E., Le Vine, A.M., and Leikauf, G.D. (2002). Genetic susceptibility to respiratory syncytial virus infection in inbred mice. Journal of Medical Virology. *67*, 92–100.

Stobart, C.C., Hartert, T.V., Lin, S., Gaston, K.A., Anderson, L.J., Oomens, A.G.P., Boyoglu-Barnum, S., Moore, M.L., Ziady, A.G., Chirkova, T., et al. (2015). CX3CR1 is an important surface molecule for respiratory syncytial virus infection in human airway epithelial cells. Journal of General Virology. *96*, 2543–2556.

Subramanian, K.N., Weisman, L.E., Rhodes, T., Ariagno, R., Sánchez, P.J., Steichen, J., Givner, L.B., Jennings, T.L., Top, F.H., Carlin, D., Connor, E. (1998). Safety, tolerance and pharmacokinetics of a humanized monoclonal antibody to respiratory syncytial virus in premature infants and infants with bronchopulmonary dysplasia. MEDI-493 Study Group. The Pediatric Infectious Disease Journal. J. *17*, 110–115.

Sullender, W.M. (2000). Respiratory syncytial virus genetic and antigenic diversity. Clinical Microbiology Reviews. *13*, 1–15.

Sullender, W.M., Sun, L., and Anderson, L.J. (1993). Analysis of respiratory syncytial virus genetic variability with amplified cDNAs. Journal of Clinical Microbiology. *31*, 1224–1231.

Svenda, M., Berg, M., Moreno-López, J., and Linné, T. (1997). Analysis of the large (L) protein gene of the procine rubulavirus LPMV: identification of possible functional domains. Virus Research. *48*, 57–70.

Swedan, S., Andrews, J., Majumdar, T., Musiyenko, A., and Barik, S. (2011). Multiple functional domains and complexes of the two nonstructural proteins of

human respiratory syncytial virus contribute to interferon suppression and cellular location. Journal of Virology. *85*, 10090–10100.

Tan, L., Lemey, P., Houspie, L., C. Viveen, M., Jansen, N.J.G., van Loon, A.M., Wiertz, E., van Bleek, G.M., Martin, D.P., and Coenjaerts, F.E. (2012). Genetic variability among complete human respiratory syncytial virus subgroup A genomes: bridging molecular evolutionary dynamics and epidemiology. PLoS ONE 7, e51439.

Tan, L., Coenjaerts, F.E.J., Houspie, L., Viveen, M.C., van Bleek, G.M., Wiertz, E.J.H.J., Martin, D.P., and Lemey, P. (2013). The comparative genomics of human respiratory syncytial virus subgroups A and B: genetic variability and molecular evolutionary dynamics. Journal of Virology. *87*, 8213–8226.

Techaarpornkul, S., Collins, P.L., and Peeples, M.E. (2002). Respiratory syncytial virus with the fusion protein as its only viral glycoprotein is less dependent on cellular glycosaminoglycans for attachment than complete virus. Virology *294*, 296–304.

Teng, M.N., Whitehead, S.S., Bermingham, A., St Claire, M., Elkins, W.R., Murphy, B.R., and Collins, P.L. (2000). Recombinant respiratory syncytial virus that does not express the NS1 or M2-2 protein is highly attenuated and immunogenic in chimpanzees. Journal of Virology. *74*, 9317–9321.

Teng, M.N., Whitehead, S.S., and Collins, P.L. (2001). Contribution of the respiratory syncytial virus G glycoprotein and its secreted and membrane-bound forms to virus replication *in vitro* and *in vivo*. Virology *289*, 283–296.

The IMpact RSV Study Group (1998). Palivizumab, a humanized respiratory syncytial virus monoclonal antibody, reduces hospitalization from respiratory syncytial virus infection in high-risk infants. Pediatrics *102*, 531–537.

Trento, A., Galiano, M., Videla, C., Carballal, G., García-Barreno, B., Melero, J.A., and Palomo, C. (2003). Major changes in the G protein of human respiratory syncytial virus isolates introduced by a duplication of 60 nucleotides. Journal of General Virology. *84*, 3115–3120.

Trento, A., Casas, I., Calderón, A., Garcia-Garcia, M.L., Calvo, C., Perez-Breña, P., and Melero, J.A. (2010). Ten years of global evolution of the human respiratory syncytial virus BA genotype with a 60-nucleotide duplication in the G protein gene. Journal of Virology. *84*, 7500–7512.

Villenave, R., O'Donoghue, D., Thavagnanam, S., Touzelet, O., Skibinski, G., Heaney, L.G., McKaigue, J.P., Coyle, P.V., Shields, M.D., and Power, U.F. (2011). Differential cytopathogenesis of respiratory syncytial virus prototypic and

clinical isolates in primary pediatric bronchial epithelial cells. Virology Journal. *8*, 43.

Walsh, E.E., and Falsey, A.R. (2012). Respiratory syncytial virus infection in adult populations. Infectious Disorders Drug Targets *12*, 98–102.

Wertz, G.W., Collins, P.L., Huang, Y., Gruber, C., Levine, S., and Ball, L.A. (1985). Nucleotide sequence of the G protein gene of human respiratory syncytial virus reveals an unusual type of viral membrane protein. Proceedings of the National Academy of Sciences of the United States of America. *82*, 4075–4079.

Wertz, G.W., Krieger, M., and Ball, L.A. (1989). Structure and cell surface maturation of the attachment glycoprotein of human respiratory syncytial virus in a cell line deficient in O glycosylation. Journal of Virology. *63*, 4767–4776.

White, L.J., Waris, M., Cane, P.A., Nokes, D.J., and Medley, G.F. (2005). The transmission dynamics of groups A and B human respiratory syncytial virus (hRSV) in England & Wales and Finland: seasonality and cross-protection. Epidemiology & Infection. *133*, 279.

Whitlow, Z.W., Connor, J.H., and Lyles, D.S. (2006). Preferential translation of vesicular stomatitis virus mRNAs Is conferred by transcription from the viral genome. Journal of Virology. *80*, 11733–11742.

Zhang, L., Peeples, M.E., Boucher, R.C., Collins, P.L., and Pickles, R.J. (2002). Respiratory syncytial virus infection of human airway epithelial cells is polarized, specific to ciliated cells, and without obvious cytopathology. Journal of Virology. *76*, 5654–5666.

Zhao, X., and Sullender, W.M. (2005). *In vivo* selection of respiratory syncytial viruses resistant to palivizumab. Journal of Virology. *79*, 3962–3968.

Zhou, L., Xiao, Q., Zhao, Y., Huang, A., Ren, L., and Liu, E. (2015). The impact of viral dynamics on the clinical severity of infants with respiratory syncytial virus bronchiolitis. Journal of Medical Virology. *87*, 1276–1284.

Zhu, Q., McAuliffe, J.M., Patel, N.K., Palmer-Hill, F.J., Yang, C., Liang, B., Su, L., Zhu, W., Wachter, L., Wilson, S., MacGill, R.S., Krishnan, S., McCarthy, M.P., Losonsky, G.A., Suzich, J.A. (2011). Analysis of respiratory syncytial virus preclinical and clinical variants resistant to neutralization by monoclonal antibodies palivizumab and/or motavizumab. The Journal of Infectious Diseases. *203*, 674–682.

CURRICULUM VITAE

GRACE YOONHEEKEE OLINGER

(b. 1990)

22 WATER STREET APT 431

CAMBRIDGE, MA 02141

(618) 509-3358

kyh6kr@gmail.com

EDUCATION

2013-2017 BOSTON UNIVERSITY SCHOOL OF MEDICINE

Boston, MA

Master of Science, Microbiology

Advisor: W. Paul Duprex, PhD

2010-2013 UNIVERSITY OF MISSOURI Columbia, MO

Bachelor of Science**,** Biological Sciences

Minor: Chemistry

RESEARCH EXPERIENCE

2013-2017 BOSTON UNIVERSITY SCHOOL OF MEDICINE Boston, MA

Graduate research assistant

Advisor: W. Paul Duprex, PhD

2010-2013 UNIVERSITY OF MISOURI Columbia, MO

Undergraduate research assistant

Advisor: Marc Johnson, PhD

TEACHING, LEADERSHIP, COMMUNICATION EXPERIENCE

2014-2015 BOSTON UNIVERSITY SCHOOL OF MEDICINE Boston, MA

Genetics tutor

2014-2015 BOSTON UNIVERSITY SCHOOL OF MEDICINE Boston, MA

PiBS journal club organizer

2011-2013 UNIVERSITY OF MISSOURI Columbia, MO

Genetics tutor

2011-2012 UNIVERSITY OF MISSOURI Columbia, MO

HHMI collaboration, computation, communication fellow

PUBLICATION

Gregory, D.A., Olinger, G.Y., Lucas, T.L., and Johnson, M.C. (2014) Diverse viral glycoproteins as well as CD4 co-package into the same human immunodeficiency virus (HIV-1) particles. Retrovirology *11*:28

POSTER PRESENTATIONS

Olinger, G.Y., Rennick, L.J., Duprex, W.P. (2016) Insertion of Venus Reporter Gene into the L Gene of Human Respiratory Syncytial Virus and Recovery of a Recombinant Virus. Annual meeting of American Society of Virology conference at Virginia Tech

Olinger, G.Y., Johnson, M.C. (2013) Why can't we get along: The role of GaLV Env in its incompatibility with HIV. University of Missouri Life Sciences Week Poster Session

Olinger, G.Y., Johnson, M.C. (2012) The role of Gibbon ape leukemia virus envelope cytoplasmic tail in its pseudotyping incompatibility with HIV-1. Annual international meeting on Retroviruses at Cold Spring Harbor Laboratories

Olinger, G.Y., Johnson, M.C. (2012) Glycoprotein recruitment specificity of simian immunodeficiency virus. Missouri Capitol Undergraduate Research Day